sustainability

Review

A Review of Heat Batteries Based PV Module Cooling—Case Studies on Performance Enhancement of Large-Scale Solar PV System

Karthikeyan Velmurugan [1], Rajvikram Madurai Elavarasan [2], Pham Van De [3], Vaithinathan Karthikeyan [4], Tulja Bhavani Korukonda [5], Joshuva Arockia Dhanraj [6], Kanchanok Emsaeng [7,8], Md. Shahariar Chowdhury [1], Kuaanan Techato [1,9,*], Bothaina Samih Abou El Khier [10] and El-Awady Attia [11,12]

1 Faculty of Environmental Management, Prince of Songkla University, Hat Yai 90112, Thailand; karthi230407@gmail.com (K.V.); mdshahariar.c@psu.ac.th (M.S.C.)
2 Department of Electrical and Electronics Engineering, Thiagarajar College of Engineering, Madurai 625015, India; rajvikram787@gmail.com
3 Faculty of Technology, Dong Nai Technology University, Bien Hoa 76000, Dong Nai, Vietnam; phamvande@dntu.edu.vn
4 James Watt School of Engineering, University of Glasgow, Glasgow G12 8QQ, UK; kvecers@gmail.com
5 Centre for Energy Studies, Indian Institute of Technology, Delhi 110016, India; tulja.bhavani058@gmail.com
6 Centre for Automation and Robotics (ANRO), Department of Mechanical Engineering, Hindustan Institute of Technology and Science, Padur, Chennai 603103, India; joshuva1991@gmail.com
7 Faculty of Education, Pibulsongkram Rajabhat University, Phitsanulok 65000, Thailand; forteletter@gmail.com
8 Faculty of Humanities and Social Science, Mahasarakham University, Maha Sarakham 44150, Thailand
9 Environmental Assessment and Technology for Hazardous Waste Management Research Center, Faculty of Environmental Management, Prince of Songkla University, Hat Yai 90112, Thailand
10 Architectural Engineering Department, Faculty of Engineering and Technology, Future University in Egypt, New Cairo 11835, Egypt; bothaina.samih@fue.edu.eg
11 Department of Industrial Engineering, College of Engineering, Prince Sattam Bin Abdulaziz University, Al Kharj 16273, Saudi Arabia; E.attia@psau.edu.sa
12 Mechanical Engineering Department, Faculty of Engineering (Shoubra), Benha University, Cairo 13511, Egypt
* Correspondence: Kuaanan.t@psu.ac.th

check for updates

Citation: Velmurugan, K.; Elavarasan, R.M.; De, P.V.; Karthikeyan, V.; Korukonda, T.B.; Dhanraj, J.A.; Emsaeng, K.; Chowdhury, M.S.; Techato, K.; El Khier, B.S.A.; et al. A Review of Heat Batteries Based PV Module Cooling—Case Studies on Performance Enhancement of Large-Scale Solar PV System. *Sustainability* **2022**, *14*, 1963. https://doi.org/10.3390/su14041963

Academic Editor: Chi-Ming Lai

Received: 23 December 2021
Accepted: 30 January 2022
Published: 9 February 2022

Abstract: Several studies have concentrated on cooling the PV module temperature (T_{PV}) to enhance the system's electrical output power and efficiency in recent years. In this review study, PCM-based cooling techniques are reviewed majorly classified into three techniques: (i) incorporating raw/pure PCM behind the PV module is one of the most straightforward techniques; (ii) thermal additives such as inter-fin, nano-compound, expanded graphite (EG), and others are infused in PCM to enhance the heat transfer rate between PV module and PCM; and (iii) thermal collectors that are placed behind the PV module or inside the PCM container to minimize the PCM usage. Advantageously, these techniques favor reusing the waste heat from the PV module. Further, in this study, PCM thermophysical properties are straightforwardly discussed. It is found that the PCM melting temperature (T_{melt}) and thermal conductivity (K_{PCM}) become the major concerns in cooling the PV module. Based on the literature review, experimentally proven PV-PCM temperatures are analyzed over a year for UAE and Islamabad locations using typical meteorological year (TMY) data from the National Renewable Energy Laboratory (NREL) data source in 1 h frequency.

Keywords: PV module cooling; heat battery; thermal conduction barrier; composite PCM (heat battery); thermal collector; power enhancement; PR improvement

1. Introduction

Renewable energy sources are actively adopted as non-conventional energy sources to reduce fossil fuel consumption and global warming [1,2]. Among the alternative and renewable energies, solar energy being pioneer, photovoltaic, and thermal technologies made their way to the fastest and futuristic commercialization [3,4]. With silicon-based solar cell modules, solar photovoltaics have become increasingly popular for both stand-alone and grid-integrated power generation across the world. The solar PV systems are developed for applications of a few watts to several megawatts of demands and installed across various geographic locations varying from deserts to water bodies and mountains to plains [5–7]. The solar PV power plants are operated with a performance ratio of about 80–90% with the photovoltaic conversion efficiency (PCE) of 15 to 20%. Thus, the system is economically viable, with returns on investment being typically a minimum of 3–5 years [8]. PV with electrical battery storage system also in practice for rural and remote areas where there is no national grid supply is not applicable [9–12]. As solar cells are the structural unit, it is important to understand the dynamics of the cell. The cell/device is a semi-conducting current generator that works on the photovoltaic effect; that is, it absorbs the photonic energy/photons from the solar radiation that results in a potential difference resulting in photocurrent to flow [13,14]. While the photocurrent is a function of the incident solar radiation, this radiation has side effects on the device, eventually affecting the power conversion efficiency [15]. The device is exposed to thermal radiation, which gradually heats the device/module temperature. This increase in module temperature (T_{PV}) mainly affects the voltage profile of the PV module [16].

Furthermore, the photocurrent generated is also reduced. Despite favorable bright daylight, this unwanted rise in T_{PV} is a persistent problem throughout the year for arid and semi-arid locations. Particularly during summers, the ambient temperature (T_{amb}) is often high, so the PV module's thermal dissipation is less, and it starts to increase the T_{PV}. The lower wind speed is attributed to natural convection releasing the thermal energy from the PV module yet is ineffective for high T_{amb} [17]. Although the PV module generates higher power (Wh) in summer [18–21], the performance ratio is less due to the abrupt rise in T_{PV} [19–21]. A study proved that an increase in T_{PV} from Standard Temperature Condition (STC) by 1 °C can cause the system's electrical output to drop by 0.3–0.4% [22,23]. This T_{PV} loss reduces the output power at a higher side than other losses such as soil loss [24], shading loss, inverter loss, and grid loss [25]. This increase in T_{PV} lowers the power generation and degrades the PV module lifetime and payback period. Thus, there is a need to address this open-ended research and identify appropriate technology to deal with it.

Diversified experimental studies are performed to reduce the T_{PV} and extract the maximum electrical output from the PV system. Pumping the fluids, with high specific heat capacity, over the module has initially opted for this purpose [26]. Water is one of the abundant and effective thermal absorbers with a specific heat storage capacity of 4.2 J/g.K, which is often applied as a heat sink in high temperature and desert regions [26,27]. In a study by Shenyi et al., an improvement of about 10% in electrical system efficiency is reported by employing a gas expansion-based rainwater pumping technique to be sprayed over the PV module surface [28]. Syringe-type nozzles are used to make a thin and continuous water layer over the front surface of the PV module to achieve uniform cooling with optimum groundwater utilization [29,30].

Besides spraying techniques, the PV module immersed 0–15 cm depth of the water with an interval of 5 cm to reduce the T_{PV}. All the immersed PV modules enhanced the electrical output power than the non-immersing PV module. The highest power production was achieved for 5 cm depth as solar radiation fails to penetrate the water beyond this depth [31–33]. However, the spraying mentioned above and immersing method consumes a huge amount of water or groundwater reserves. In some cases, thermal collectors are attached to the back surface of the PV module and use an external pump and thermosiphon technique to extract the heat from the PV module. Although this technique removes heat and is utilized for a low-temperature thermal application as photovoltaic-thermal (PVT) hybrid systems, it involves complexity in integration and maintenance [34]. Chandrasekar et al. attempted to minimize water consumption by experimenting with a cotton wick coiled in the spherical shape on the PV module back-surface with a water reservoir. The wicks aid the water to diffuse sufficiently, eliminating the use of an additional pumping system, thereby reducing the complex installation and economics of the system. Whenever the T_{PV} rises, wetted cotton wick extracts the thermal energy from the PV module and reduces T_{PV} by 30% [35]. However, most water-cooling technologies fail due to power consumption in operating the pumps for fluid circulation and the requirement of groundwater in case the fluid chosen is water.

Air, yet an abundant and well-explored coolant for PV modules, is one of the oldest and accustomed, due to which there are no restrictions in the usage of air to cool the PV module. Although natural airflow over and under the PV modules removes heat, particularly for cold regions, it is not significantly high to cool down the module to standard operating temperature. Hence, forced air circulation is widely adopted for cold climatic conditions [36,37]. For effective utilization of the resource, ambient air is pumped over to the back surface of the PV module by creating a cavity [37]. Again, this technique also requires additional power to blow the air. The technique is further improvised by sandwiching the PV module between the layers of glass to pass the air from both front and back surfaces of the PV module, and this technique achieved a greater reduction in T_{PV} [38,39]. Sophisticatedly, a fin-aligned thermal collector is installed on the back surface of the PV module to create resistance in the air, which could increase the heat extraction from the PV module [36]. The air's density and specific heat capacity are less than water [40], thus achieving the effective T_{PV} reduction, and the airflow duct should be in optimal range unless it is difficult to create the resistance in the air [41].

Besides water and air, heat sink-based T_{PV} reductions are optional for real-time operations at gusty locations [42]. Other techniques include immersing the PV module into the water or other liquids, thermoelectric generator incorporation to reduce the $T_{PV,}$ but these techniques are still under investigation and have not been demonstrated for practical applications [43,44]. Currently, phase change material (PCM)-based T_{PV} reduction techniques have gained considerable attention among research groups and have delivered promising results in real-time applications [45–47] as shown in Table 1. PCMs are often called heat batteries as it stores and discharges heat energy. In recent years, researchers are using the term heat batteries to attract readers and it directly promotes the usage of PCMs. Although PCM is an effective heat storage material, in real-time applications it is not as well known as electrochemical batteries. Initially, in the solid state, PCM stores thermal energy in the form of solid-specific heat capacity (J/g.K); following that, PCM reaches its melting temperature (T_{melt}) and then the material turns into a mushy state. Advantageously, mushy state stores thermal energy in the form of latent heat of fusion (J/g). This mushy state stores higher thermal energy without increasing its internal temperature, unlike specific heat capacity. Finally, in the liquid phase, the PCM utilizes its latent heat of fusion (L or Hm) completely and retains energy in a liquid-specific heat capacity J/g.K). Equation (1) is expressed below as three different forms of thermal energy storage in PCMs [48]. Generally, any specific heat material such as water stores thermal energy by raising its internal temperature (4 J/g.K). PCM also increases the internal temperature for a solid and liquid phase; moreover, its specific heat capacity is less than water (1.8–3 J/g.K) but H_m is high (130–300 J/g) which does not exist in sensible heat storage materials (water), although H_m makes PCM a unique heat storage material [49].

$$Q = \int_{T_i}^{T_m} mC_{p,s}\, dT + mL + \int_{T_m}^{T_e} mC_{p,l}\, dT \tag{1}$$

Table 2 shows various review studies conducted on the PV module cooling. From this literature study, it is clear that several researchers have focused on finding the novelty mostly in categorizing the cooling techniques, namely active cooling and passive cooling techniques. It is noted that, so far, no review study has discussed the PCM thermophysical property on cooling the PV module. Figure 1 shows the formation of this review study according to the proposed objective.

Table 1. Recent publications of PCM (heat battery)-based cooling methods.

Author	Year	Findings
Elavarasan et al. [50]	2020	OM29 organic PCM poured directly under the PV module without using any intermediate layer. A maximum 1.2 °C PV module temperature reduction is noticed.
Velmurugan et al. [49]	2020	Developed composite PCM integrated behind the PV module without using a physical contact to avoid the potential induced degradation (PID) loss. Different thickness of the PCM matrix is analyzed and validated experimentally. An increase in thickness of PCM enhanced the cooling but linearity was achieved at 2.5 cm thickness.
Poongavanam et al. [51]	2020	A novel eutectic PCM is developed for Chidambaram climatic conditions. Operational variation of PCM is analyzed for summer and winter. During high melting temperature of PCM enables higher cooling than a low melting temperature of PCM.
Velmurugan et al. [16]	2020	A novel cylindrical tube-based PCM matrix is developed for the hot climatic condition of Thailand. Developed cylindrical tube PCM container placed behind the PV module without physical contact to avoid the mechanical stress and PID loss. Cylindrical tube PCM container consumes less amount of PCM as compared to other techniques.
Savvakis et al. [52]	2020	RT27 and RT31 commercial PCM is examined for Chaina, Crete location. It is noted that RT31 reduced 7.5 °C which is 1.1 °C higher than RT27.
Velmurugan et al. [8]	2021	Eutectic cold PCM is developed for PV module cooling. A 3 cm and 5 cm thickness of cold PCM is examined resulting higher cooling effect achieved for 5 cm thickness.
He et al. [53]	2021	Stearic acid and Lauric acid are mixed to prepare the eutectic combination to cool the PV module. Developed eutectic PCM reduced the PV module temperature maximum of 20 °C.
Velmurugan et al. [54]	2021	Cascaded PCM structure is developed for tropical and subtropical climatic conditions. The PCM selection algorithm is developed based on the existing experimental results. India and France require to be cooled only in summer and Thailand require cascaded structure for both summer and winter.
Divyateja et al. [55]	2021	Simulation is conducted with RT25HC commercial PCM to cool the PV module, in addition, CuO is composited to enhance the thermal property of the PCM. Nano-enhanced PCM reduced maximum of 2.02 °C.

The main objective of this study is given below:

- Non-PCM-based cooling technique defects are reviewed.
- PCM based cooling techniques are majorly classified into pure PCM, composite PCM, and PCM thermal collectors.
- The benefits and drawbacks of PCM thickness studies are reviewed.
- Recent trends in PCM-based active cooling techniques are studied.
- PCM thermophysical properties are exclusively studied especially, PCM Tmelt necessity and economic viabilities.
- Merits and demerits of the PCM-assisted cooling techniques are explored.
- Research gaps and recommendations are identified for further development in PV module cooling.
- Typical meteorological year (TMY) data from National renewable energy laboratory (NREL) data source in 1 h frequency enables studying the sites' weather condition over a year. This would benefit in determining the PCM for varying environmental conditions.
- With the reference values associated with experimentally proven PV PCM temperature from "Hasan et al. [56] and Waqas et al. [57]" to assess the performance of a typical MW scale solar PV system.

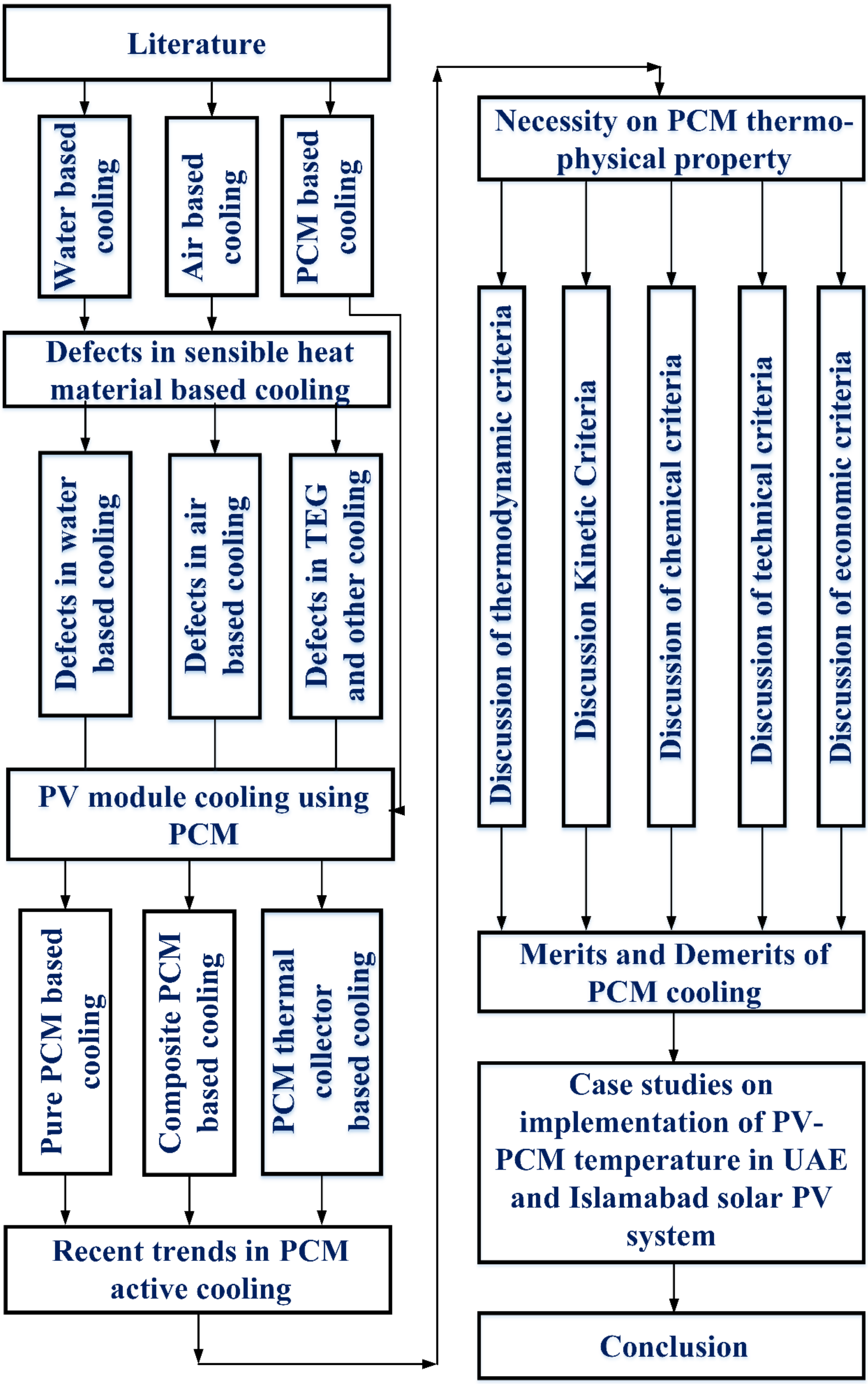

Figure 1. Flow chart of a complete overview of PV module cooling techniques.

Table 2. Recent review studies of PCM and non-PCM based PV module cooling techniques.

Author	Objective	Key Findings
Senthil et al. [58]	Different types of solar thermal heat pipes are reviewed.	• The optimal range of the heat pipe diameter is 8–12 mm. • Heat pipe inclination 50–70° achieves higher thermal efficiency. • Adding 2–3% of nanofluid enhanced the heat absorbing capability.
Velmurugan et al. [54]	• Types of PCMs used for PV module cooling are reviewed. • A simplified PCM selection procedure is proposed.	• Following paraffin wax, commercial Rubitherm PCMs gained second place in cooling the PV module. • Organic eutectic PCMs are achieving proper endothermic and exothermic peaks though not involved majorly. • The study finds that Thailand requires a cascade structure as compared to France.
Anand et al. [59]	• A comprehensive review is conducted for PV module cooling using water, air, thermoelectric generator, and PCM.	• The active cooling system enhances electrical output power generation, but it consumes more external sources to pump/circulate the fluids. • Thermoelectric generator found to be an efficient coolant medium with enhanced efficiency of 1–18%. • Using PCM and nanofluid enhanced the electrical efficiency by 8–10%.
Kumar et al. [60]	PCM and nano-PCM based cooling techniques are reviewed.	• PVT system is mainly developed by aluminum and copper. • Modified heat transfer channels such as thin absorber sheet, porous air flow duct/heat pipe, fin-based heat pipe enhanced the heat transfer rate. • Nano-PCM with nanofluid enhanced the cooling effect.
Browne et al. [61]	A comprehensive review was conducted on BIPV and concentrated PV cooling methods using PCM.	• This study found that the PCM technique enhanced the cooling effect than other sensible heat storage materials. • Water and air are efficient heat removing materials though it does not regulate the temperature of the PV module longer period.
Kandeal et al. [62]	Conductive, convective, and radiative cooling techniques are reviewed.	• Nano fluid-based PVT system efficiency reached up to 61.23%. • The air cooling technique improved the performance maximum of 26%. • The radiative cooling technique is one of the promising techniques, yet the emissive factor must be developed to achieve greater impact.
Ghadikolaei et al. [63]	A detailed review of water, jet impregnation, and PCM based cooling.	• Heat pipes with internal and external fin enhanced the power output. • Selecting inappropriate PCM melting temperature deteriorates the efficiency of the PV system. • Nano fluid with thermal collector maintained the T_{PV} under control for a longer duration.
Maleki et al. [64]	Active and passive cooling methods are reviewed.	• Passive cooling methods tend to be the simplest and most efficient technique in turns of non-additional power consumption. • Active cooling methods mainly rely on fluid channel constructions.

Table 2. *Cont.*

Author	Objective	Key Findings
Mahian et al. [65]	Building-integrated PCM-based PV module cooling techniques are reviewed.	• Few research was found in the field of economic aspects and optimization. • A cooling system that is incorporated with HVAC, low operating temperature application seems to be good in economic aspect. • It is found that concentrated PV systems are not majorly incorporated with PCM-based cooling systems.
Present study	• Current research trend in PCM based active cooling techniques is reviewed. • PCM thermophysical properties are discussed and their relationship in cooling the PV modules are addressed. • Study of resource data associated with Experimental results for a different geographical location.	• The current active cooling method shows that thermal collector designs are the major key point in PV power enhancement. • PCM thermophysical properties addressed especially T_{melt}, H_m, and K_{PCM}. • Collection of resource data to determine the PV PCM from NREL data source • Theoretically calculated Power from PV and PV-PCM temperature. Considering the default losses from explicitly modeled values from NREL(PV-watts).

2. Technical Barriers and Defects in Existing PV Module Cooling Techniques

2.1. Defects in Water-Based Cooling

Although water is a practical material in removing heat commercially and technically, it is complicated to cool the PV module at a large scale due to resource and maintenance difficulties. Resource management becomes crucial due to the degrading statistics of the groundwater level and absence of water in arid and semi-arid regions, which are favorable sites for the PV plants, owing to their alternative advantages.

2.1.1. Water Spraying Technique

Water spraying is suggested to minimize the water consumption, effective utilization is subjected to the spacing between the PV modules as they act as sites for leakage. Despite recovering three-quarters of sprayed water, filtering fine dust and dirt particles adds to difficulties in maintenance and resource cost of the PV plant [28].

2.1.2. Syringe-Type Water Spraying Technique

Although a syringe-type of water spraying technique is installed to optimize the water utilization, an external pump is essential to maintain the constant pressure and flow in the water channel for uniform water spreading, which adds complexity to the existing system. However, this system is great for areas where the water resource is enormous, as shown in Figure 2a,b.

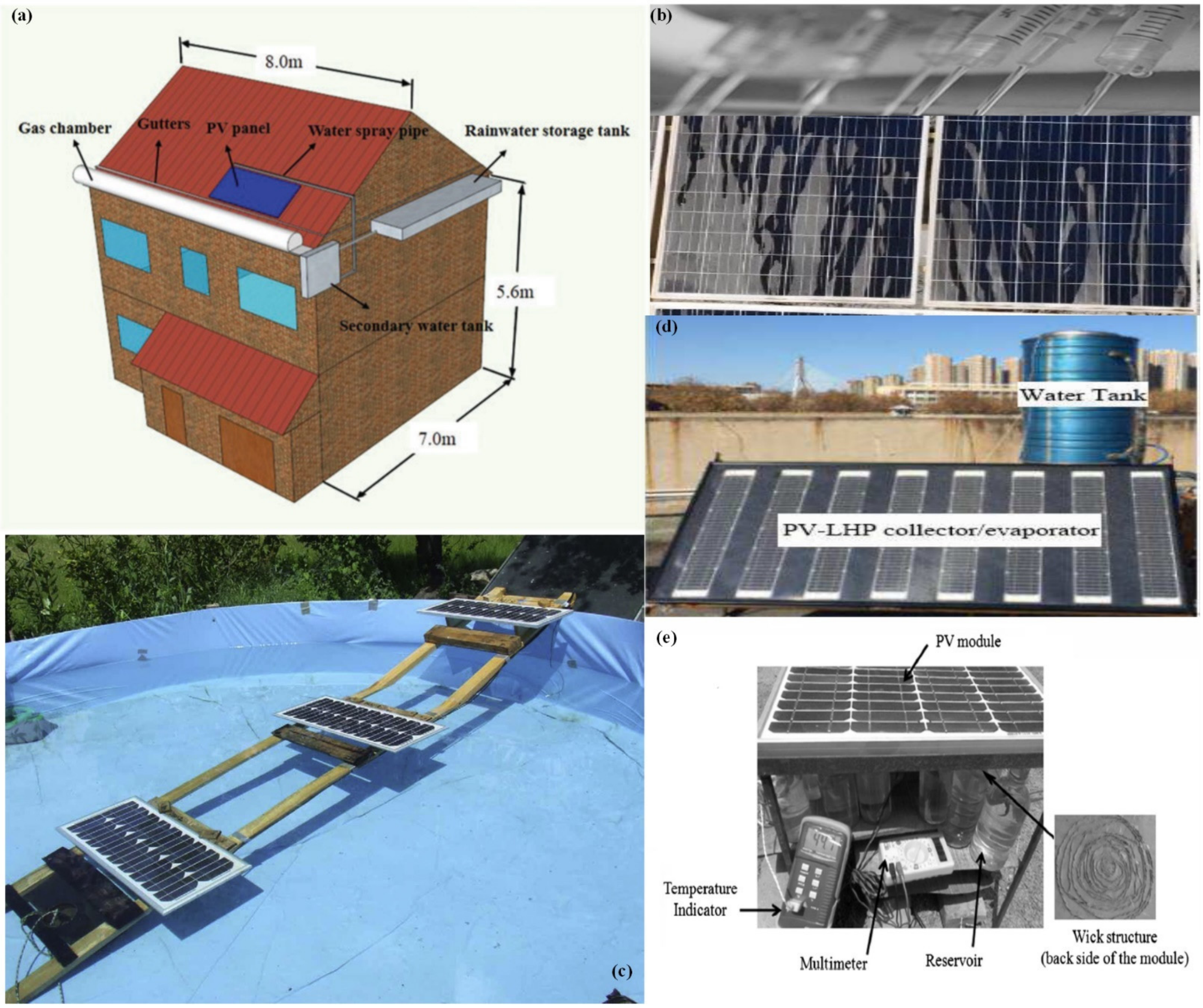

Figure 2. PV module cooling using (**a**) stored rainwater spraying technique [28]; (**b**) nozzle type water spraying [66]; (**c**) immersing at different depth of water [32]; (**d**) heat pipe [67]; (**e**) wetted cotton wick [35].

2.1.3. Cotton Wick Cooling Technology

Besides high-end technology in cooling the PV module, cotton wick with bottled water reservoir also reduces the temperature of the PV module. Perhaps the investment cost of the cotton wick and bottled water is not as expensive as water spraying and PVT techniques as shown in Figure 2e. However, the heat transfer rate as well as the reduction in the rate of T_{PV} is so low that it was correspondingly found to be worth the investment for small and mid-sized power plants.

2.1.4. Immersing Cooling Technique

Other than any of the above-mentioned techniques, immersing the PV module inside the water bodies could restrain the PV module's temperature in higher order especially, by immersing the PV module in clean rivers rather than a lake or polluted river as shown in Figure 2c. The polluted river or lake could contaminate the glass surface of the module by producing unwanted layer formation that possibly reduces the solar radiation penetration for energy conversion. On the other hand, cleaning the PV module is difficult and useless, as contamination can coat the surface in a short period.

2.1.5. Heat Pipe Cooling Technique

Based on the continuous drop in electrical efficiency and increase in thermal load, waste temperature from the PV module could be captured and reused for low and mid-temperature applications. Thermal heat-removing sheets and tubes are placed on the Tedlar surface, whereas the PV module acts as a semiconductor device and flat plate thermal collector. Based on the electrical and thermal load demand, water flow arrangements are made in the flat plate thermal collector, as shown in Figure 2d. The major drawback in accompanying thermal collectors with PV modules is that it greatly increases the weight of the system. Therefore, safety and security become a questionable argument due to the constant pressure in the thermal collector and water storage tank which could cause an explosion. On the other hand, a photovoltaic thermal hybrid system creates noise and vibration during the water flow in the channels or tubes.

Non-uniform cooling occurs in PVT systems though it is widely adopted in cold regions under hybrid electrical and thermal energy generator models. This PVT system is not suitable for large-scale systems as the temperature from the PV module is not sufficiently high to run a turbine to generate electricity. It would increase the total investment with a long payback period. Overall, it is considered that water-based PV module cooling techniques are feasible under certain criteria, and it is permissible to deploy them in the common platform as a solution.

2.2. Defects in Air-Based Cooling

Likely, the air is an effective medium to cool the PV module than water because air is abundant in nature and can be applied as a coolant for any environmental conditions. However, air-based cooling techniques are not reported for large-scale systems, as it requires modifying the front or back surface of every PV module to facilitate heat extraction, which is practically impossible. Once the front or back surface of the PV module is modified, an external pump is necessary to assist in any climatic conditions as natural thermal dissipation is restricted in air-based techniques, as shown in Figure 3a. For commercial-grade implementation at a larger scale, air-assisted cooling methods are not appropriate. Especially in hot and humid climatic conditions, water can be sprayed over the PV module during the peak daytime hours to reduce thermal stress. The rest of the period can be set for natural dissipation without any effort. However, this condition is not applicable for air-based cooling techniques, since the front or back surface of the PV module becomes entirely suppressed by interacting with the ambient environment or surroundings. If the external air pump fails, T_{PV} could increase exponentially than the unmodified PV module. These constraints depict that air is technically not recommended for large-scale systems; however, it can be widely used for a small and mid-sized PV system to warm the building or room temperature in cold climatic conditions. Reportedly, a PV module without an air pump can be adopted for hybrid application, although it is a demerit for PV module cooling because natural convection is capable to remove the heat from the PV module, but not for the entire duration of daytime hours.

2.2.1. Forced Air Flow Technique

In recent years, several researchers have recommended the forced convection method to enhance the electrical and thermal efficiency of the PV system where a fin-aligned thermal collector with forced convection doubles the benefit of cooling the PV module by creating the resistance in air flow which increases the heat absorption capability of the air as shown in Figure 3c. Notably, pressurized air in the thermal collector increases air leakage, which requires additional care in insulating the thermal collector. Glass wool or other high fire point insulation material is required to minimize the fire accident as short circuits in electrical connections are more vulnerable.

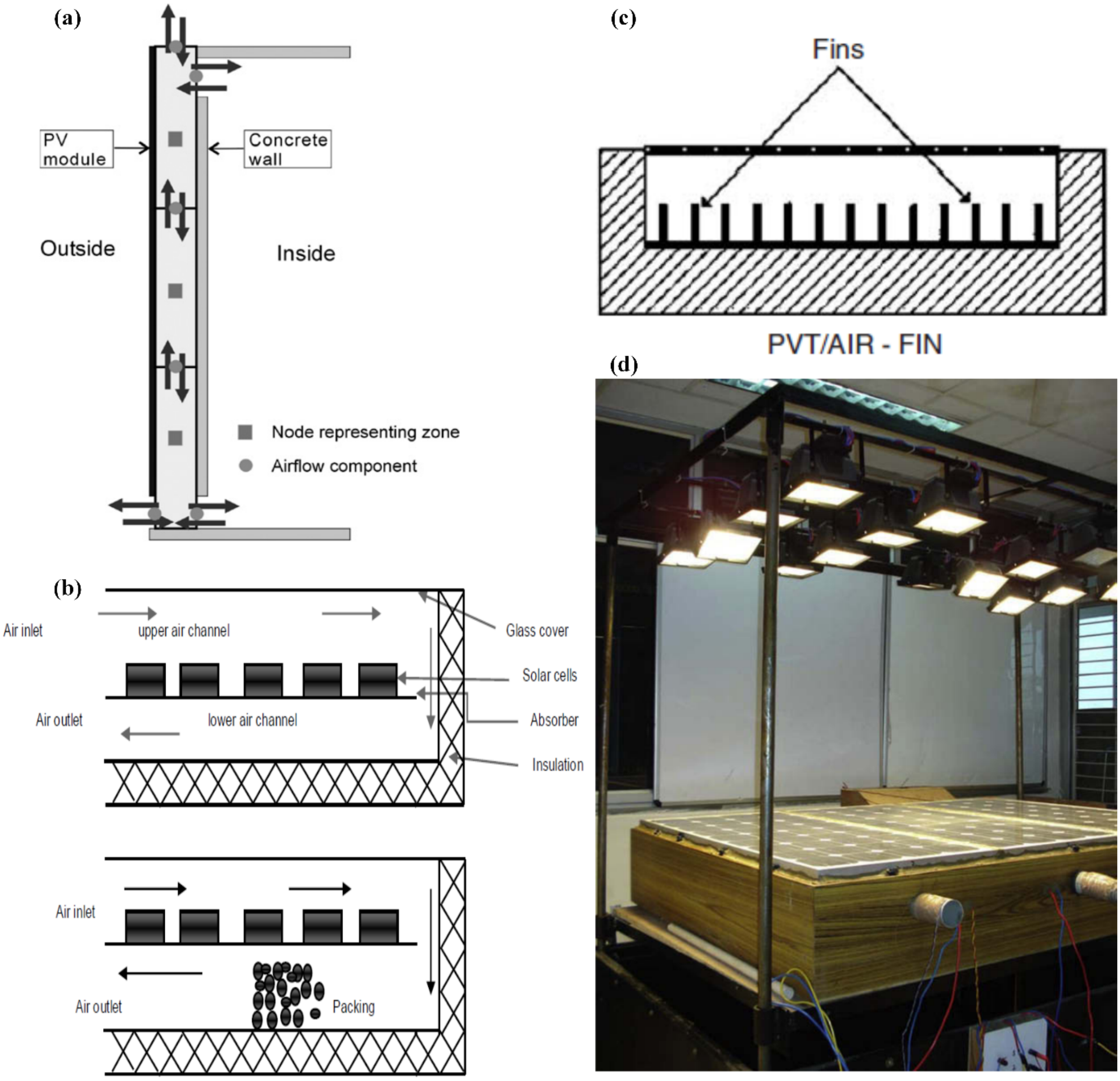

Figure 3. Overview of PV module cooling using (**a**) single passing air [37]; (**b**) double passing air [38]; (**c**) aligned internal fins [36]; (**d**) variable duct depth air [41].

2.2.2. Double Side Air Passing Technique

As mentioned earlier, the double side air passing method cools the PV module effectively and acts as a double cooling agent on both the front and back surface of the PV module as shown in Figure 3b. This modified front surface of the PV module lacks an antireflection coating that affects the absorption of solar radiation. Overall, the air-based technique is advised for small and mid-sized power plants this technique is subjected to several operational issues for scaled-up applications.

2.3. Defects in TEG and Others

TEG is a well-known energy converter and is mainly used in high-temperature applications such as thermal plants, industrial furnaces, heat engines, and others to convert waste heat into useful electrical energy. TEG requires a higher temperature difference between the hot and cold sides, whereas the charge carriers are excited on the hot side and move towards the cold side, generating voltage. In this case, T_{PV} is the TEG source applied on the hot side while the cold side faces the ground in an open environment. Converting T_{PV} into useful electrical energy boosts the system's electrical output technically, but economically, TEG failed to meet the return on investment. TEG is economically favorable when the temperature difference between the hot and cold sides is high. Mostly, T_{PV} lies around 50–70 °C during peak daytime hours and approximately 30 °C of the temperature difference between T_{PV} and ambient can be noticed. TEG will not make the effective electrical conversion that makes TEG not economically favorable with this temperature difference. Other than TEG, placing the heatsink behind the PV module could enhance the heat transfer. It requires a proper mounting structure unless the Tedlar surface of the PV module can break easily because of its brittleness and fragile nature conditions.

2.4. Drawbacks of Non-PCM Technique

The major drawback in non-PCM-based cooling technology is non-uniformity in PV module surface cooling. The higher temperature difference between the sensible heat material and PV module enables a higher heat transfer rate; water and air absorb a high amount of heat energy when it enters into the header or footer section of the PV module. During the motion of the fluid from header to footer or footer to the header, the fluid gains a higher temperature and fails to absorb the same heat energy resulting in non-uniformity in cooling to occur. The same situation occurs for other sensible heat storage materials. That is why PCM has gained significant attention in cooling the PV module because PCM is a stationary unit and removes the heat uniformly during the entire period of operation.

3. Outline of PV Module Cooling Using PCM

In the recent decade, researchers have been using PCM as coolant material to enhance the electrical efficiency of the PV module [54,68]. This passive cooling technique does not require a flowing medium, or external energy needed to circulate the coolants, thus making PV-PCM systems/technology more economical with low maintenance costs compared to conventional PV-thermal systems. The compactness of the auxiliary design and reliability is yet another reason for the massive adaption of this cooling system. PCM has a high energy density and stores thermal energy with a negligible temperature rise. This makes the material and the technology robust and safe-fail; thus, even to be used in complex projects such as the Pioneer-Venus spacecraft in 1979 [69]. Later, in the late 1990s, Hausler et al. demonstrated the simplest PV-PCM system to boost the PV module performance by improving the thermal conductivity of the PCM [70]. One of many ways to improve the thermal conductivity is by simply fitting a metal container filled with PCM to the PV module Tedlar surface [71].

Effective recovery and utilization of thermal energy dissipating through a rise in temperature of the PV modules are of higher importance, particularly in renewable energy systems for the generation of power. PV-PCMs can be regarded as the best existing solution for designing future hybrid systems for better energy conservation and utilization [8,9]. Despite these facts that the technology is familiar and offers unmatchable benefits, low thermal conductivity, low heat storage density, leakage, and high material costs are the main areas of concern that need further investigation. Thus, on the whole, understanding the properties and types of PCM and identifying the appropriate PCM for the application plays a crucial role in developing a matured PV-PCM system. Classification of PCM cooling systems based on PCM type is shown in Figure 4 and their respective material properties are discussed broadly in the forthcoming sections.

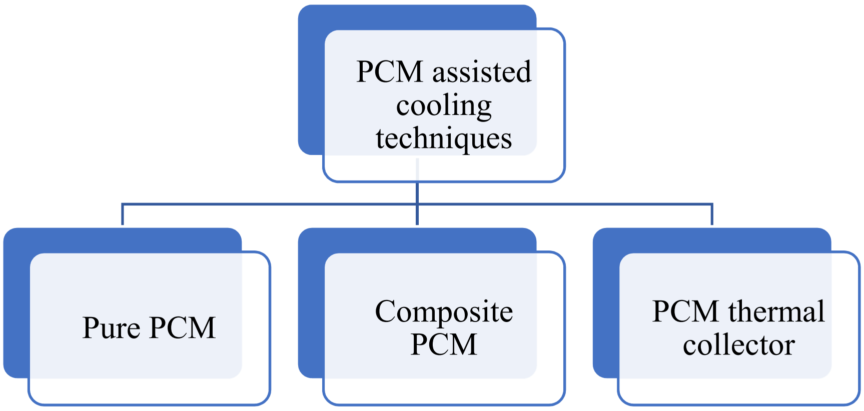

Figure 4. Operational types of PCM in the PV module cooling.

3.1. Overview of Pure PCM-Based PV Module Cooling

Primarily, there are several types of PCM available in the market and each one of them is unique in its way in terms of major benefits and storing and discharging heat with minor defects. Commercially available pure PCMs becomes an alternative organic PCM type that stand tops in terms of the simple material design and usage, likely most of them are paraffin wax, fatty acids, or oils. While most of the PCM integrated systems need to be tailored to the requirement, pure PCM, which means the raw PCM, does not require any further processing and can be integrated behind the PV module as such. Secondly, considering the change in phase of the PCM it can be filled in the container to avoid leakage, which makes the system robust. Generally, organic PCMs are identified as non-corrosive and have ease of maintenance compared to their inorganic types of counterparts.

3.1.1. PV-PCM Construction

Figure 5 shows the overview of PV-PCM operational conditions using a different construction technique. Yuli et al. showed that PCM integration is more effective for ground mounting than the rooftop PV system. The reason is that the PCM container's back surface does not get exposed to the ambient or surrounding, which results in thermal stress occurrence around the PCM container, leading to restriction in dissipating its heat. Therefore, it is necessary to consider the thermal dissipation factor of the PCM container as one of the key parameters to enhance the electrical efficiency of the PV module [72]. Notably, building integrated photovoltaic (BIPV) with PCM integration also failed to reduce the T_{PV} due to resistance in thermal dissipation and a lack of wind interaction [73]. As mentioned earlier, PCMs are filled in a container to avoid leakages during the phase change and most of the time PCMs are packed in a metal container to maintain perfect physical contact with the PV module. Nikolaos Savvakis et al. developed a three-segment PCM container constructed using galvanized steel to increase the mechanical strength as well as physical contact closeness ratio with the PV module. In this study, RT27 commercial organic PCMs were filled in the segmented PCM container and integrated on the Tedlar surface. With the help of perfect physical contact, a segmented PCM container enabled higher heat transfer, resulting in the reduction in T_{PV} to the maximum of 20 °C for 150 min compared to PV without PCM [74]. Several researchers used thermal conducting adhesive material between the PV module and PCM container to attain 100% physical contact since there is a different property for every adhesive material used, thus limiting the heat transfer. Considering this issue, liquid PCMs are directly filled on the PV module Tedlar surface and sealed on the backside of the PCM using a glass/metal sheet [75,76]. The direct filling PCM technique transfers the PV module heat to PCM without any intermediate adhesive material resulting in the achievement of a higher heat transfer rate. This method attained a PV module temperature reduction of a maximum of 10–12 °C under Malaysian climatic conditions [77,78]. Even though this technique limits the thermal barriers, PCM leakage becomes the biggest issue and thus is not an affordable one for solar power plants.

3.1.2. PV-PCM Operational Difficulties

Other than the construction and placement of the PCM container in the given system, several researchers focused on the thermal properties of the PCM such as T_{melt}, H_m, and congruent in the material. In most cases, organic PCMs are examined for cooling the PV module as they are congruent in material with high H_m. Selecting PCM T_{melt} is one of the major parameters in cooling the PV module as PCM is a temperature-dependent material and sensitive to climatic conditions [79]. To illustrate this, Indartono et al. [80] studied two different T_{melt} PCM materials on Indonesian climatic conditions. The first one was made up of coconut oil as this sort of PCM failed to reduce the T_{PV} effectively due to higher T_{amb}, while on the other hand PCM made up of crude oil reduced the T_{PV} to a better extent rather than that of coconut oil. It was noted that the PCM material with low T_{melt} turns to liquid before the peak sunshine which results in restriction in the transfer of heat between the PV module and PCM. Following Indartono et al., the study by Eqwan M. R et al. [81] revealed that examining with inappropriate PCM adversely affects the heat removal from the PV module, even to the extent that under certain conditions, it rather increases the T_{PV} than the conventional PV module. The main reason behind this negative impact is due to H_m not being appropriately utilized [79,82]. Precisely, to optimize the PCM T_{melt}, Waqas et al. [83] conducted a numerical simulation using a different melting range of PCM (30 °C, 35 °C, 40 °C, and 44 °C) for hot climatic conditions in Pakistan. It was noted that 44 °C of PCM T_{melt} cools the PV module effectively with a higher T_{PV} reduction of 28 °C. From this study, it was concluded that to select the appropriate PCM, summer T_{amb} must be averaged and from that 10 °C (average T_{amb} + 10 °C = PCM T_{melt}) must be added to optimize the PCM T_{melt}. Following the PCM T_{melt} selection, optimizing the PCM thickness for a balanced cooling effect is necessary. It is well known that an increase in thickness of PCM directly increases the PCM's total energy storage capacity (Table 3), resulting in H_m, sustained for a longer period, and heat energy from the PV module is effectively transferred to the PCM [84]. Waqas et al. revealed that by increasing the PCM thickness beyond 2 cm, the linear cooling effect is disturbed, suggesting it is the optimum thickness for the reported climatic conditions [83]. Sourav Khanna et al. [85] examined the necessity of increasing the thickness of PCM under variable wind azimuth angles and wind speed for the existing experimental work of M. J. Huang [86] and Pascal Henry Biwole [87]. Moreover, Sourav Khanna showed the necessity of PV module inclination (0–90°) to find the effective heat transfer for an existing experimental work by Taieb Nehari [76]. The increase in inclination of PV-PCM reduced the T_{PV} in higher order for up to 45° and beyond that, a reduction in T_{PV} was not as effective due to a restriction in the liquid PCM circulation inside the container. This restriction in liquid PCM circulation creates a convection barrier and is forced to conduct the heat by conduction mode [88].

It is well known that the thermal conductivity of PCM (K_{PCM}) lies from 0.2–2.0 W/m.K which is lower than most of the sensible heat storage material. Reportedly, several researchers found that a low K_{PCM} may increase the thermal resistance that directly affects the cooling effect. As mentioned earlier, the direct filling method minimizes the heat transfer loss to a certain extent; however, it is not practically applicable. The only way to reduce the heat transfer loss during the peak daytime period is through increased PCM thermal conductivity. Through such measures, the contact loss with PV and PCM containers can be negotiable. It can be achieved by imparting a thermal distribution fin or modifying the material by blending with expandable graphite (EG) or metal scrap. However, copper powder and metal foams with PCM play a major role in reducing the overall thermal resistance and a detailed discussion is provided in the following subsection.

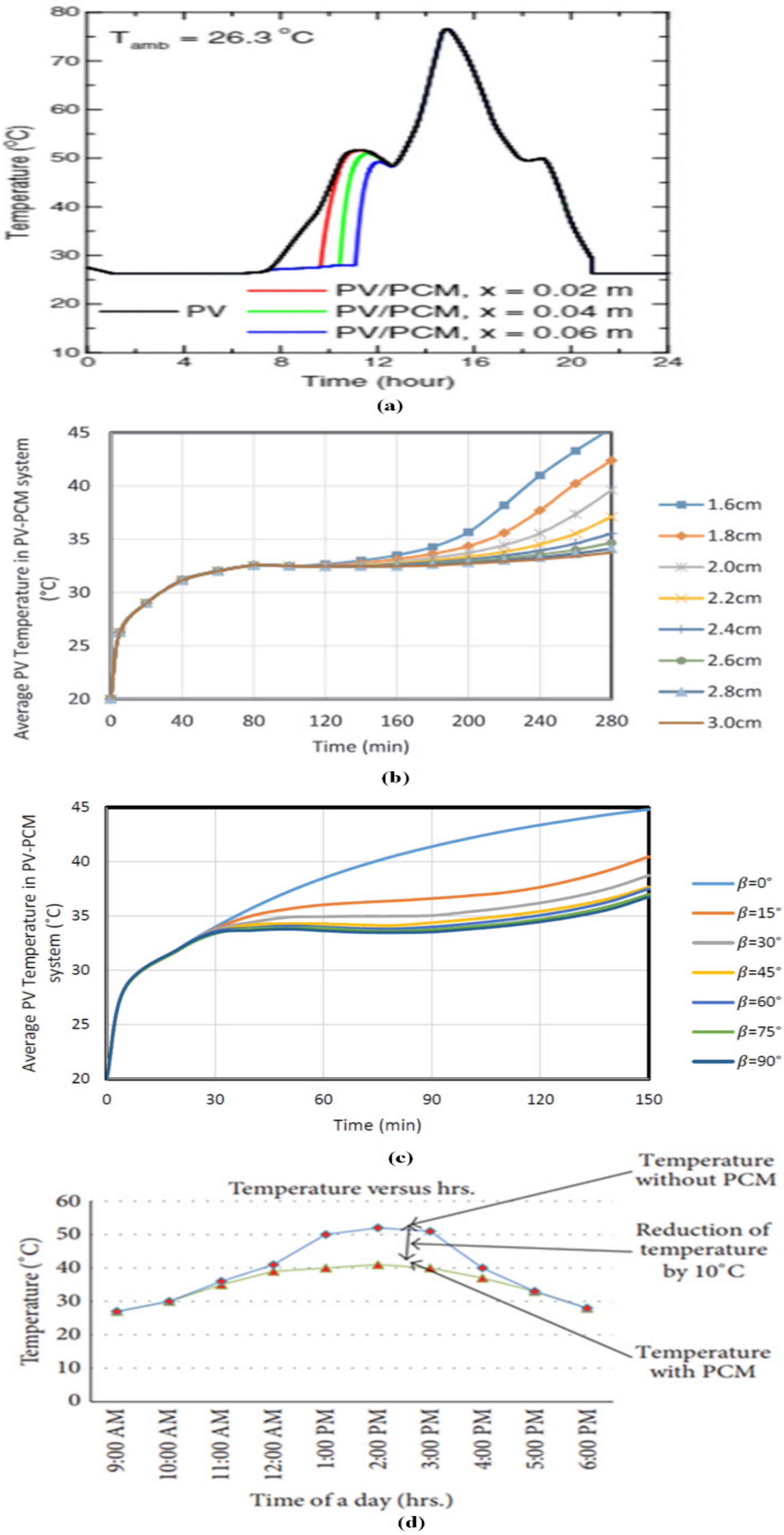

Figure 5. Overview of PV module cooling using (**a**) different thickness of PCM under real time condition [84]; (**b**) different thickness of PCM under indoor condition [85]; (**c**) different tilted PCM container [85]; (**d**) PCM direct filling technique [77].

Table 3. Importance of PCM thicknesses in cooling the PV module.

Authors	PCM Thickness	PCM Name	Major Findings
Ahmad et al. [89]	20 mm, 40 mm, 70 mm, 90 mm, 110 mm	RT42, RT31, RT25	• An increase in PCM depth/thickness enhanced the thermal regulation. • A 20 mm thickness of organic PCM regulated the T_{PV} for 3 h afterward started to rise and reach the unmodified T_{PV}.
Gan and Xiang [90]	20 mm, 30 mm, 50 mm	Plus ice S25	• PV module surface temperature started to increase at 120 min of the experimentation for 20 mm PCM depth. • An increase in the quantity of PCM (30 mm) greatly removes the heat resulting in 30 mm regulated the T_{PV} for 190 min.
Darkwa et al. [91]	2.5 mm, 5 mm, 10 mm, and 20 mm	n-Octadecane	• A 2.5 mm PCM thickness has a lower reduction in T_{PV} as compared to other thicknesses. • An increase in PCM thickness enhances the system performance at the same time when the PCM completely turns to liquid, it creates a conduction barrier.
Liu et al. [92]	20 mm, 30 mm, and 40 mm	$CaCl_2.6H_2O$	• A 20 mm thickness of PCM output energy is 6695 kWh and for 50 mm output energy (PVT) is 9632.5 kWh. • Linearity in PV output power generation is less for 40 mm thickness as compared to 20 mm.
Siyabi et al. [93]	30 mm and 60 mm	RT46, RT49, RT52, RT55, RT58	• Minor differences are noted for 30 mm and 60 mm using 1 Wp. • The same thicknesses with 1.5 Wp panel show vast T_{PV} variation; however, 60 mm maintained the lower T_{PV} for a longer time.

3.2. Overview of Composite PCM Based PV Module Cooling

3.2.1. PV-PCM Interfin

In early 2000, M. J Huang et al. introduced the composite PCM for PV module cooling [86]. In the beginning, the thermal distribution fin was considered a thermal enhancer that was submerged/projected into the liquid PCM from the top surface to the bottom surface of the container. The physical dimension of the thermal distribution looks like a heat sink with a series of thin metal plates (equal thickness) arranged in parallel with equal spacing between them. M J Huang cross-examined different morphologies patterns of thermal fins to optimize the spacing between them. He found that a decrease in spacing between each fin (4 mm) adequately gained higher composition with PCM and enhances the heat transfer rate. Unfortunately, it eventually affects the cooling effect due to a decrease in the overall PCM quantity. Notably, 20 mm spacing of each fin gained a high amount of PCM, but the heat transfer rate was ineffective due to less volume occupancy of thermal fins (high thermal conduction stress). This study showed that 8 mm and 12 mm spacing thermal fins minimized the conduction barrier without deteriorating the PCM performance compared to 4 mm and 20 mm [86]. Further, Nehari et al. [94] performed a 2D numerical model for the experimental setup of M. J. Huang [86] with a modified inter-fin length (0–40 mm with an increment of 5 mm). This study revealed that PCM with no fin is ineffective while 5–20 mm inter-fin performed moderately. An increase in the length of the fin improved the heat transfer rate but under this condition, a 25–35 mm fin length reduced PCM thermal stress; however, 40 mm becomes ineffective. This is because a 40 mm fin length interconnects the PCM container chamber that restricts the PCM internal convection as shown in Figure 6. Later, the same author performed a simulation for different inclinations (0–90°) for finned PCM containers. For the inclination, which is less than 45°, natural convection dominates inside the PCM and helps to melt the PCM layer by layer as shown in Figure 7. Beyond 45°, pure conduction occurred during the entire simulation period and reduced the T_{PV} reduction as compared to an inclination of less than 45° [95]. It is noted that M. J. Huang's experimental designs have been widely re-examined for further studies to develop an effective cooling system.

Pascal et al. solved a Navier stroke equation using a 2D finite element model for the same system geometry of M. J. Huang. Still, in this case, different thicknesses of PCM are filled in the plexiglass-based container rather than a metal container. As a result, the temperature of the front surface of the T_{PV} was maintained below 50 °C for more than 89 min under the constant insolation of 1000 W/m^2. A further increase in the thickness of the PCM container leads to a reduction in the T_{PV} value to the maximum of 39 °C for one hour, and for PV without PCM in a couple of minutes, T_{PV} was raised higher than PV with PCM [96]. Following other researchers, Pascal Henry Biwole et al. [87], Khanna et al. [97], and other researchers also reexamined the M. J. Huang system design to achieve effective heat transfer between PV and PCM to enhance the electrical efficiency of the PV module.

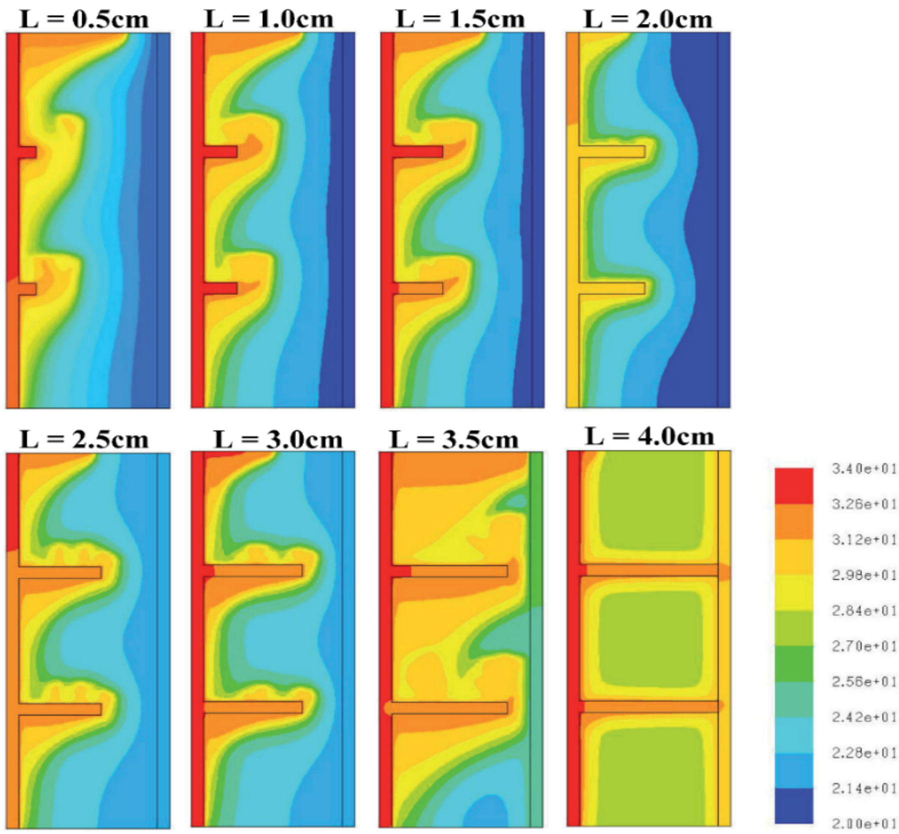

Figure 6. PV module temperature and thermal distribution in PCM using different lengths of interfin [94].

3.2.2. PV-PCM Metal Scrap

Other than fins (as for thermal conductivity enhancer), Subarna Maiti et al. [98] used a metal scrap as composting material to improve the heat transfer; advantageously, since metal scrap is a low-cost material, it is easy to incorporate with PCM and is as effective as thermal distribution through the inter-fin design as shown in Figure 8a. This study takes 5.5 kg of paraffin wax as PCM by solving the energy balance equation. The performed indoor experimental result showed that 23 °C of average T_{PV} reduction is monitored for a maximum of 3 h. After a continuous 3 h of experimentation, PCM completely turns to liquid resulting in an increase in the value of T_{PV}, 62 °C, which is lower than the value compared to the T_{PV} value of PV without PCM.

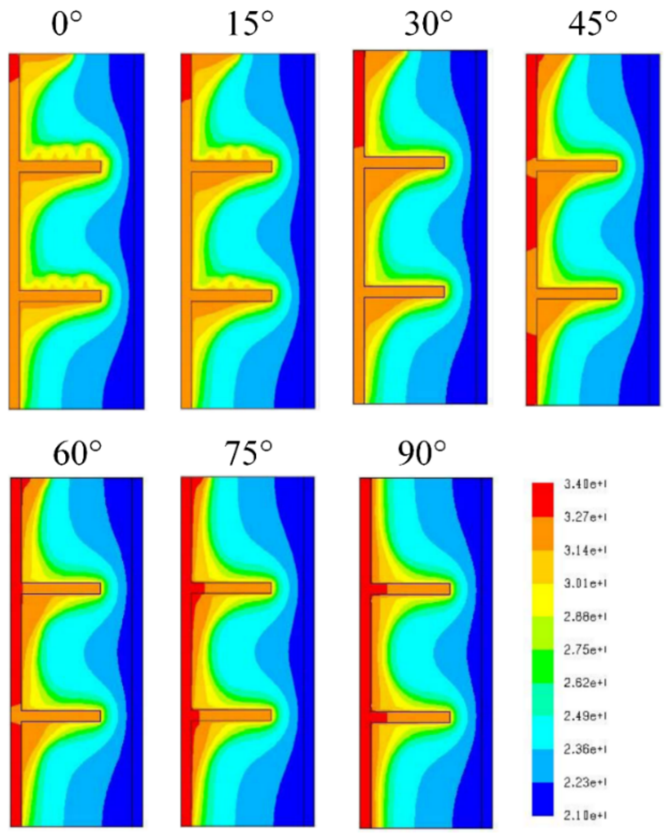

Figure 7. PV module temperature and thermal distribution in PCM using different inclinations [95].

3.2.3. PV-PCM Nano-Compounds

Thermal distribution fin and metal scraps are a well-known thermal conductivity enhancer; however, less volume occupancy and improper mixture with PCM encouraged [99] to blend the copper and graphite powders with PCM resulting in a composite PCM. The results showed that the composite PCM reduced 5.6 °C and 2.9 °C of T_{PV} compared to PV without PCM and pure PCM, respectively.

3.2.4. PV-PCM Graphite

Following nanomaterial, Karthikeyan et al. found that expandable graphite (EG) as a thermal enhancer has advantages such as being readily available on the market, low cost, lightweight, and low density. At first, EG is heated by an electric furnace for a 1 min duration of 800 °C to expand its physical dimension with a volume of about 200–300 times and higher porosity as shown in Figure 8b. Compositing high pores of expanded graphite with PCM creates improper mixing texture in the mixture. Therefore, to attain the perfect blend, expanded graphite is compressed where the unwanted pores are sealed, and the bulk volume density of the expanded graphite is reduced. After compression, expanded graphite porous foam is impregnated in the liquid PCM for absorption [49]. EG is an effective thermal conductivity enhancer in terms of proper texture composition, ease of handling, and EG will not settle on the bottom surface like other nano compounds and powder materials.

3.2.5. PV-PCM Metal Foam

Following EG, metal foam is a better option to enhance the K_{PCM} than other thermal enhancers [100]. Abdulmunen R. Abdulmunen et al. [101] showed that impregnating Al foam with paraffin cools the PV module to 39.58 °C; although it is not practically viable for mid/large scale systems. However, metal foam is expensive, heavy weight (Figure 8c), not readily available in the local market, and requires additional care on the mounting structure.

Overall, it is concluded that composite PCM enhances the electrical power and efficiency; although it increased the total weight of the PCM container. Integrating a heavy PCM container with a PV module could damage the physical structure of the PV module. However, adding PCM to the PV module for cooling purposes is an external investment cost. Therefore, to rectify the temperature loss, investing more into thermal conductivity enhancers weakens the system performance economically.

Further, it is necessary to consider the waste heat to useful energy by incorporating the thermal collector with PCM. This hybrid technique will minimize the conventional low thermal application such as hot water for bathing, cooking, cleaning vegetables and vessels, hot air for room heating, and other thermal applications.

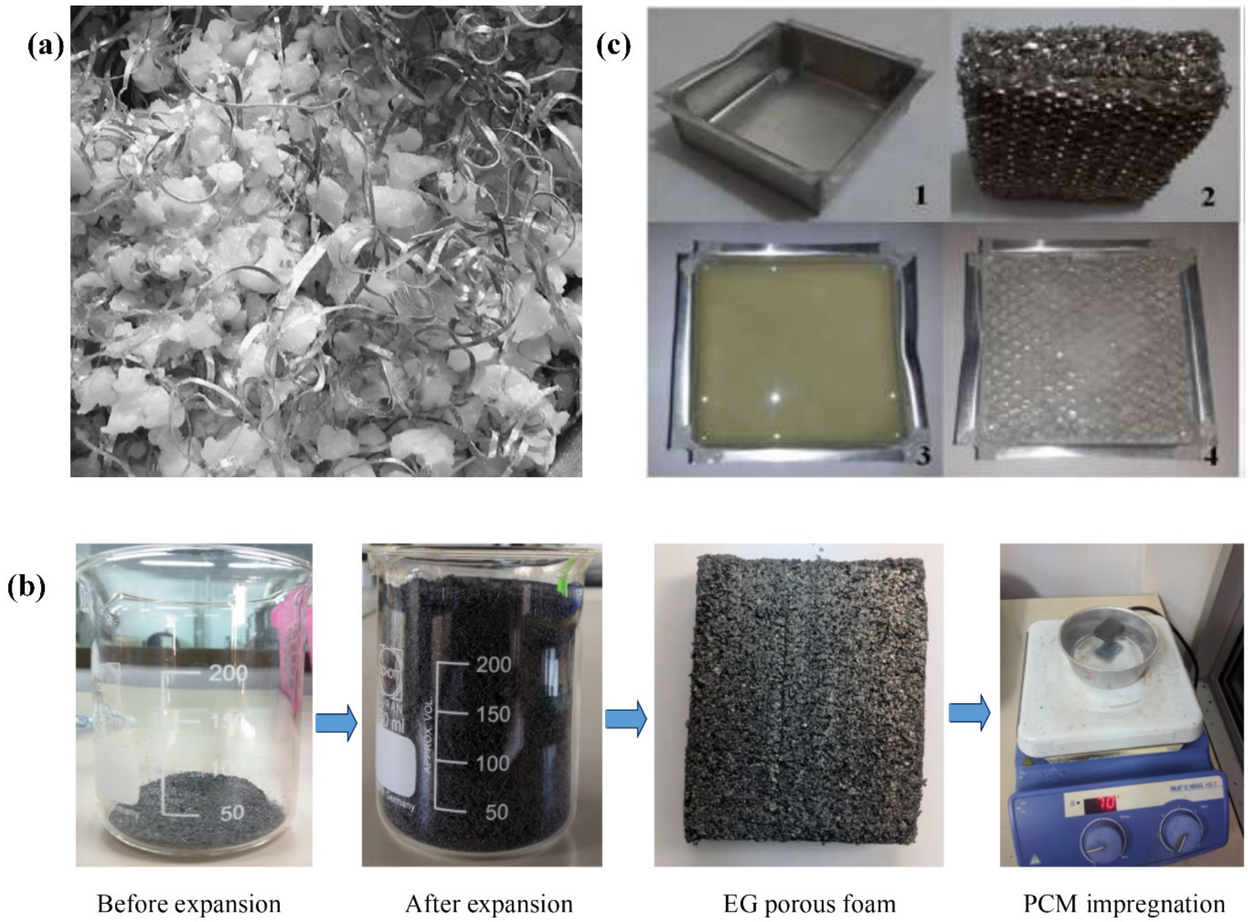

Figure 8. Overview of PCM thermal conductivity enhancer using (**a**) metal scrap [98]; (**b**) expandable graphite foam; (**c**) metal foam [101].

3.3. Overview of PCM-Thermal Collector Based PV Module Cooling

The above two subsections explained the PCM influence on cooling the PV module only to increase the electrical efficiency. It is noted that under certain conditions, heat energy from the PCM can be utilized for low-temperature applications such as warm water for cooking, cleaning vegetables and fruits, cloth washing, and indoor space warming [102].

Converting waste energy into useful heat energy will reduce the conventional thermal energy load, which directly minimizes the traditional building load. Moreover, adopting this hybrid technology could minimize the total amount of the PCM that is usually used for PV module cooling. This hybrid technique removes the heat from PCM, whereas the heat transfer rate between PV and PCM is increased in daytime hours and for next-day operations, PCM continues without any interruption or reduction in performance.

3.3.1. PVT-PCM-Air

Hagar Elarga et al. [103] performed a numerical simulation for three different locations namely Venice, Helsinki, and Abu Dhabi using RT42 (Venice/Helsinki) and RT55 organic PCMs (Abu Dhabi). The PV module and PCM together were placed in between the glass called cavity construction or double skin façades, as shown in Figure 9a. During the daytime, outdoor air is pumped into the double-skin façades to flow on both the PV module front and back surface of the PCM to remove the heat. The PV module without PCM using cavity construction increases the indoor air temperature by a rise in T_{PV}. Interestingly, the PCM-assisted system stabilized the indoor air temperature and is well suited for human comfort that minimizes the conventional building heating load. Air is abundant in nature, although the specific heat capacity of air is lower than water, making air an inefficient material compared to water. However, air is widely used to cool the PV module where the building heating load is required.

3.3.2. PVT-PCM-Water

Secondly, water-assisted thermal collectors with PCMs are widely used as they have a more efficient storage facility and direct usage for several thermal applications than air. Ankita Gaur et al. [104] developed a PCM-assisted thermal collector using selective coated rectangular copper water channels along with a wetted absorber plate and PCM container. Thermal energy from the PV module is transferred to the water channel and then the wetted absorber plate and PCM receive the heat. A 50 mm thickness of glass wool is placed on the bottom surface of the PCM to act as an insulator to prevent heat loss, as shown in Figure 9b. During the daytime, water is heated by both the PV module and PCM, and at nighttime PCM alone assists in heating the water; whenever hot water is required, a 24 W DC pump assists in flowing the water in a rectangular channel. This system design effectively enhances the electrical efficiency; the maximum T_{PV} reduced for summer and winter is 15 °C and 5 °C, respectively.

3.3.3. PVT-PCM-Nanofluid

Ali H Al-Walei et al. [105] used high conductivity nanofluid to flow inside a copper tube to enhance the heat transfer and was found to be the best replacement for water. A computational fluid dynamic (CFD) simulation was performed to optimize the flow rate and diameter of the tube. The simulation result showed that an increase in tube diameter and flow rate enhances the heat transfer [106]; however, a flow rate higher than 0.175 kg/s produced mechanical vibration and noise that likely could damage the system.

Following Ali, Mohammad Sardarabadi et al. [107] used deionized water and ZnO/water nanofluid to flow in a copper tube thermal collector to remove the heat from PCM. In this study, 2 kg of paraffin wax was used to remove heat from the PV module and enhance the electrical and thermal efficiency, as shown in Figure 9c. It is noted that deionized water and ZnO without PCM reduced the T_{PV} maximum of 10 °C and 11 °C, respectively, whereas the same system with PCM reduced the T_{PV} maximum of 17 °C.

Overall, it is noted that adding nanofluid into the PCM and working fluid greatly enhanced the heat transfer rate that favors increasing both the system's electrical and thermal efficiency. Technically, nanofluid is a great innovation for cooling the PV module but it is not economically feasible. The amount of electrical energy that has been demolished by the excess rise in T_{PV} will be cheaper than the incorporation budget of nanofluid. As mentioned earlier, nanofluid is an effective material but is not suitable for cooling the PV module considering the economic aspect; the whole point in cooling the PV module is to increase the revenue of the solar power plant. However, nanofluid can be used for the PV module cooling process when the cost of the nanofluid becomes cheaper. Based on the literature review, most of the research is conducted in cooling the PV module rather than considering whether it is economically feasible for a large-scale system. Further, researchers recommend that low-cost and easily available nanofluid can cool the PV module.

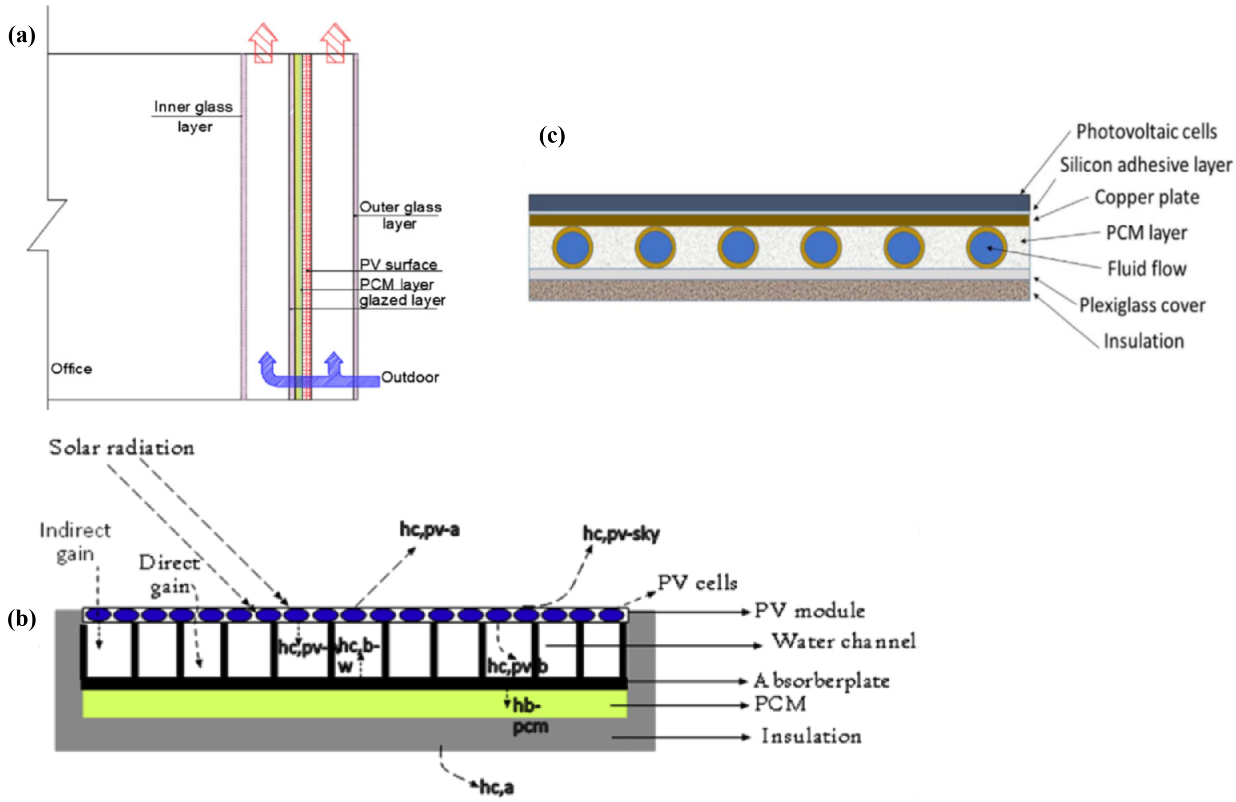

Figure 9. PV module cooling using PCM with different thermal collectors of (**a**) air double passing [103]; (**b**) wetted absorber water channel [104]; (**c**) heat pipe through the PCM container [107].

4. Recent Trend in PCM Based Active Cooling Technology

As mentioned earlier, PCM-based active cooling technology favors cooling the PV module and reduces the existing thermal load in residential and mid-commercial buildings. Integrating the thermal collector inside or above the PCM container cools the PV module effectively when the collector's surface area is more—unless an uneven cooling performance is achieved.

On other hand, PCM-based active cooling methods minimize the thermal resistance by employing the fluid in the channel. Low thermal conductivity of PCM often creates resistance in PCM; both charging and discharging periods using active fluid flow helps to maintain the higher temperature difference between PCM and the PV layer. When there is a high-temperature difference, thermal resistance in PCM is low and heat energy from the PV module is transferred to the PCM at a higher rate. This technique is often considered hybrid by utilizing the heat from PCM into a useful thermal load. This hybrid technique can be widely adopted for low and mid-sized power plants especially when the thermal load and electrical load are consumed at the same level, which is where hybrid technology will benefit.

In recent years, active cooling methods have gained attention among researchers as compared to pure PCM and composite PCM. Table 4 shows some of the recently published PCM-assisted active cooling technology (PVT).

Table 4. Recent trends in PCM thermal collector-based active cooling technology.

Author	Thermal Collector	Heat Transfer Fluid	Methodology
Carmona et al. [108]	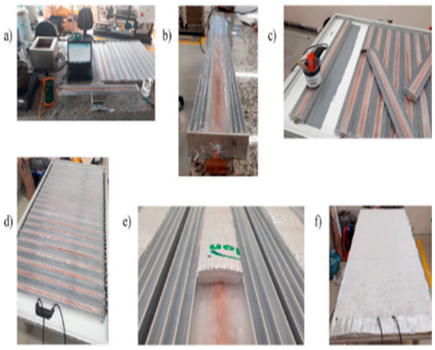	Water	• In this study, continuous 25 days of experimentation with a minute's time interval data measuring claims to be a novel method. • Following that, a flexible PCM structure made up of polyvinyl acetate foil turns to be a second novelty. • Total twenty finned plates are installed under the PV module, following that twenty flexible PCM layer is placed.
Fu et al. [109]		Water	• In this study multilayer heat exchanger technique is embedded with a PCM container. • A vacuum aluminum bag is used to fill the PCM and placed behind the PV module. • A heat exchanger is made up of a square copper tube that is placed behind the PCM layer. • To ensure the proper physical contact between PCM and heat exchanger, thermally conductive silicone gel is applied.
Naghdbishi et al. [110]	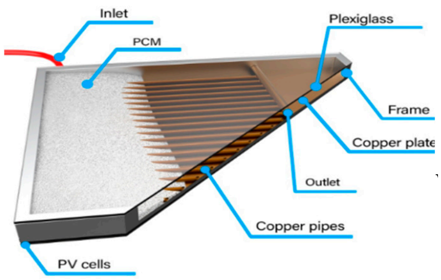	Deionized water, glycol/water, water/MWCNT, EG/MWCNT	• A heat exchanger is loaded inside the PCM to increase the heat absorption capability of the system. • The top and bottom surfaces of the PCM are covered by plexiglass and the four sides of the PCM are covered by a metal frame. • Thermal and electrical efficiencies are monitored for different heat transfer fluids.
Fu et al. [111]		MPCM slurry, water	• Paraffin wax as PCM is encapsulated in the vacuum aluminum bag. • PCM layer placed behind the PV module, following that serpentine copper heat exchanger tube is attached behind the PCM layer. • Nitrile Butadiene Rubber and Polyvinyl Chloride as insulating material with a 12 mm thickness are placed behind the heat exchanger and a 3mm composite aluminum sheet is enclosed in the insulation layer.

Table 4. *Cont.*

Author	Thermal Collector	Heat Transfer Fluid	Methodology
Ahmadi et al. [112]	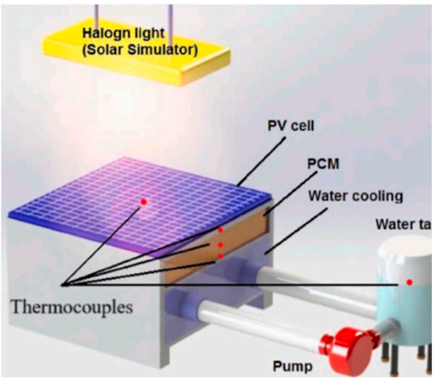	Water	• In this study, PS-CNT polyHIPE foam is used as encapsulating material for paraffin wax. • Laboratory type 5.5 × 5.5 cm^2 solar cell is embedded with PCM layer and following that aluminum water channel in place. • Water flow was maintained at 0.2, 0.6, and 1 L/minute. • Experiments are performed in both passive and active techniques to make an effective comparison.
Kazemian et al. [113]	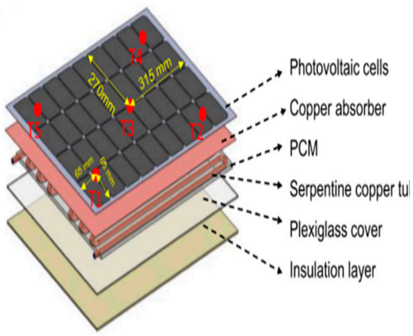	EG/water	• Three system configurations are examined namely, PV-PCM without the thermal collector, PV-PCM with a serpentine thermal collector, and glazed PV-PCM with a serpentine thermal collector. • In this study, EG is added with water to avoid working fluid freezing. • Working fluid flows in the heat exchanger in a serpentine flow with a mass flow rate of 20–60 L/hr.
Basalike et al. [114]	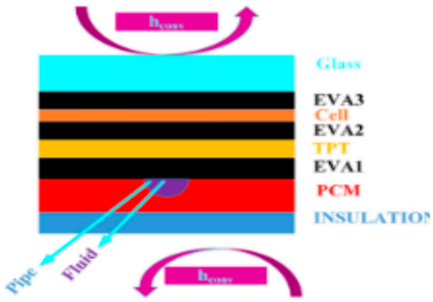	Water and Al_2O_3	• n-octadecane and eutectic capric-palmitic as PCMs are used in this simulation. • To ensure the PCM and heat pipe physical contact, 10-layer inflation was applied. • Grid independent study was approached with five different mesh sizes to find the resistance in heat transfer.
Hasan et al. [115]	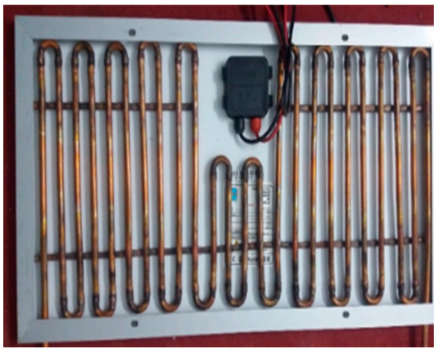	Graphene nano fluid	• The thermal collector is made up of a copper tube impregnated in the PCM container. • Graphene nano fluid flows inside the copper tube with a mass flow rate of 0.33–0.67 kg/s. • Once the working fluid removes the heat from PCM, the car radiator acts as a secondary heat exchanger to remove the heat from the nano-fluid.

Table 4. *Cont.*

Author	Thermal Collector	Heat Transfer Fluid	Methodology
Ciftci et al. [116]	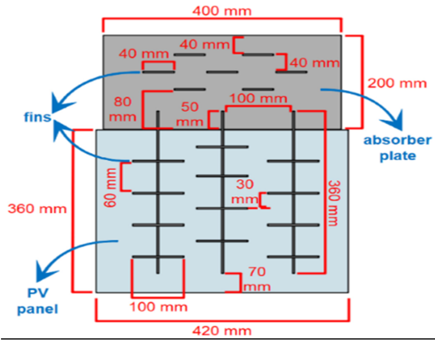	Air	• PV module placed in a vertical position to save space. • Fins are placed on the back surface of the PV module and air flows in the duct. • Fins create resistance in air flow that favors removing the heat from the PV module. • Several air flow rates are analyzed in the study. • In the daytime, 50 g of mint leaves are dried using the recovered heat from the PV module.
Yang et al. [117]	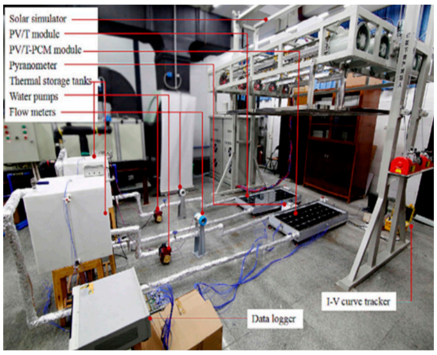	Water	• Simulation is performed in indoor controlled climatic conditions of 800 W/m^2 with a mass flow rate of 0.15 m^3/hr. • In this study separate thermal energy storage tank is placed to store the recovered heat from the PV module. • Five different melting temperature of the PCM is examined to find the relationship of PCM melting temperature with a reduction in T_{PV}.

5. PCM Thermo-Physical Property Necessity on PV Module Cooling

5.1. Discussion of Thermodynamic Criteria

5.1.1. PCM T_{melt}

As mentioned earlier, PCM T_{melt} is an essential parameter in cooling the PV module; experimenting with inappropriate T_{melt} of PCM causes a reduction in the performance of the system [79,82]. Adeel Waqas et al. [83] performed a numerical simulation to optimize the PCM T_{melt} for hot climatic conditions. Several PCMs were examined to find the PCM T_{melt} (30 °C, 35 °C, 40 °C, and 44 °C); among these, RT44 extracted high amounts of thermal energy from the PV module. This optimized PCM (RT44) reduced 28 °C of T_{PV} at the time of peak daytime hours. From this finding, Waqas concluded that the T_{amb} plays an important role in the operation of the PCM.

Following Waqas, Arici et al. [118] performed a numerical simulation for two different locations to find the PCM T_{melt} and thicknesses for an entire year. Arici also showed that T_{amb} plays an important role in cooling the PV module. From this finding, it is clear that selecting a single T_{melt} of PCM will not be effective for an entire year and also, the PCM thickness varies for each month as listed in Table 4. On the other hand, changing the PCM for each month is not practical; further, it is recommended to split the seasons (summer and winter) and choose two PCMs for an entire year cooling process or cascade PCM will be an option; low T_{melt} of PCM can be placed as the first layer and the second layer will be high T_{melt}, whereas it can serve the cooling effect for both summer and winter [54] as shown in Figure 10. On the other hand, Karthikeyan et al. revealed that PCM T_{melt} can be selected without performing lex simulation tools such as CFD/numerical simulation by only analyzing the experimental local ambient temperature of the ambient temperature in Figure 11. It is found that PCM operation in cooling the PV module is majorly classified into two categories: ineffective T_{PV} reduction and effective T_{PV} reduction. When the selected PCM T_{melt} is equal to T_{amb}, less than T_{amb}, and 6 °C higher than average, T_{amb} causes ineffective T_{PV} reduction. These conditions mostly absorb heat from the surroundings rather than absorbing from the PV module. Secondly, if the PCM failed to reach the T_{melt} in the effective daytime hours, H_m will not be utilized effectively, and the resulting negative impact will reflect in cooling the PV module as listed in Table 5. To achieve effective cooling, PCM T_{melt} must be 3–6 °C higher than T_{amb}.

Table 5. Optimization of PCM T_{melt} and thickness for Ankara and Mersin [118].

Month	Ankara (PCM T_{melt}/Thickness)	Mersin (PCM T_{melt}/Thickness)
January	4 °C/50 mm	17 °C/31 mm
February	15 °C/32 mm	27 °C/38 mm
March	3 °C/48 mm	20 °C/34 mm
April	12 °C/28 mm	25 °C/35 mm
May	22 °C/33 mm	22 °C/31 mm
June	26 °C/50 mm	28 °C/26 mm
July	35 °C/47 mm	35 °C/39 mm
August	25 °C/38 mm	35 °C/34 mm
September	22 °C/34 mm	30 °C/45 mm
October	14 °C/38 mm	29 °C/47 mm
November	10 °C/42 mm	23 °C/43 mm
December	5 °C/37 mm	13 °C/31 mm

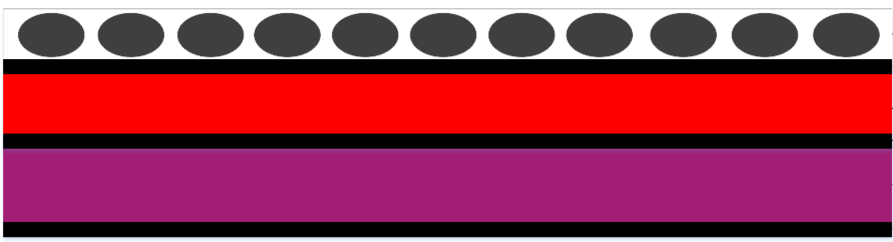

Figure 10. Cascaded PCM construction for annual PV module cooling [54].

Thongtha et al. [79] experimented with controlled indoor climatic conditions to study the nature of paraffin wax which melts at 59 °C. It was found that 2–6% of cooling is achieved due to the higher melting temperature of PCM. Yuan et al. [119] stated that T_{amb} plays a crucial role in cooling the PV module. Interestingly, when the T_{melt} is equal to T_{amb}, a moderate or less cooling effect is achieved. PCM struggles to remove the heat from the PV module because PCM starts to absorb from T_{amb} as well. On the other hand, Elavarasan et al. [50] revealed that examining with low T_{amb} causes a non-favorable cooling effect because the PCM turns to liquid before the peak daytime especially in summer. With a rise in solar radiation, T_{amb} also increases, resulting in PCM interacting with the surroundings that cools the PV module. Within an hour of experimentation, PCM influenced the PV module to gain a higher temperature than the unmodified PV module. Overall, this study showed the negative impact on the modified PV module due to inappropriate PCM selection. However, the same PCM works perfectly in winter because of the lower T_{amb} [75,76]. Anna Machniewicz et al. [120] conducted a simulation for climatic conditions in Poland using different PCMs (RT10HC, RT15HC, RT18HC, RT25HC, and RT35HC PCM) to find a suitable PCM for winter and summer. In winter, RT10HC enhanced the cooling effect and the same PCM for summer failed in cooling the PV module effectively. In summer, RT18HC and RT25HC showed an extraordinary cooling process. Following that, Hendricks et al. [84] revealed that an uneven cooling effect is noticed. In Utrecht, PCM starts to cool the PV module at 8 a.m., and the for Malaga PCM cools the PV module at 10 a.m. This analysis showed that PCM must be selected for each location using the meteorological data unless the system delivers a negative impact on the cooling process.

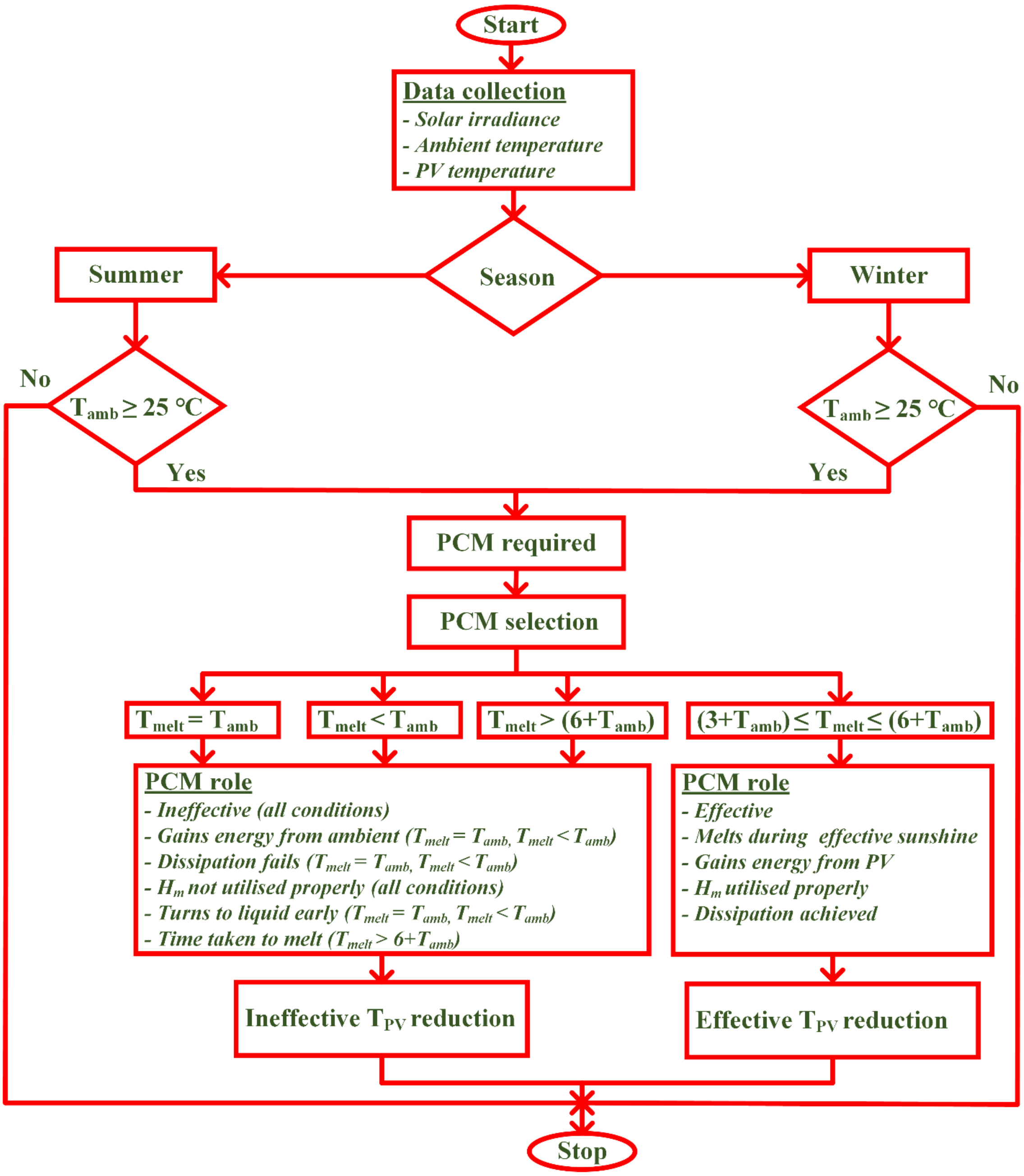

Figure 11. PCM selection procedure without performing the complex simulation tools [54].

5.1.2. Latent Heat of Fusion

The reason behind selecting the PCM as a cooling element for PV modules is its high energy density and latent heat of fusion [121]. PCMs H_m is not temperature-dependent material. It stores a high amount of thermal energy during the PCM melting state without increasing the PCMs temperature while charging compared to sensible heat storage material [122,123]. Selecting a high H_m material can store a large amount of thermal energy and directly enhance the cooling effect and cooling durability each day. On the other hand, selecting a high H_m reduces PCM thickness, whereas PCM consumption is less and has a higher cooling effect. As mentioned earlier, in PV module cooling using PCM as heat removal, it is necessary to consider the T_{melt} at first, if H_m is less means it only shortens the cooling durability [124]. However, this issue can be resolved by increasing the thickness of the PCM container to withstand the cooling effect for a longer period [125].

5.1.3. Density

The density of PCM directly correlates with thermal conduction loss because low-density material intakes large volumes in containers, whereas the thickness is increased. Especially, organic PCM owes low density, and integrating them with PV modules slightly increases the thickness of the PCM container. On the other hand, organic PCM's low thermal conductivity directly imposes a thermal conduction barrier with an increase in thickness of the PCM container [126,127]. It was noted that the density of PCM is correlated with the cooling effect; although it is often negligible compared to T_{melt} optimization [49].

5.1.4. Specific Heat Capacity

Specific heat capacity is often not considered basic criteria for selecting the appropriate PCM for PV module cooling due to its low thermal conductivity [54,125]. Several studies state that the specific heat capacity of PCM is not efficient to cool the PV module, especially under hot and humid climatic conditions. Karthikeyan et al. showed that specific heat capacity is useful when the K_{PCM} is enhanced unless it is recommended to proceed with the PCM selection process without considering the specific heat capacity as a parameter [49].

5.1.5. Thermal Conductivity

K_{PCM} is the second essential parameter in cooling the PV module. To enhance the cooling effect, it is necessary to increase the K_{PCM} unless the conduction barrier reduces the heat transfer rate between the PV module and PCM [128–130]. Several researchers claim that incorporating a thermal distribution heat sink inside the PCM container helps transfer the thermal energy from the PV module to the PCM's inner surface [93,94,104]. This technique enhanced the electrical efficiency greatly as compared to pure PCM. However, fabricating interfin with the PCM container is difficult and also creates leakage in the PCM container. Following interfins, several studies have been conducted on nano material, metal powder, and metal foam, resulting in higher T_{PV} reductions; although, it not feasible for longer operations. The nano compounds or metal powder degrade the thermal stability of the PCM [130], and metal foam increases the total weight of the PCM requiring additional care to the PV module mounting structure. As mentioned above, all K_{PCM} enhancing techniques lack in certain features mostly in the simplest way to enhance the K_{PCM} without degrading the property or increasing the mass of the PCM container, notably expandable graphite is not increasing the K_{PCM} as compared to metal foam, though it is easy to handle and fabricate. Moreover, it increases the K_{PCM} by up to 16.6 W/m.K [131,132]. It is noted that EG increases the thermal conductivity as compared to several nano compounds, which are non-metallic. Further, the combination of EG and metal powder is recommended to composite with PCM. This combination of metallic powder with EG will not allow it to settle down in the PCM container. Considerably, this technique increases the K_{PCM} to a higher order to reduce the T_{PV} effectively with minimal thermal resistance.

5.1.6. Congruent Melting

Inorganic PCMs are not widely examined due to their incongruence in melting after several hundred thermal cycles. Continuous heating and cooling cycle breaks the salt and hydrates separately; as a result, semi-liquefication and freezing occur and can be noticed in the endothermic and exothermic curves [54]. Several researchers reported that organic PCM, especially paraffin wax, is congruent in melting and is an effective material for PV modules as coolants over several thousand thermal cycles [49].

5.2. Discussion of Kinetic Criteria

Supercooling

During daylight hours, PCM removes heat energy from the PV module and stores it in the PCM by changing the phase solid to liquid. In most cases, PCM turns to a liquid/mushy state at the end of the day. To conduct the consecutive day PV module cooling, PCM must be solidified in the nighttime otherwise the cooling process will not be effective. This is the reason why the selected PCM must be non-supercooling and congruent in the material. Further, it is necessary to examine the supercooling nature of the PCM before experimenting with the PV module, especially for inorganic PCMs, in which examining the thermal properties (thermal cycling) is not recommended to incorporate with the PV module because the supercooling effect is high in inorganic PCM as compared to others. Other than the natural super cooling effect, an increase in thickness of PCM creates a barrier in discharging the stored heat energy and fails to solidify the PCM. Under this condition, PCM also turns into an ineffective material for cooling the PV module. However, this artificial supercooling effect can be rectified by increasing the K_{PCM}. Notably, this artificial supercooling effect is less in composite PCM and thermal collector-based PCM incorporation with the module [116,117,119].

5.3. Discussion of Chemical Criteria

5.3.1. Chemical Stability and Decomposition

The low melting temperature of inorganic PCM is moderately stable chemically and thermally; this is the reason most of experiments are performed with commercial PCMs and paraffin [54,133]. Commercial PCM achieves perfect endothermic and exothermic reaction without any restriction in operation; the only drawback in commercial PCM is investment costs. In most cases, PCM integration investment is higher than the temperature loss which makes commercial PCM unsuitable for real-time applications [16]. As mentioned earlier, paraffin wax is widely examined as it is inexpensive, readily available in the market, and easy to handle. Following commercial PCMs and paraffin, it is recommended to examine organic eutectic and fatty acids as coolant materials for PV module cooling purposes. They are inexpensive compared to commercial PCMs; a wide range of melting temperatures is available besides paraffin wax, and a eutectic mixture can be easily prepared to obtain the expected operating temperature for any desired location [8]. On the other hand, fatty acids and organic eutectic PCMs are thermally and chemically stable even after several thousand thermal cycles and are outnumbered in the literature to cool the PV modules which make them alternative PCMs [134–136].

5.3.2. Corrosive

In most cases, PCMs are filled in a container that is made up of stainless steel and aluminum. Notably, inorganic PCMs are highly corrosive with metal, especially salt hydrates [137,138]. Aluminum is a higher conducting metal than stainless steel, but the corrosion rate is higher for inorganic PCMs and moderate for other PCMs compared to stainless steel [139,140]. Over time, the corrosion rate increases gradually and destroys the PCM container's mechanical strength and thermal stability [137,141]. Under certain conditions, an increase in corrosion rate leads to liquid PCM leakage. To minimize this loss, PCM must be examined with aluminum or stainless steel to find the corrosion rate before integrating for PV module cooling. Several researchers state that organic PCMs are less corrosive to metal and easy to handle for PV module cooling purposes. Further organic PCMs are recommended for real-time cooling purposes for a longer period of operation.

5.3.3. Toxic

PCM is a non-hazardous and environmentally friendly thermal energy storage material. Benefits of integrating PCM as a coolant material include reducing the T_{PV} without consuming manpower, natural resources, and less maintenance costs [142,143]. However, laboratory-grade gloves and masks are essential safety devices to use while handling the

PCM, some PCMs have a strong odor that makes mild headaches especially inorganic salt, without safety measures, creating rashes and itches on human skin. Other than these minor side effects, PCMs are ecofriendly and can be incorporated with PV modules without contaminating nature.

5.3.4. Flammable and Explosive

In most experiments, organic PCMs are involved in cooling the PV module as compared to the inorganic and eutectic mixture. Moreover, locally available paraffin wax plays a major role in PV module cooling than fatty acids. Following that commercial PCM also widely influenced as listed in Table A1. In prior notice, paraffin wax and commercial PCM are flammable starting from 150 °C; however, the PV module operating temperature will not reach 150 °C but accidental electrical failure or a short circuit in the electrical system may cause a fire in PCM. In such a case, it is necessary to maintain the electrical systems in good condition and fire extinguishers must be kept in the power station. The extinguishers should work autonomously to control the fire before it ignites the entire power plant. It is noted that paraffin is flammable under certain conditions but not explosive, with proper precaution and safety measures, paraffin can be incorporated as a cooling system. Inorganic PCM is non-flammable but scarcity in the corrosion and supercooling effect makes salt hydrates unsuitable for cooling purposes. Other than salt hydrates, fatty acids, and fatty acids eutectic mixtures are replacement heat storage materials than paraffin wax.

5.4. Discussion of Technical Criteria

Compactness, Reliability and Simplicity

PCM is a compact heat battery as compared to other sensible heat storage materials. However, it is heavier and larger as compared to electrical batteries. PCM stores and discharges thermal energy without raising the temperature, making heat batteries reliable for thermal applications. PCMs have been widely adopted as heat removal material over the last two decades because of their simplicity in fabrication, installation, and operational performance.

5.5. Discussion of Economic Criteria

Large Scale Availability and Low Cost

Economic analysis should be conducted for further commercialization as some of the commercial and research-grade PCMs are highly expensive than the loss that occurs from T_{PV}. Ahmad Hasan et al. [144] experimented with calpric-palmitic and calcium chloride hexahydrate eutectic under Ireland and Pakistan climatic conditions. For Ireland, the PCM-integrated PV module enhanced the power maximum of 10.7 W and 15.8 W, respectively. Economically, PCM increased the revenue, EUR 51.5 and EUR 76, noticeably this financial enhancement is lower than the net cost of the PCM and its construction which was EUR 92 and EUR 98. However, the same PCM under Pakistan climatic conditions enhanced the output power of 22 W and 33.7 W. The same PCM performed well in Pakistan than in Ireland. It can be concluded that PCM integration is economically viable if the reduction in T_{PV} is higher-order and also based on the grid tariff. Table 6 shows the recent studies on the economic feasibility of the PV module cooling technology using PCM as a cooling agent.

Table 6. Economic feasibility study of PCM cooled PV module.

Author	PCM Name	Material Cost	Findings
Hasan et al. [56]	RT42	PCM = USD 1/kg, payback period = 10 years.	• According to the international electricity tariff, RT42 organic PCM under the hot climatic condition of UAE benefits 2.2 $/m^2$. • RT42 actual cost is 1 USD/kg, under this price, the payback period of the system is 10 years. • Instead of RT42, salt hydrates with similar thermophysical properties will reduce the payback period from 10 years to 3 years. • Salt hydrates are nearly 7 times more inexpensive than RT42.
Smith et al. [145]	-	PCM = 4.93 EUR/kg, Aluminum = 1.6 EUR/kg, PV/PCM = 244.31 EUR/m^2	• PCM as coolant material is analyzed for several world locations, specifically, the US (Arizona), India, China, Ghana, and Germany. • Integrating PCM behind the PV module shows a significant improvement in temperature reduction and output power. • Technically PCM is an excellent coolant material but economically PCM failed to achieve the payback period. • According to the US electric tariff in 2013, PCM assisted PV module requires a 7.9 times higher price than the actual price. • Following that India, China, Germany, and Ghana requires 9.2, 23.3, 7.9, and 3.1 times enhancement in the actual tariff.
Sun et al. [146]	Paraffin wax	PCM = 37 (RMB)/kg	• This study found that using PCM for building-integrated PV modules is not economically viable. • Building without PCM payback period is 17.51 years and for the building with PCM is 18.57 years. • Systematically, PCM embedded building reduced the conventional thermal load that directly favors carbon emission control but not economically.
Arici et al. [118]	-	PCM = 100 EUR/m^2, Aluminum = 32 EUR/m^2,	• According to the manufacturer, the PV module lifetime is 25 years, cooling the PV module will extend to 30 years. • The operational and maintenance (OM) cost of the PCM is higher than the conventional PV module. • Adding OM to the investment, increased the payback period of the system. • Hereby, this study states that PCM is not economically feasible, however, if the OM and PCM cost is reduced in the future, PCM can be the efficient material on the economic aspect.
Zhao et al.	Paraffin wax	PCM = 30 RMB/kg	• It is found that 10 mm thickness of paraffin wax under government subsidy makes 16 years of payback. • Higher thickness of PCM could increase the payback period. • It is noted that 16 years of payback period is not affordable as the lifetime of the PCM is about 5–8 years in general.

6. Benefits and Drawbacks of PV Module Cooling Using PCM

Benefits: The main benefit of using raw PCM is the high amount of Hm that can be utilized for an effective PV module cooling process. On the other hand, it can be easily filled in the PCM container/PV module back surface by melting the PCM. As mentioned earlier, numerous heating and cooling cycles of the PCM face volume changes which deteriorate the cooling process; advantageously, using raw PCM as a coolant material can be refiled easily whenever the PCM volume change is noticed. Adding thermal additives with PCM enables the heat transfer capacity between PV and PCM, resulting in a higher cooling effect. It is well known that the solid and liquid specific heat capacity of the PCM is ineffective in cooling the PV module; however, when the PCM is incorporated with thermal additives, it turns out to be an effective material. On the other hand, the enhanced thermal conductivity of the PCM using EG and other lightweight materials maintains the stability of the system, and thermal dissipation from the PCM enhances the cooling effect and consecutive day cooling performance effectively. Other than PCM as coolant material, it stores excess heat from the PV module and utilizes it for various low thermal applications that minimize the conventional thermal load. Secondly, the thermal collector helps to minimize the total amount of PCM usage in cooling the PV module because fluid motion in the PCM chamber greatly maintains the PCM in a mushy state for a longer period than non-thermal collector-based PV-PCM, resulting in higher temperature differences between the PV module and PCM being maintained. The unique benefit in both composite and thermal collector-assisted PCM favors enhancing the electrical efficiency in the early daytime period itself compared to pure PCM.

Drawback: Overall, using PCM as a coolant material increases the overall system weight. It deteriorates the PV module's back surface thermal dissipation, especially during off-peak daytime hours, as PCM is ineffective in cooling the PV module. The main drawback of raw PCM is its low thermal conductivity; notably, organic PCMs are widely performed in cooling the PV module that has a maximum of 0.3 W/m.K. Although PCM is a high-energy-density material, a lack of thermal conductivity increases the heat transfer resistance between the PV module and PCM. Notably, the low thermal conductivity of PCM failed to achieve consecutive cooling processes, especially in hot and humid climatic conditions, PCM failed to discharge stored thermal energy due to high ambient temperature, resulting in the incorrect utilization of H_m on a consecutive day. Although adding additives in the PCM enables the heat transfer rate, it is particularly difficult to construct inter-fin-based compositing materials, as they lead to liquid PCM leakage, increasing the system's total weight. Moreover, adding nano compounds in the PCM deteriorates the thermophysical property of the PCM. Although thermal collector-based PCM favors cooling the PV module greater than other techniques, it is not appropriate for large-scale systems. Mainly, the thermal collector with PCM increased the weight of the system and produced mechanical vibration and noise due to an increase in the flow rate of the fluid. Moreover, recovering heat from the large-scale system will not be converted into useful energy considering the safety issues of the powerplant and grid stability.

As mentioned earlier, PCM is an efficient and effective material that can cool the PV module, but it is not convenient for all climatic conditions. Table 7 shows the importance of PCM and recent research activities in cooling the PV module. However, it is necessary to find a suitable PCM according to the experimental location to achieve an effective payback period, because the operation of PCM is mainly correlated with outdoor climatic conditions. The T_{PV} reduction from different researchers with different PV module cooling techniques is listed in Table 7 and represented graphically in Figure 12. It is found that most previous studies were only performed for a short period in a particular location; for example, some experiments were conducted for less than a day and month—selective days in a particular month and season. In most cases, researchers failed to attempt the annual performance of the PCM cooling. Under this condition, it is difficult to recommend these cooling technologies for large-scale solar power plants. Strategically, only two studies were found in the literature: Hasan et al. [56] and Waqas et al. [57] showed an annual simulation for UAE and Islamabad locations, respectively. In the next section, deep an analysis was conducted for the 15 MWp using the NREL meteorological data.

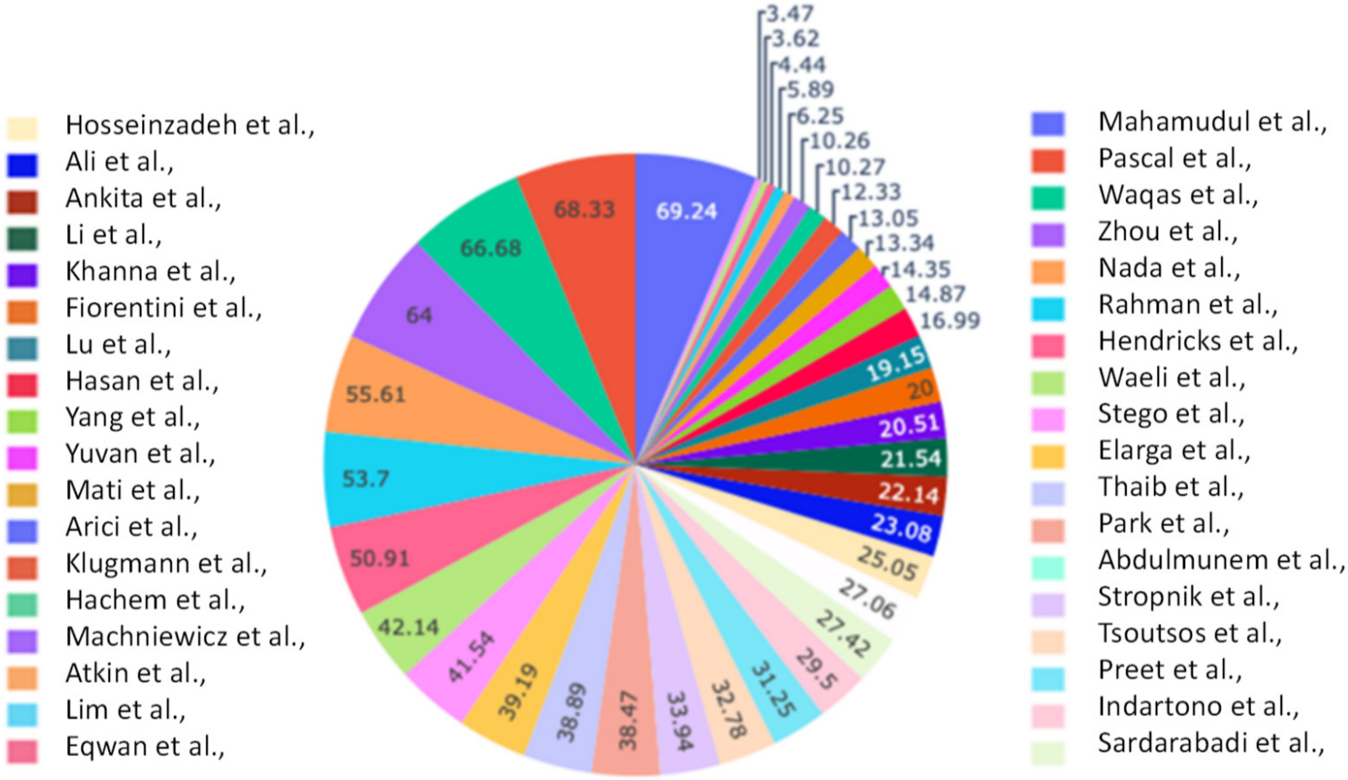

Figure 12. Reduction in T_{PV} using different techniques by different researchers.

Table 7. List of PCM and experimental details of the PV-PCM.

Reference	System	PCM Name	Location	Study Type	Solar Irradiation	Experiment Type/Period	Study Environment	Highlights	T_{PV} without PCM (°C)	T_{PV} with PCM (°C)
[124]	PV-cPCM	GR40	Belfast, UK	Simulation and Experiment	750	Indoor	The developed system is performed in indoor climatic simulation and validated with experimental results under the constant irradiance of 750 W/m^2 and 23 °C of T_{amb}.	A 6 mm thickness of two interfin is projected inside the PCM container.	NA	38
								A 0.5 mm thickness of a total 32 interfin is projected inside the PCM container.	NA	29
								A Strip aluminum matrix is installed behind the PV module without PCM.	NA	55
[73]	PV-PCM	RT42	Indoor	Experiment	1000	Indoor	Concentrated PV cells have experimented with under 28–35 °C of T_{amb} and 1000 W/m^2 constant irradiance using a solar simulator.	PCM is filled in a 13 mm thickness of Perspex box type container and integrated on the PV module back surface.	60.9	58.7
[84]	PV-PCM	RT27	Utrecht	Simulation	-	365 days	The developed numerical model is performed to find the annual performance of different thicknesses of PCM integration.	During the peak daytime, 2–3 h PCM utilized its latent heat of fusion effectively and lowers the T_{PV}. An increase in thickness of PCM has shown the variation in enhancing the electrical efficiency and reduction in T_{PV}.	55	27
[94]	PV-cPCM	RT25, Paraffin wax 32	Indoor	Simulation	750	Indoor	Different length of interfin is examined to optimize the fin length without restricting the PCM mushy state convection.	An increase in length of interfin enhanced the heat transfer better than a 40 mm fin length as it connects the front and bottom layer of the PCM that restricts mass convection in PCM.	NA	55

Table 7. *Cont.*

Reference	System	PCM Name	Location	Study Type	Solar Irradiation	Experiment Type/Period	Study Environment	Highlights	T_{PV} without PCM (°C)	T_{PV} with PCM (°C)
[95]	PV-cPCM	RT25, Paraffin wax 32	Indoor	Simulation	750	Indoor	The different inclinations of the fin intruded PCM container is performed to analyze the effectiveness of the conduction and convection relationship.	A PCM container at lower than 45° inclination encourages convection mode inside the PCM, following 45° to 90° inclination pure conduction dominates.	NA	45
[96]	PV-PCM	RT25	Indoor	Simulation	1000	Indoor	Different heights of the PCM containers are developed and performed under constant irradiance of 1000 W/m^2 to find the effectiveness of heat transfer.	An increase in height of the PCM container reduced the T_{PV} for a longer time compared to the shorter height. An increase in PCM height directly enhances the heat storage capacity of the PCM.	~87	40
[87]	PV-cPCM	RT25	Indoor	Simulation	1000	Indoor	PCM container with and without interfin is exposed to the constant irradiance of 1000 W/m^2.	PCM containers without interfin struggle to extract the thermal energy from PV modules compared to PCM with interfin.	~35	~30
[98]	PV-cPCM	Paraffin wax	Rajasthan, India	Simulation and Experiment	1900	Less than a month	Metal scraps are reinforced with paraffin wax to enhance the thermal conductivity of the PCM.	V-through concentration increased the T_{PV} abruptly compared to conventional PV module, however, prepared composite PCM reduced the T_{PV} effectively compared to PV without PCM.	90	78
[77]	PV-PCM	RT35	Malaysia	Simulation and Experiment	1000	Less than a month	A 2 cm thickness of liquid PCM is directly filled on the Tedlar surface and fiber optic glass is used to cover the back surface of the PCM like sealant material.	PCM receives thermal energy directly from the Tedlar surface without any intermediate layer that helps to reduce the thermal resistance resulting electrical output of the PV module being greatly enhanced.	70	35

Table 7. *Cont.*

Reference	System	PCM Name	Location	Study Type	Solar Irradiation	Experiment Type/Period	Study Environment	Highlights	T_{PV} without PCM (°C)	T_{PV} with PCM (°C)
[79]	PV-cPCM	Paraffin wax 59	Indoor	Experiment	1000	Indoor	PCM with interfin is exposed to the constant irradiance of 500 W/m^2, 600 W/m^2, 800 W/m^2, and 1000 W/m^2.	Higher T_{PV} reduction achieved for 1000 W/m^2 and 800 W/m^2 than 500 W/m^2 and 600 W/m^2. Low irradiance requires a low melting temperature of PCM.	72.1	69.6
[85]	PV-PCM	RT25HC	Indoor	Simulation	1000	Indoor	Different thickness of PCM is examined to find the optimum level under varying environmental conditions such as different wind speed, wind azimuth.	A 3 cm thickness of PCM maintained the TPV at 33 °C and the same with 1cm thickness PCM was maintained at 45 °C. An increase in thickness of PCM enables higher T_{PV} reduction.	NA	33
[74]	PV-PCM	RT27	Greece	Experiment	1020	Summer	The developed experiment was performed in outdoor climatic conditions using RT27 at the Technical University of Crete, Chania, Greece climatic condition.	Three equal dimensions of PCM containers are integrated on the PV module to minimize the mechanical stress on the PV module surface.	60.1	40.4
[71]	PV-cPCM	Coconut oil and Vaseline	South Korea	Simulation and Experiment	660	Summer, Winter	Coconut oil and Vaseline are used as PCM under summer, intermediate and cloudy conditions.	Both PCM are packed in honeycomb and macro type nylon containers, resulting in honeycomb-structured PCM enhanced higher heat from PV module than nylon due to the thermal conductivity of the PCM container.	34	32

Table 7. *Cont.*

Reference	System	PCM Name	Location	Study Type	Solar Irradiation	Experiment Type/Period	Study Environment	Highlights	T_{PV} without PCM (°C)	T_{PV} with PCM (°C)
[81]	PV-PCM	Candle wax	Malysia	Experiment	1605	Less than a month	Heat sink and PCM as coolant material integrated with the PV module and performed at TNB Research in Kajang, Selangor, Malaysia.	The heat sink degrades the output power and efficiency as it failed to extract the heat from the PV module compared to candle wax as PCM.	45.1	43.1
[78]	PV-PCM	RT35	Malaysia	Experiment	1000	Less than a month	A 2 cm thickness of RT35 is examined under the typical climatic condition of Malaysia.	The developed system reduced the T_{PV} maximum of 10 °C and this reduction sustains for 6 h.	52	42
[72]	PV-PCM	Petroleum Jelly	Indonesia	Experiment	1120	Less than a month	1 kg of PCM is filled in a rectangular tube and is integrated into the PV module to study the performance under Indonesian climatic conditions.	Rectangular tube PCM container greatly enhanced the T_{PV} reduction as PCM container wall acts as a thermal distribution fin.	60	54.3
[88]	PV-PCM	RT25HC	Indoor	Simulation	1000	Indoor	A 2cm thickness of PCM container is performed under different inclinations.	It was found that 15° to 90° inclination extracts higher thermal energy than 0° inclination.	43.4	34.5
[80]	PV-PCM	Crude oil and Palm oil	Indonesia	Simulation	-	Less than a month	Coconut oil and palm oil-based different thickness of PCM is performed as a coolant device.	The highest PCM thickness of 9 cm yields higher T_{PV} reduction but linearity in T_{PV} is stopped at 8 cm thickness of PCM.	~75	~60
[147]	PV-PCM	RT27, RT20, SP25A8	Greece	Simulation	-	January-August	Finite difference method simulation is performed and compared with existing simulation tools to find the accuracy of the simulation.	A 5 cm thickness of RT 25 enhanced higher T_{PV} reduction annually.	~65	~38

Table 7. *Cont.*

Reference	System	PCM Name	Location	Study Type	Solar Irradiation	Experiment Type/Period	Study Environment	Highlights	T_{PV} without PCM (°C)	T_{PV} with PCM (°C)
[83]	PV-PCM	RT44	Pakistan	Simulation and Experiment	-	June	Different T_{melt} and thickness of PCMs are performed under hot climatic conditions of Pakistan to establish the proposed method for large-scale integration.	Linearity in T_{PV} reduction is achieved at 2.5 cm thickness of RT44 throughout the year.	86.5	57.8
[103]	PVT-PCM	RT42, RT55	Venice, Abhu Dabi	Simulation	900, 820	Summer and winter	A numerical simulation is performed for the Double skin façade of PV and PCM under the Venice, Helsinki, and Abhu Dhabi climatic condition.	A double façade allows the air to flow over the PV module and behind the PCM container that helps to enhance the heat transfer from the PV module to PCM.	74	45
[104]	PVT-PCM	OM37	France	Simulation	875	Summer and winter	The numerical model is performed for wetted water channel-based PCM containers to cool the PV module under France climatic conditions.	PCM associated fully wetted absorber channel with constant water flow helps to maintain the T_{PV} constant during peak daytime as a fully wetted absorber channel without PCM.	69.17	53.86
[102]	PVT-PCM	S21	Australia	Experiment	560	June and August	A building management system is equipped to monitor the thermal and electrical load of the proposed model at the University of Wollongong Innovation Campus.	PCM is encapsulated by HDPE and applied for the dual purpose to reduce the T_{PV} as well as heating, ventilation, and air-conditioning purpose.	-	~29
[105]	PVT-PCM	Paraffin wax 50	Malaysia	Simulation and Experiment	-	Indoor	Different thermal collector tubes and flow rates are performed using CFD simulation using different solar irradiance.	Thermal conductivity enhanced PCM and nano fluid-based thermal collector favors to reduce the PCM temperature as well as T_{PV} in higher order.	65	50

Table 7. *Cont.*

Reference	System	PCM Name	Location	Study Type	Solar Irradiation	Experiment Type/Period	Study Environment	Highlights	T_{PV} without PCM (°C)	T_{PV} with PCM (°C)
[107]	PVT/PVT-PCM	Paraffin wax 42–72	Iran	Experiment	1050	August and September	Conventional PV and PVT, and a novel PVT-PCM (nanofluid) systems have been experimented under Iranian climatic condition	PVT-PCM enhanced the electrical efficiency higher than conventional PV modules also nano fluid-based PVT without PCM enhanced the electrical efficiency.	~62	~45
[82]	PVT-PCM	Paraffin wax 42-44, RT42, Ceresin	Indoor	Experiment	1000	Less than a month	Different thickness of PCM and flow rate of water is examined under indoor condition.	Increase in thickness of PCM and mass flow rate of water enhanced the better performance than PV without cooling.	~73	~64
[106]	PV-cPCM/PVT-PCM	RT42	UAE	Experiment	960	Less than a month	Different types of PCM-based PV module cooling are performed under UAE climatic conditions.	Water assisted system maintained the PCM temperature in lower order as compared to interfin PCM.	53	44
[120]	PV-cPCM	RT35, RT10HC, RT18HC, RT25HC	Central Europe	Simulation	550, 100, 550, 500	November and June	Different T_{melt} of PCM with honeycomb thermal enhancer is performed for real-time outdoor conditions.	During winter RT10HC performs well and for summer RT25HC reduced the T_{PV} better than other PCMs.	~39	35
[99]	PV-cPCM	White petroleum Jelly	Lebanon	Experiment	800	Less than a month	Pure PCM, graphite, and copper powder-based thermal conductivity enhanced PCM performed in indoor conditions.	Pure and cPCM enhanced the electrical efficiency by 3% and 5.8% as compared to PV without PCM.	63.3	56.8
[101]	PV-cPCM	Paraffin wax 42	Indoor	Experiment	800	Indoor	The indoor experiment is carried out for pure PCM and aluminum foam impregnated PCM.	Aluminum foam impregnated PCM shows a wide variation in T_{PV} reduction compared to pure PCM, an increase in thermal conductivity of the PCM helps to extract the higher thermal energy from the PV module.	61.39	39.58

Table 7. *Cont.*

Reference	System	PCM Name	Location	Study Type	Solar Irradiation	Experiment Type/Period	Study Environment	Highlights	T_{PV} without PCM (°C)	T_{PV} with PCM (°C)
[148]	PVT-PCM	PCM 28-34	Indoor	Experiment	800	Indoor	Copper absorber plate associated with heat pipe is structure is performed using with and without PCM. The experiment is conducted in controlled indoor climatic conditions.	PCM integrated thermal collector reduced the T_{PV} linearly compared to PVT without PCM for a maximum of an entire period of experimentation (550 min).	66.6	56.7
[57]	PV-PCM	RT44	Pakistan	Simulation	-	365 days	Movable PCM containers are placed behind the PV module to increase the PCM discharge rate during the off-daytime hours.	Movable PCM container enhanced the electrical efficiency by 9% at the peak daytime hours.	63.30	42.10
[149]	PVT-PCM	RT35	-	Simulation	-	Summer, winter, and mid season	Numerical simulation is developed for double-skin façade of PV-PCM to find the operational variation throughout the year, different climatic conditions (summer, winter, and mid-season).	The developed double-skin façade model enhanced the electrical efficiency and waste heat from the PV module is extracted and utilized for room heating and ventilation purpose.	NA	NA
[150]	PV-cPCM	RT55	Egypt	Experiment	1100	August, September, October	Pure PCM and Al_2O_3 nanoparticles mixed composite PCM is performed under Egypt climatic condition	Nanoparticles enhanced PCM reduced the T_{PV} effectively in the whole period of experimentation compared to pure PCM.	75	49.3
[151]	PV-PCM	RT28	Slovenia	Simulation and Experiment	560	365 days	A 3.5 cm thickness of PCM is directly filled on the PV module back surface and transparent acrylic glass is used to cover the back side of the PCM to prevent liquid PCM leakage.	During winter PV power enhancement is not high as compared to the summer season for Ljubljana climatic conditions however the experimental results are in a good match with simulation.	65.30	43.14

Table 7. *Cont.*

Reference	System	PCM Name	Location	Study Type	Solar Irradiation	Experiment Type/Period	Study Environment	Highlights	T_{PV} without PCM (°C)	T_{PV} with PCM (°C)
[152]	PV-cPCM	RT55	Egypt	Experiment	1100	Less than a month	Pure and composite PCM is performed for Egypt's climatic conditions.	Al_2O_3 nanoparticles combined with PCM enhanced the electrical efficiency by 7.1% as compared to pure PCM.	75	59
[153]	PVT-PCM	PCM 15	China	Simulation and Experiment	1000	January and April	Encapsulated and regular PCMs are integrated behind the thermal collector to analyze the system performance under Hefei, China's climatic condition.	Encapsulated PCM failed to reduce higher T_{PV} as compared to regular PCM with thermal collectors because encapsulated PCM attained poor physical contact with thermal collectors.	~75	~60
[154]	PV-PVT PVT-PCM	Paraffin wax 46–48	Iran	Experiment	1000	August and September	Nano fluid-assisted thermal collector with and without PCM is developed and examined under Iran climatic conditions.	ZnO/water nano fluid assisted PV module with and without PCM enhanced the overall efficiency of 40% and 53% as compared to conventional PV module, respectively.	56.62	47.22
[155]	BIPVT-PCM	PCM-45	China	Simulation	540	Summer and winter	The PCM-assisted heat pipe is developed and performed for both summer and winter of Changsha location.	An increase in the mass flow rate of water enhanced the T_{PV} reduction and electrical efficiency.	70	25.2
[156]	PV-PCM	RT38–43	Croatia	Simulation	905	January, March, and June	RT42 and pork fat as PCM with the thickness of 23 mm is performed for Croatia climatic conditions.	For January and March, both PCM reduced similar T_{PV}, however for June RT42 PCM enhanced the heat transfer better than pork as PCM.	-	62.93

Table 7. *Cont.*

Reference	System	PCM Name	Location	Study Type	Solar Irradiation	Experiment Type/Period	Study Environment	Highlights	T_{PV} without PCM (°C)	T_{PV} with PCM (°C)
[157]	CPV-PCM	RT27	UK	Experiment	926	Indoor	A 2.0 Concentrated photovoltaic system is integrated with RT27 to study the effectiveness of cooling under UK climatic conditions.	A 4.2 cm thickness of PCM enhanced the electrical efficiency maximum of 5%.	40.2	32.5
[158]	PV-PCM	Paraffin wax 25	South Korea	Simulation and Experiment	240	May and June	A 3 cm and 5 cm thickness of PCM is integrated with a rooftop PV module to study the heat transfer capability in South Korea's climatic conditions.	Developed PV-PCM enhanced the output power by 3%.	65	40
[159]	PV-PCM	RT35	Egypt	Experiment	820	Indoor	A 2 cm thickness of PCM with Al_2O_3 and cylindrical tube interfin based system performed under Egypt climatic conditions.	Al_2O_3 and Cylindrical fin enhanced the T_{PV} reduction of 46.3% and 52.3%, respectively.	74.5	34.5
[160]	BIPV-PCM	Paraffin wax, Beewax	Indonesia	Experiment	1042	July	Beeswax and paraffin wax is examined under Indonesian climatic condition using the experimental configuration of [86].	Beewax reduced higher T_{PV} than paraffin wax with the help of its low T_{melt}; however, both PCM reduced the T_{PV} effectively compared to PV without PCM.	54	33
[161]	PV-TEG/PV-PCM-TE	Paraffin wax 47, NaOH-KOH	China	Simulation	900	Less than a month	A concentrated PV module with TEG is performed to cool the PV module using with and without PCM.	TEG without PCM under 500 times concentration reduced the T_{PV} lower than with PCM as TE alone failed to extract thermal energy from the PV module.	85	62

Table 7. *Cont.*

Reference	System	PCM Name	Location	Study Type	Solar Irradiation	Experiment Type/Period	Study Environment	Highlights	T_{PV} without PCM (°C)	T_{PV} with PCM (°C)
[162]	PV-cPCM	Paraffin wax 40	Indoor	Simulation	920		A 3 cm thickness of PCM is composited with graphite porous matrix and heat sink.	PCM with graphite porous matrix enhanced less electrical conversion than PCM with heatsink.	80	75
						Indoor		PCM with graphite porous matrix and heatsink enhanced the PV module efficiency maximum of 12.97%.	80	69
[163]	PVT-PCM	Paraffin wax 49	Malaysia	Experiment	700	April, July, October, and November	Nano compound mixed PCM incorporated with the PV module, and nano fluid SiC-water flows inside the PCM to enhance the heat transfer.	Heat removal from the PV module is effective when the working fluid flows inside the PCM and in this proposed system also electrical efficiency is greatly enhanced.	68.3	39.52
[157]	PV-PCM	RT27	UK	Experiment	926	Indoor	A 21 Wp triple-junction solar cell is examined under low concentration.	PCM, TEG, and heatsink are integrated like a sandwich layer to control the excess rise in T_{PV}. Favorably electrical efficiency is enhanced maximum of 0.56%.	65	51
[164]	PVT-PCM	Paraffin wax 30	India	Experiment	1200	-	Thermal collector with and without PCM is performed under Punjab climatic conditions.	An increase in the flow rate of water enhanced the electrical efficiency greatly compared to the thermal collector without PCM, however, thermal efficiency is high for the only thermal collector because PCM assisted thermal collector allows the thermal energy to store in PCM reduces the water temperature.	80	55

7. Case Studies on Implementation of PV and PV PCM Temperature in Solar PV System for Two Different Geographical Locations UAE and Islamabad

The resource assessment for a given geography is of primary importance in developing an MW scale solar PV system. To estimate the year around performance, cost, and payback period requires accurate resource data. The NREL (National Renewable Energy Laboratory) is a national laboratory of the U.S. Department of Energy that provides a TMY (typical meteorological data) in an hourly frequency, available in different formats and data from different sources (NSRDB) 1961–1990 data, TMY2 1991–2010, TMY3 and EnergyPlus weather files. The available weather parameters are:

- Beam irradiance (W/m^2)
- Diffuse irradiance (W/m^2)
- Ambient temperature (°C)
- Wind speed (m/s)
- Plane of array irradiance (W/m^2)

These resource data are analyzed to select the PCM material concerning its thermal properties. In this study, two different geographies are considered, namely UAE and Islamabad, measured PV-PCM temperatures are taken from "Hasan et al. [56] and Waqas et al. [57]" for a respective location and compared with reference NREL data to figure out the impact of PV-PCM temperature on performance enhancement. The experiment requires module temperature to study the effectiveness of PCM material for a given geography and period. The Faiman module temperature transposition method has been used to convert ambient temperature to module temperature using Equation (2). The model is adopted in IEC 61853 standard and uses an empirical heat loss factor.

$$T_{PV} = T_a + \frac{E_{POA}}{U_0 + U_1 \times WS} \tag{2}$$

Solar irradiation availability data over a year is the key weather parameter for investment in a solar PV system. Having satellite and ground measured data will provide the necessary knowledge in determining the potential site. Another dominant weather parameter is ambient temperature. The project size-AC/DC ratio will vary based on the ambient temperature availability to compensate for the loss produced from high temperature operating conditions. To understand the distribution of weather parameters in hourly, daily, and monthly granularity, box plots have been used. Monthly, hourly average, maximum, and minimum temperatures. These plots will assist in identifying the right PCM material before testing it on the field conditions, knowing the thermal properties of the PCM. Apart from understanding the maximum and minimum of weather parameters, it is imperative to understand the spread of weather parameters in ranges, in the sense of the distribution from the median and the density of the dataset.

7.1. UAE and Islamabad Irradiance

The distribution of irradiation for UAE and Islamabad locations is observed in this study. Over the year, during daytime hours the UAE location on average yields 543.38 W/m^2 with a peak irradiation of 1085.47 W/m^2 and 854.73 W/m^2 in the third quartile meaning 75% of time observed values in this range. Similarly, the Islamabad location yields 495.66 W/m^2 on average with a peak irradiation of 1030.25 W/m^2. Figure A1 "Month" January has recorded the lowest irradiance on an average of 261.44 W/m^2 with the maximum of 994.4 W/m^2 and the month of May has recorded the highest irradiance of 325.25 W/m^2 with a maximum of 1040.36 W/m^2. Subsequently, for the Islamabad location, the monthly average of irradiation over the year has been studied, Explicitly the month of May has seen a higher distribution with an average of 334.5 W/m^2 with a maximum and minimum of 1015.4 W/m^2 and 16.12 W/m^2, respectively.

Figure A1 "hour": For instance, hourly distribution of irradiation has to be studied to ensure the active time of PCM's utilization. During the early daytime hour of 07:00, the average irradiation is 250.91 W/m^2. At a peak hour from 12:00 to 12:59, the average irradiation is 914.40 W/m^2 with a maximum of 1085.7 W/m^2. Figure A2: For Islamabad location, the average irradiation during a peak hour noon is 789 W/m^2 with a peak of 1030.25 W/m^2.

7.2. Ambient Temperature of UAE and Islamabad

Ambient temperature is an important weather parameter that estimates the generation for a given geography with higher precision, as it directly affects voltage generation from a solar PV system. For any geography understanding, a temperature profile is necessary in terms of the site feasibility study. On average, UAE has recorded 30.5 °C with a maximum and minimum temperature of 47.2 °C and 5.2 °C, respectively. Furthermore, for a location such as Islamabad, the average ambient temperature is 25.5 °C with a maximum and minimum of 48.56 °C and 6.43 °C, respectively.

Figure A3 ″Month″ depicts the highest and lowest temperature recorded during July and December, respectively. For July, the average temperature is 35.09 °C with maximum and minimum temperatures of 47 °C and 26.5 °C, respectively. For December, the maximum and minimum temperatures are 29.7 °C and 18.57 °C, respectively. Figure A4: For Islamabad location, the average and maximum ambient temperatures are 34.12 °C and 48.56 °C during May. Figure A3 ″hour“ hourly ambient temperature distribution depicts that morning 06:00–07:00 recorded a lower temperature and 12:00 to 13:00 recorded the highest temperature over the year. The average temperatures during the hour 07:00 and 13:00 are 25.06 °C and 32.8 °C, respectively. The maximum and minimum temperatures are 46 °C and 17.12 °C for the hour 13:00 and 39.4 °C and 19 °C for the hour 07:00. From Figure A4 for Islamabad, the average and maximum recorded ambient temperatures were 31.2 °C and 48.53 °C at hour 12:00.

7.3. Wind Speed of UAE and Islamabad

Wind speed helps in reducing the module temperature naturally by convective heat transfer. The higher the wind speed the higher the heat dissipation. Choosing a site with a high average wind speed potentially increases the yield not just by dissipating the heat, but also by the deposition of soil on the surface of the panel.

For the UAE location, the average wind speed during the daytime hours over a year is 4.35 m/s, and the maximum wind speed reaches up to 24.2 m/s and 1.41 m/s on average for Islamabad. Figure A5: “Month” depicts during June there was a higher distribution of wind speed. The average wind speed is 4.95 m/s with the maximum and minimum of 15 m/s and 0.1 m/s, respectively. In the 3rd quartile, the recorded wind speed is 6.2 m/s. Figure A6 for Islamabad 2.08 m/s on average with a maximum wind speed of 4.01 m/s during May. Figure A5: “hour” depicts the hours 12:00 and 17:00 carrying a large distribution. From 12:00 to 13:00 over the year the average recorded wind speed is 4.76 m/s with a maximum and minimum of 13.1 m/s and 0.5 m/s. At 17:00 the maximum wind speed of 24.2 m/s with an average of 5.3 m/s. Figure A6: At hour 11:00, average wind speed is 1.11 m/s.

7.4. PV Module Temperature of UAE and Islamabad

Module temperature maintaining close to STC is one of the ways to increase the yield. The average module temperature is 33.48 °C, the maximum and minimum module temperature is 76.59 °C and 4.161 °C for UAE and Islamabad the average module temperature over the year is 33.42°C and the maximum temperature is 82.77 °C. Figure 13 “Month”: On average, January recorded the lowest temperature. From Figure 13 it is clear that the average module temperature is 24.02 °C, which is less than the nominal operating cell temperature. These temperatures are sufficient to set up the PCM for the later part of reducing the temperature of the module at a high operating cell temperature. The minimum and maximum temperatures are 10.49 °C and 58.06 °C, respectively. From Figure 13, the month of July has seen vigorous environmental conditions to run the solar PV system efficiently;

these are the months required for an external cooling system to improve the performance of a solar PV system. The average, maximum, and minimum temperatures are 40.96 °C, 76.59 °C, and 26.17 °C, respectively. From Figure 14, the average module temperature is 43.35 °C and the maximum temperature is 82.77 °C during May. Figure 13 "Hour" for UAE: During the peak daytime hour of 12:00 the average cell temperature is 52.04 °C, the maximum and minimum temperatures are 75.02 °C and 20.45 °C, respectively. Figure 14: for Islamabad location 55.23 °C on average and 78.53 °C at 12:00.

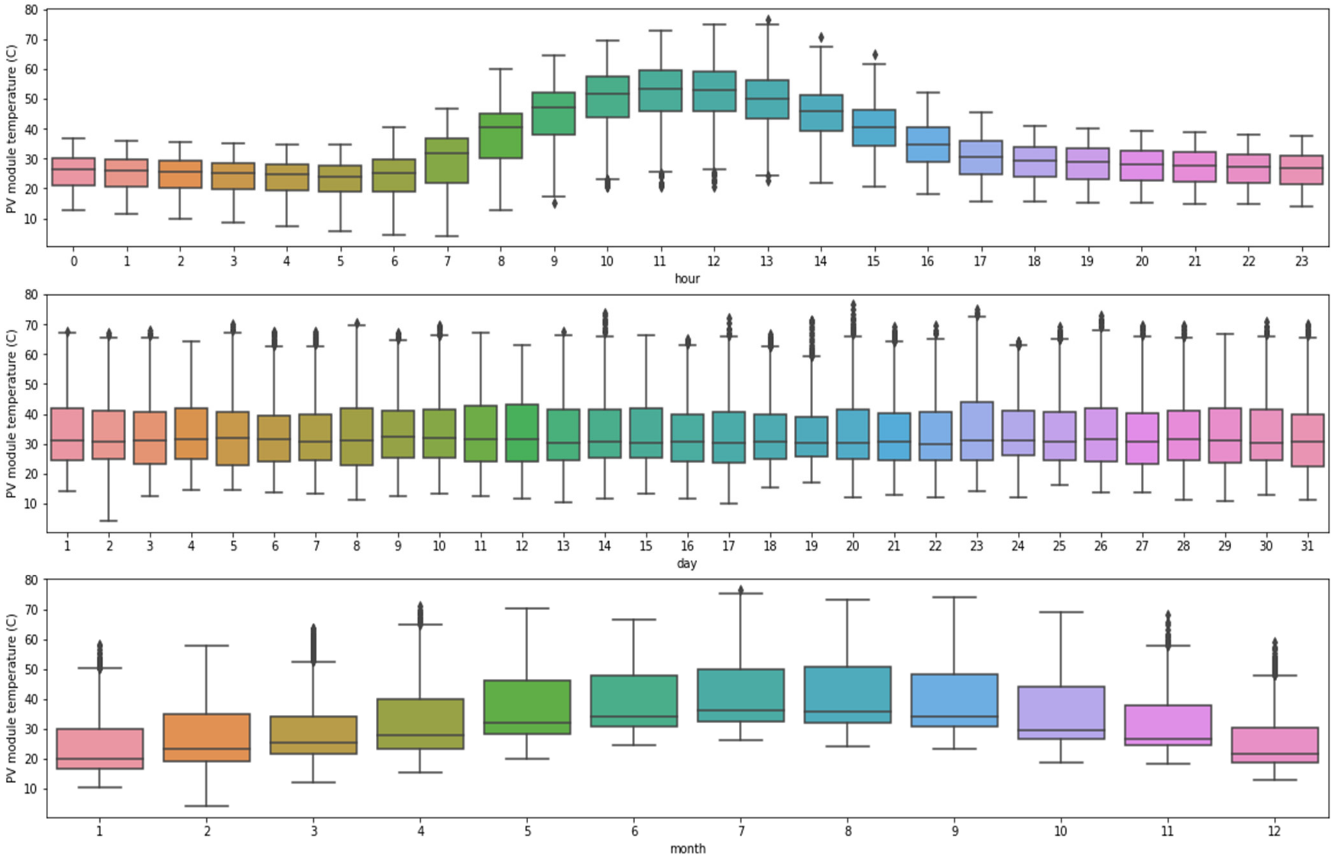

Figure 13. Hourly, daily, and monthly PV temperature for UAE location.

7.5. PV-PCM Performance Assessment

7.5.1. PV Temperature and PV-PCM Temperature

Figure 15 depicts the peak module temperature for each month and the experimental values of a PV-PCM for the respective months are plotted against each other. Year around PV-PCM temperature was lower as compared to the PV module temperature. From the figure, the maximum temperature is 76.59 °C while the PV-PCM temperature is 66.52 °C. That precise hour shows a difference of 10 °C in temperature reduction. Similarly, the lowest ones are 57.2 °C and 47 °C for February.

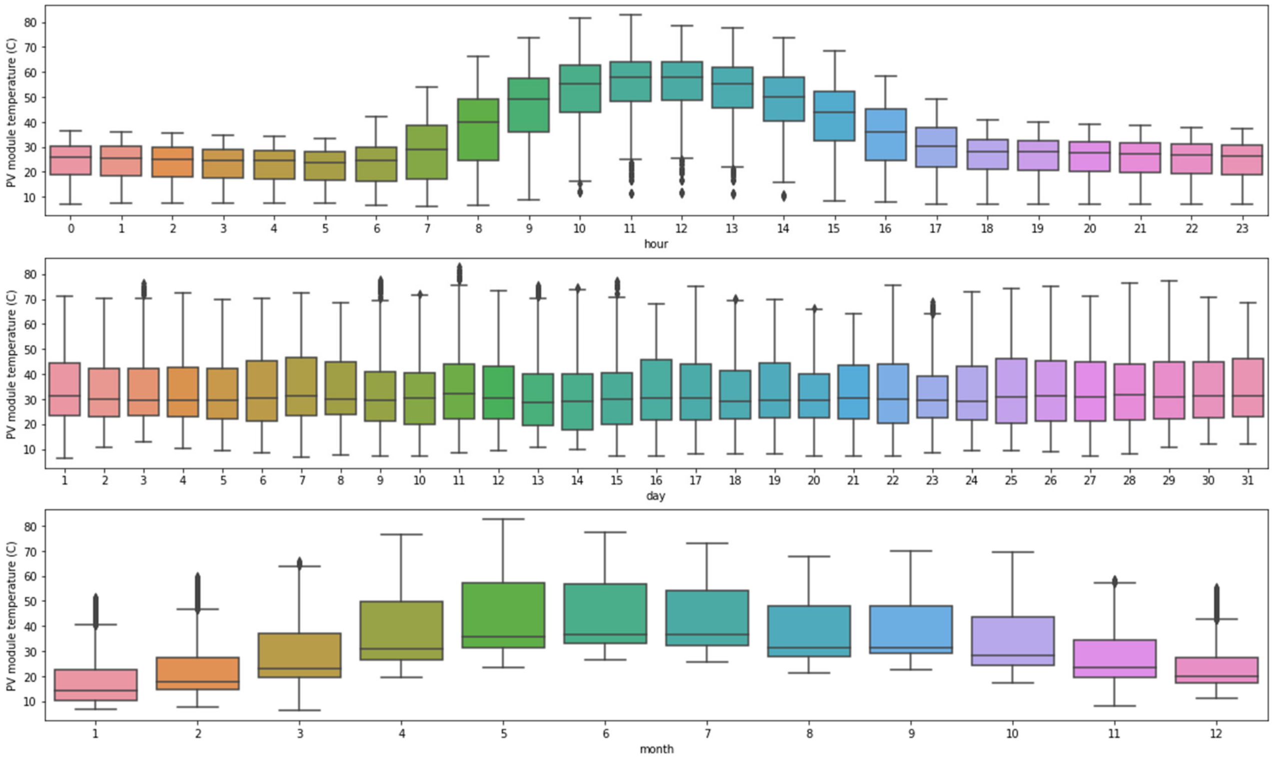

Figure 14. Hourly, daily, and monthly PV temperature for Islamabad location.

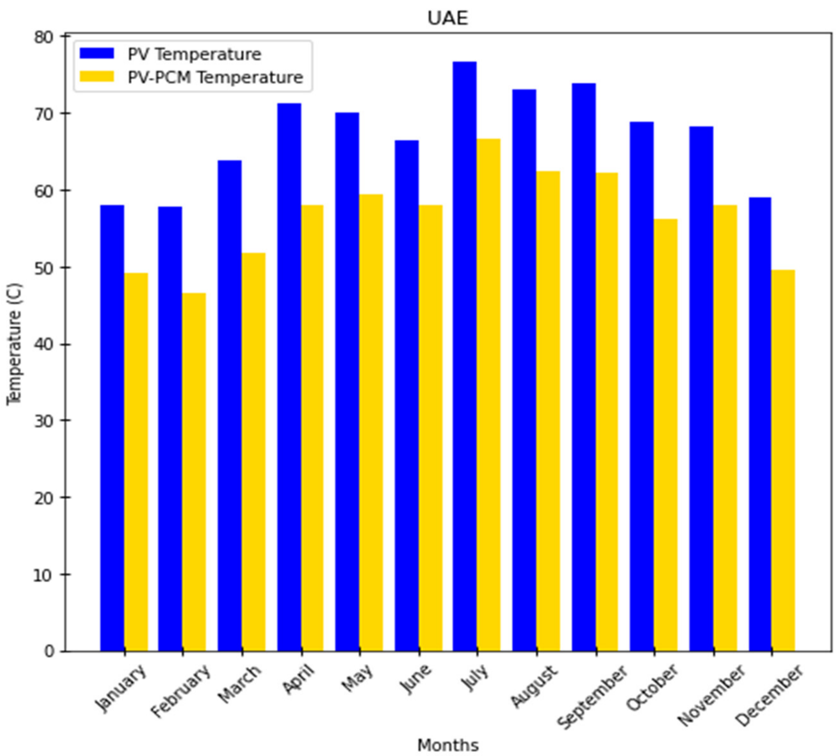

Figure 15. Temperature profile of PV and PV-PCM for UAE.

Figure 16. For Islamabad location during May (the hottest month), the PV module temperature is 81.2 °C, while the PV PCM temperature is 72.1 °C. Similarly, January has recorded the lowest temperatures. The PV module temperature is 52.1 °C while the PV-PCM temperature is 42.3 °C.

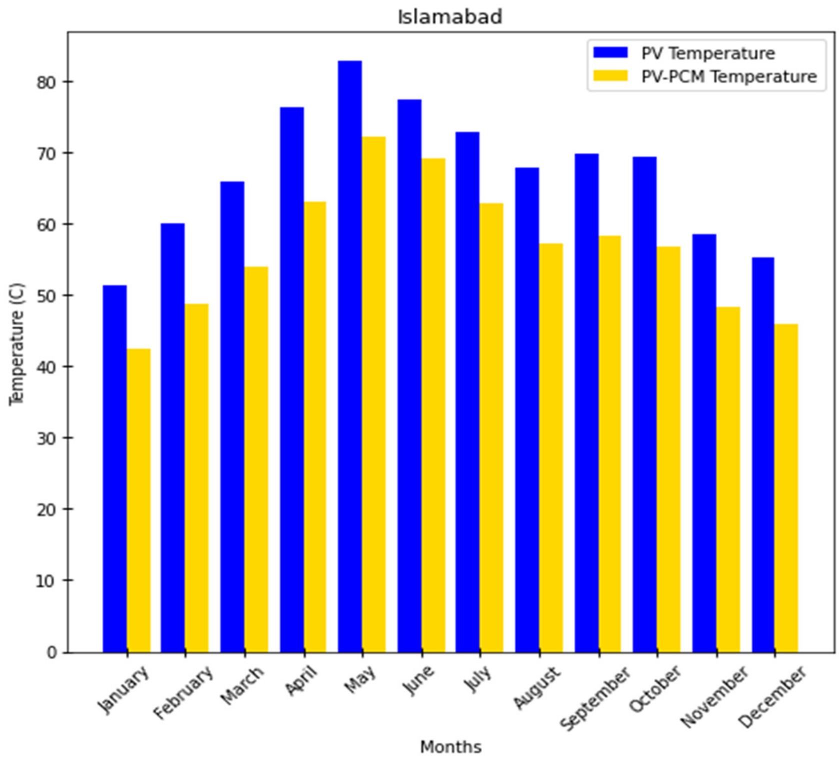

Figure 16. The temperature profile of PV and PV-PCM for Islamabad.

7.5.2. Power Profile of PV and PV-PCM for UAE and Islamabad

To examine the impact of the PV module and PV PCM temperature, an MW scale solar PV system was designed. A 400 Wp Mono-crystalline solar panel with a temperature degradation coefficient(β) of −0.36%/°C is considered. A 15 MW Solar PV system with a 400 Wp panel requires 37500 panels with 20 panels in series and 1875 in parallel. Theoretically, power was calculated for given irradiation, module temperature, reference temperature, temperature degradation coefficient, and capacity using Equation (3) [165,166].

$$Power = (\mathrm{POA} \times 0.001 \times \mathrm{pdc} \times (1 + \beta * (T_{PV} - T_{STC}))) \tag{3}$$

DC losses applied in Equation (4) are explicitly modeled percentages available in PV-watts NREL that were considered. Default percentage for loss parameters such as soiling 2%, mismatch 2%, shadow 3% wiring 2%, light-induced degradation 0.5%, and nameplate rating 1% applied for both UAE and Islamabad locations.

$$\text{Loss total } (\%) = 100 \times [1 - \pi_i \left(1 - \frac{L_i}{100}\right)] \tag{4}$$

Estimated power (MW) with PV temperature and PV PCM temperature as shown in Figures 17 and 18. For UAE location the enhancement of power generation during peak hours occurred throughout the year, during February and March even for low insolation produced a maximum power because of low operating conditions. In March, the UAE location saw a rise from 12.41 MW to 13.04 MW as a result of using PV PCM. Similarly, for the Islamabad location during March, 11.55 MW of power generation enhanced to 12.13 MW with the advent of PV PCM temperature.

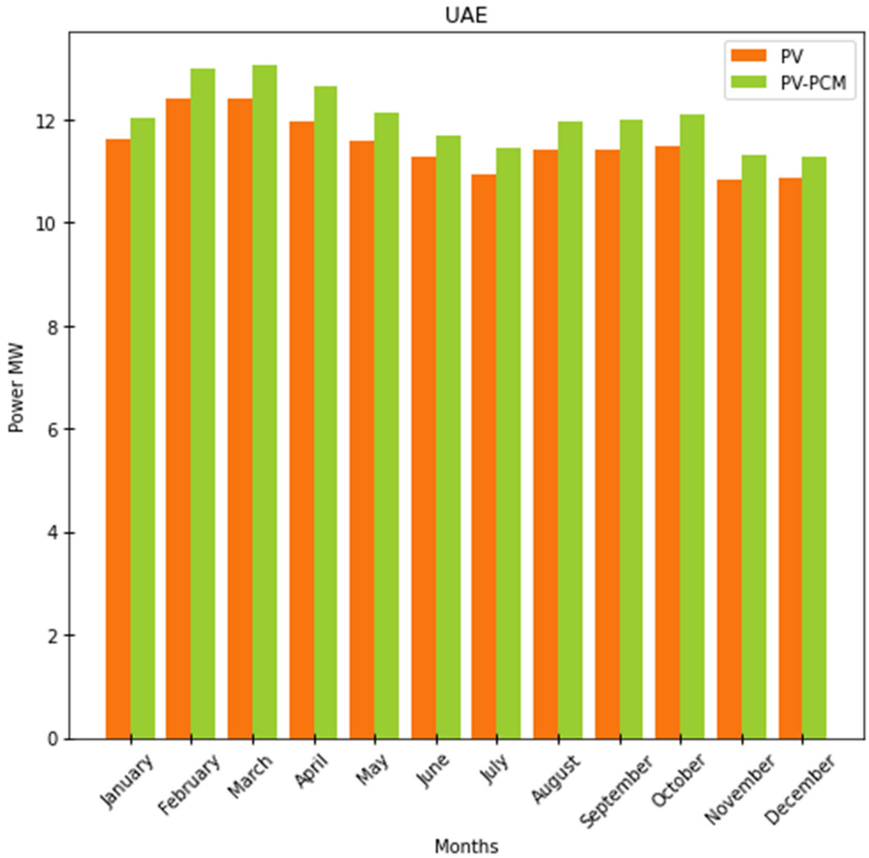

Figure 17. Power profile of PV and PV-PCM for UAE location.

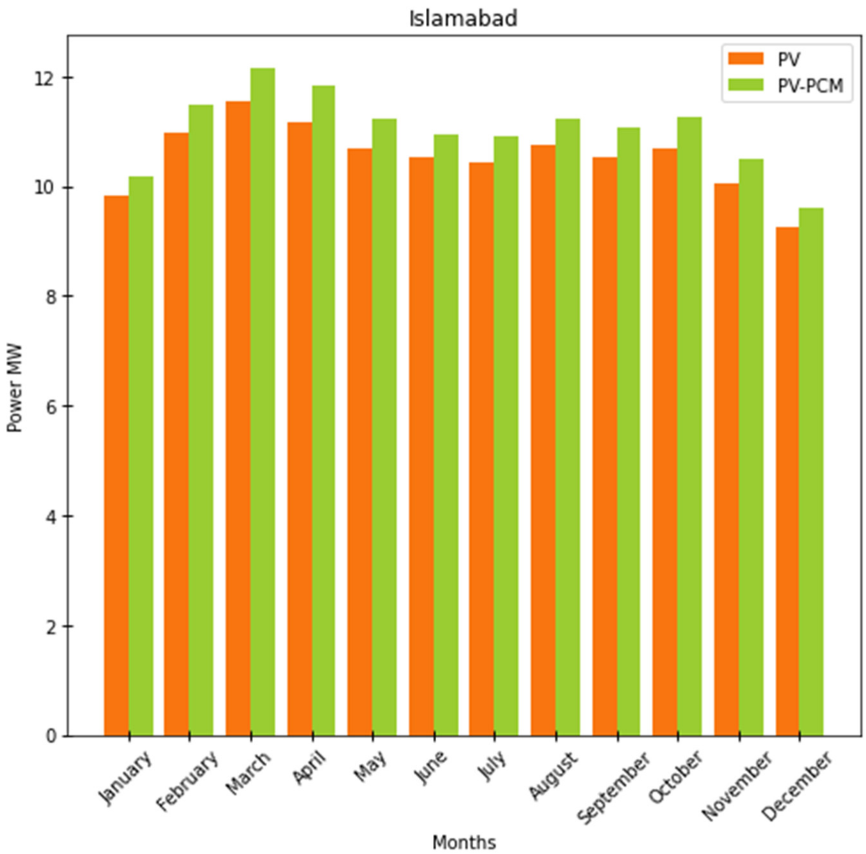

Figure 18. The power profile of PV and PV-PCM for the Islamabad location.

7.5.3. Performance Ratio Metric for UAE and Islamabad

Equation (5) was used to calculate the performance ratio (PR) of the solar power plant. The percentage of power increased was validated with the help of performance metrics IEC 61724. The percentage of PR increased is phenomenal for UAE locations for February, March, and April by 4.42%, 4.78%, and 5.39% respectively as shown in Figure 19. For February, PR improved from 78.17% to 82.59%. Similarly, Islamabad location during March, April, and September saw a rise in PR by 4.82%, 5.50%, and 4.82%, respectively, as shown in Figure 20. In April, PR improved from 72.26% to 77.77%.

$$PR = \frac{Generated\ output\ power}{Installed\ capacity \times \frac{Solar\ irradiation}{1000}} \quad (5)$$

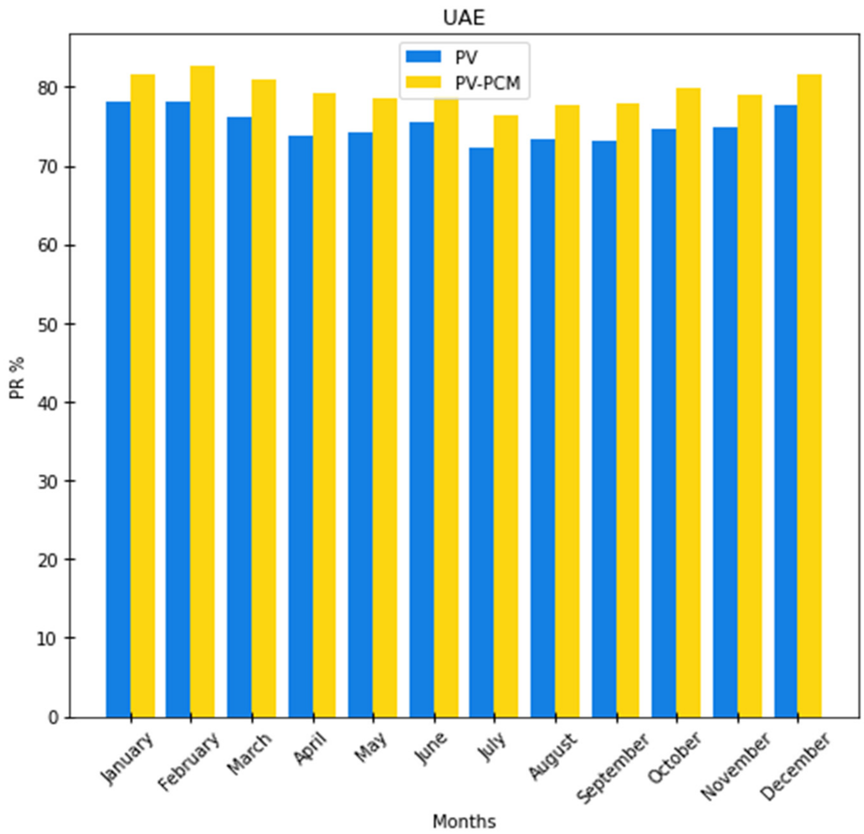

Figure 19. Performance ratio of PV and PV-PCM for UAE location.

7.5.4. Power Generation Correlation Concerning PV-PCM Temperature

Figure A7 depicts the power generation (MW) concerning irradiation and module temperatures. A lower module temperature is recorded during December and 11.27 MW is generated for a peak module temperature of 48 °C. It is clear that even for low irradiation the output from the system is high, because the peak PV-PCM temperature is low. During July, even for high irradiation, the generation is 11.4 MW and PV-PCM temperature is 64.27 °C. Figure A8 depicts 12.3 MW at 55 °C peak PV-PCM temperature and 11.25 MW at 72 °C PV-PCM temperature.

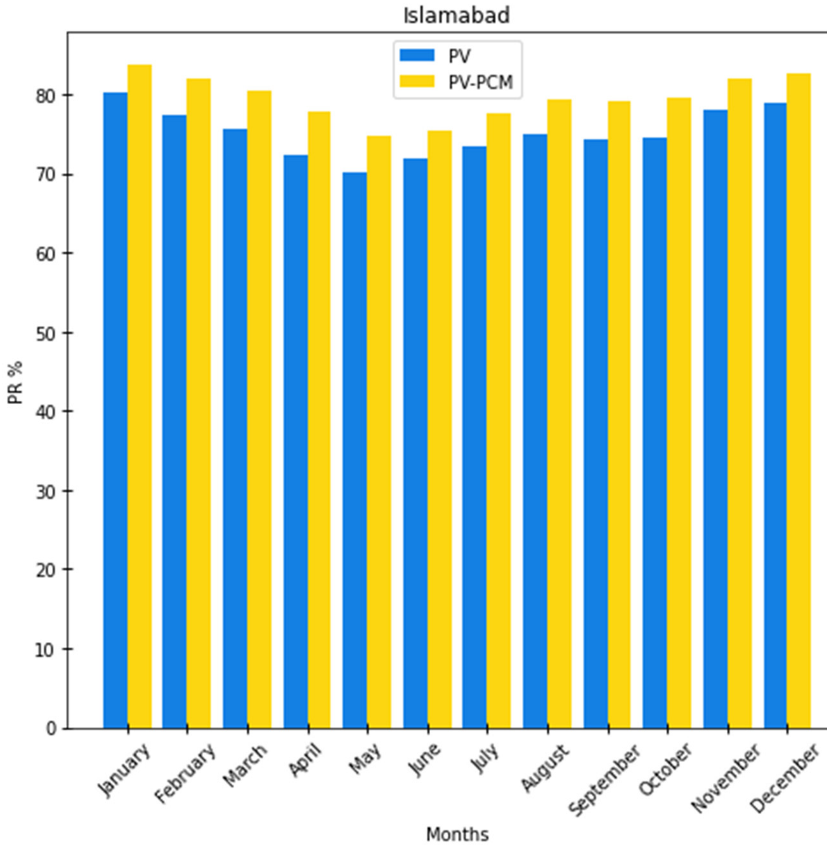

Figure 20. Performance ratio of PV and PV-PCM for Islamabad location.

From Table 8 for UAE's location, the maximum PV temperature for each month has been considered to analyze the peak performance of a PV-PCM. It is observed that PV-PCM temperature is always lower than the PV module temperature, indicating high certainty of improved performance of the PV module over the year. This is evident from Table 8 as the power (MW) improved by 4.36% on average. Similarly, from Table 9, for Islamabad location, PV-PCM temperature shows a lower trend as compared to PV temperature. This is evident with the power (MW) enhancement. The average increase in power output percentage is 4.35%.

Table 8. UAE power and PR profile for PV and PV-PCM.

Month	Plane of Array (W/m^2)	PV (°C)	PV-PCM (°C)	Power (PV) MW	Power (PV-PCM) MW	Power %	PR (PV) %	PR (PV-PCM) %
January	991.21	58.06	49.21	11.61	12.03	3.49	78.10	81.59
February	1057.67	57.84	46.51	12.40	12.98	4.42	78.17	82.59
March	1085.47	63.77	51.77	12.42	13.04	4.78	76.28	81.06
April	1078.37	71.25	58.05	11.95	12.63	5.39	73.89	79.29
May	1040.36	70.03	59.43	11.59	12.12	4.36	74.28	78.64
June	998.19	66.39	58.06	11.30	11.69	3.40	75.44	78.85
July	1011.51	76.59	66.59	10.95	11.44	4.23	72.19	76.42
August	1039.53	73.09	62.49	11.43	11.96	4.41	73.30	77.72
September	1043.12	73.84	62.24	11.43	12.01	4.82	73.06	77.89
October	1025.47	68.82	56.22	11.49	12.10	5.11	74.67	79.78
November	966.13	68.19	57.97	10.85	11.32	4.17	74.87	79.04
December	931.74	58.97	49.57	10.87	11.29	3.71	77.81	81.52

Table 9. Islamabad power and PR profile for PV and PV-PCM.

Month	Plane of Array (W/m^2)	PV (°C)	PV-PCM (°C)	Power (PV) MW	Power (PV-PCM) MW	Power %	PR (PV) %	PR (PV-PCM) %
January	817.07	51.32	42.47	9.84	10.18	3.40	80.25	83.65
February	944.73	60.02	48.69	10.98	11.49	4.46	77.48	81.93
March	1019.26	65.99	53.99	11.55	12.14	4.82	75.57	80.39
April	1030.25	76.33	63.13	11.17	11.82	5.51	72.27	77.78
May	1015.96	82.77	72.17	10.70	11.22	4.60	70.21	74.81
June	976.91	77.43	69.1	10.54	10.93	3.56	71.92	75.48
July	949.22	72.85	62.85	10.45	10.90	4.17	73.38	77.55
August	954.65	67.84	57.24	10.74	11.22	4.32	74.98	79.30
September	945.56	69.83	58.23	10.54	11.07	4.74	74.34	79.09
October	957.3	69.37	56.77	10.70	11.27	5.12	74.49	79.61
November	860.64	58.52	48.3	10.06	10.48	4.02	77.95	81.97
December	780.44	55.37	45.97	9.24	9.59	3.66	78.96	82.62

Table 10 shows UAE's location average peak PV temperature over the year is 67.23 °C; with the advent of PCM the average peak PV temperature dropped to 56.50 °C (PV-PCM temperature), which is clear in the power output and performance ratio (PR). The PR (%) on a peak PV temperature and PV-PCM temperature has increased from 79.53% to 75.17% on average over the year. While for the Islamabad location, the average peak PV temperature over the year is 67.30 °C and with PV-PCM the PR (%) of the PV system increased from 79.51% to 75.15%. Comprehensively, both the locations have similar weather conditions over the year.

Table 10. Average power and PR profile for Islamabad and UAE.

Location	Maximum Plane of Array (W/m^2)	Average T_{PV} (°C)		Average PR (%)		Average Power (MW)	
		PV	PV-PCM	PV	PV-PCM	PV	PV-PCM
Islamabad	1030.25	67.30	56.57	75.15	79.51	10.54	11.02
UAE	1085.47	67.23	56.50	75.17	79.53	11.52	12.05

8. Conclusions and Future Prospects

Several researchers claim that reducing T_{PV} enhances the electrical conversion efficiency of the PV module. Conventional, water, and air-assisted cooling techniques were widely performed, followed by TEG, heatsink, and other techniques. However, effective PV module cooling is questionable for several locations due to resource unavailability. In recent years, PCM has broken the availability of a cooling process that helps control the excess rise in T_{PV} for all locations. PCM is a stationary unit with a minimum lifetime of 5 years and is readily available in the local market.

- PCM can store a high amount of thermal energy within a small quantity, which makes PCM unique as a sensible heat storage material. In such a way, paraffin wax and Rubitherm commercial PCM's are widely used and have achieved higher T_{PV} reduction. However, PCM also lacks several issues that question the performance of the PCM integration.
- PCM is a low thermal conducting material that creates a thermal conduction barrier during charging and discharging mode. Several researchers claim that an increase in the thickness of PCM also creates the conduction barrier. Further, thermal conductivity enhancers are used to increase the K_{PCM}. In such a way, interfin plays a major role in PV module cooling techniques than nano compounds and metal-based enhancers. Secondly, non-metal-based thermal enhancers have gained higher attention in the cooling process, especially EG. The main benefit of EG as a thermal enhancer will not increase the weight of the system and is free from corrosion.

- A further increase in the thickness of PCM failed to discharge the entire stored thermal energy in the nighttime that causes to fail the consecutive charging process. To minimize this loss, thermal collectors or heat pipes are attached inside the PCM to remove the thermal energy from the PCM by flowing working fluid inside the tube. Notably, heat from the PCM is utilized for thermal comforts such as heating and ventilation processes. Secondly, the thermal collector minimizes the usage of PCM and conduction barriers.
- From this study, it is clear that before experimenting with PCM, numerical or theoretical work has to be carried out to optimize the T_{melt} of PCM and appropriate thickness. Inappropriate PCM T_{melt} postpones or prepones the cooling process that makes PCM ineffective. If the selected PCM T_{melt} is less than the optimal range, the cooling process will start in the early daytime and end before the peak daytime. If the selected PCM T_{melt} is higher than the optimal range, PCM will initiate the cooling process in late peak daytime. In such a case, PCM turns ineffective and creates a negative effect on increasing the thermal resistance and T_{PV}. These two surveys will reduce the negative impact of the PCM integration. EG is recommended as a thermal enhancer rather than interfin because EG will not increase the system's total weight such as a conventional thermal enhancer. Moreover, eutectic PCM played a minor role in the PV module cooling technique because it is not readily available PCM. However, organic eutectic material is thermally stable for more than 2000 thermal cycles. Further, it is recommended to use the effectiveness of eutectic material to cool the PV module and minimize PCM's cost.
- Case study: NREL resource data associated with experimental values were implemented upon two geographical locations—UAE and Islamabad. Theoretical power output was compared between PV and PV-PCM temperature. Results indicate that throughout the year the PV-PCM outperforms PV module temperature; more specifically, February, March, and April showed an increased electrical output power by 4.42%, 4.78%, and 5.39%, respectively Similarly, Islamabad location during March, April, and September saw a rise in performance by 4.82%, 5.50%, and 4.82%, respectively.
- Analyzing resource data before any geographical location would help determine a suitable PCM. Having higher insolation, low average temperature, windy conditions, and a module with a good thermal coefficient would ensure higher yield and reduced loss. Economically, this reduces the payback period and cuts the project cost by enabling a reduced AC/DC ratio(sizing).

Author Contributions: Conceptualization, K.V.; methodology, K.V. and R.M.E.; writing—original draft, K.V., V.K. and K.E.; visualization, K.V., P.V.D. and J.A.D.; investigation, R.M.E., P.V.D., V.K., T.B.K., J.A.D., M.S.C., B.S.A.E.K. and E.-A.A.; writing—review and editing, R.M.E., V.K., T.B.K., J.A.D., K.T., B.S.A.E.K. and E.-A.A.; resources, K.V., K.T. and M.S.C.; validation, K.V. and K.T.; supervision, K.T. All authors have read and agreed to the published version of the manuscript.

Funding: This research was funded by Prince of Songkla University and the Ministry of Higher Education, Science, Research and Innovation, Thailand, under the Reinventing University Project (Grant Number REV64009).

Institutional Review Board Statement: Not applicable.

Informed Consent Statement: Not applicable.

Data Availability Statement: Not applicable.

Conflicts of Interest: Authors declare no conflict in interest.

Nomenclature

Q	Total amount of heat energy stored in the PCM
T_i	Initial or starting temperature
T_m	Melting temperature
m	Mass of PCM
$C_{p,s}$	Solid specific heat capacity
L	Latent heat of fusion
$C_{p,l}$	Liquid specific heat capacity
T_e	Ending temperature
T_{PV}	PV module temperature
T_a	Ambient temperature
E_{POA}	Irradiance plane of array
U_0	Constant heat transfer co-efficient
U_1	Convective heat transfer co-efficient
WS	Wind speed
POA	Plane of array irradiation W/mm
T_{PV}	PV module temperature
T_{STC}	Standard test temperature
β	Temperature co-efficient (0.0036 per °C for STC)
Pdc	Capacity

Appendix A

Table A1. List of PCM used for T_{PV} reduction.

Type of PCM	T_{melt} (°C)	Latent Heat of Fusion (J/g)	Location	Temperature Drop (°C)	Ambient Temperature (°C)	Solar Irradiance (W/m^2)	Reference
RT25 [167]	26.6	232	Indoor	-	20	1000	[86]
Paraffin wax [168]	32	251	Indoor	-	20	1000	[86]
Aluminum [169]	-	-	Indoor	-	20	1000	[86]
GR 40 [167]	43	82	Belfast, UK	-	23	750	[124]
Paraffin wax [170]	57	255	Rajasthan, India	16	-	1900	[98]
RT42 [167]	38–43	165	Venice	42	-	900	[103]
RT55 [167]	51–57	170	Abhudabi	10	-	820	[103]
Paraffin wax	42–44	130	Indoor	8	23	1000	[82]
RT22 [167]	20–23	200	Indoor	-	23	1000	[82]
Ceresin [171]	61–78	160	Indoor	-	23	1000	[82]
OM 37 [172]	37	211	Lyon, France	-	23	875	[104]
RT 35 [167]	29–36	160	Malaysia	10	-	1000	[77]
Paraffin wax	59	137.67	Indoor	2.5	-	1000	[79]
RT42 [167]	38–43	165	Indoor	2.2	35	1000	[73]
RT 27 [167]		184	Greece	21	32	1020	[74]
Fatty acid ester (coconut oil) [173]	24	-	Seosan, South Korea	2	4	660	[71]
Petroleum jelly (Vaseline) [72]	44		Seosan, Soth Korea	5	4	660	[71]
S21 [174]	22	170	Australia	-	22	560	[102]
Paraffin wax	50		Malaysia	-	-	-	[105]
RT 35 [167]	29–36	160	Malaysia	10	35	1000	[78,175]
Paraffin wax	42–72	200–220	Iran	19	30	1050	[107]

Table A1. *Cont.*

Type of PCM	T_{melt} (°C)	Latent Heat of Fusion (J/g)	Location	Temperature Drop (°C)	Ambient Temperature (°C)	Solar Irradiance (W/m^2)	Reference
RT 35 [167]	34–36	240	Central Europe	11	-	550	[120]
RT 10HC [167]	9–10	200	Central Europe	8	-	100	[120]
RT 18HC [167]	17–19	260	Central Europe	12	-	550	[120]
RT 25HC [167]	22–26	230	Central Europe	11	-	500	[120]
Petroleum jelly [72]	44		Indonesia	6	26	1120	[72]
RT25HC	22–26	230	Indoor	-	20	1000	[88]
pure PCM (white petroleum jelly)	36–60		Lebanon	6.5	32	800	[99]
Pure PCM 70% + copper 20% + graphite 10%	36–80		Lebanon	6.3	32	800	[99]
RT25HC	22–26	230	Indoor	-	20	750	[97]
RT42 [167]	38–43	165	UAE	20	30	960	[56,106]
RT 27 [167]		184	Utrecht	12	12.2	-	[176]
Crude palm oil and coconut oil [177]			Indonesia	37	30	-	[80]
RT 27 [167]		184	Greece	5.5	19	-	[147]
RT 20 [167]	15–26	132.1	Greece	14	19	-	[147]
SP25A8	22–32	141.5	Greece	5	19	-	[147]
RT44	41–44	250	Pakistan	28.7	43	-	[83]
RT44	41–44	250	Pakistan	35	40	-	[57,178]
RT35	35	160	-	-	-	-	[149]
RT55	51–57	170	Egypt	10.6	39	1100	[150]
RT28	28	245	Slovenia	34	19	560	[151,179]
Paraffin wax	46–48	200–220	Iran	16	31	1000	[154]
PCM	45	-	China	-	20	540	[155]
RT	38–43	165	Croatia	-	31	905	[156]
Pork fat	36–45	170	Croatia	-	31	905	[156]
Paraffin wax	40	198	Malaysia	-	35	-	[180]
RT27	28	179	UK	10	24	926	[157,181]
Paraffin wax [182]	25	184	South Korea	4	26	240	[158]
RT35HC	34–36	240	Egypt	34	-	820	[159,183]
Paraffin wax	49	196	Malaysia	31	35	700	[163]
Lauric acid	44–46	228.90	Malaysia	8	36.5	999	[184]
Paraffin wax [154]	46–48	200–220	Iran	14	30	850	[185]
Paraffin wax	27.67	204.5	China	5	28	901	[186]
Paraffin wax	26–28		Italy	-	-	-	[187]
Octadecane [188]	28	244	Saudi arabia	30	-	-	[189]
Paraffin wax [190]	56	226	-	-	39	610	[191]
RT44HC	44	220	Qatar	14.5	40	900	[192]
RT50	50	130	Qatar	14	40		[192]
RT54HC	54	170	Qatar	20	40	900	[192]
Eutectic (capric: palmitic acid)	22.4	195	Ireland	10	-	-	[193]
Poly ethylene glycol 1000	38–40	159	Iran	15	-	-	[194]

Table A1. *Cont.*

Type of PCM	T_{melt} (°C)	Latent Heat of Fusion (J/g)	Location	Temperature Drop (°C)	Ambient Temperature (°C)	Solar Irradiance (W/m^2)	Reference
$Na_2HPO_4.12H_2O$	40	280	Spain	6	-	-	[195]
$Na_2SO_4.10H_2O$	32	251	Spain	9	-	-	[195]
Eutectic (capric-palmitic acid)	22.5 [196]	173 [196]	Ireland	7	24	950	[197]
Calcium chloride hexahydrate	29.8 [198]	191 [198]	Ireland	10	24	950	[197]

Appendix B

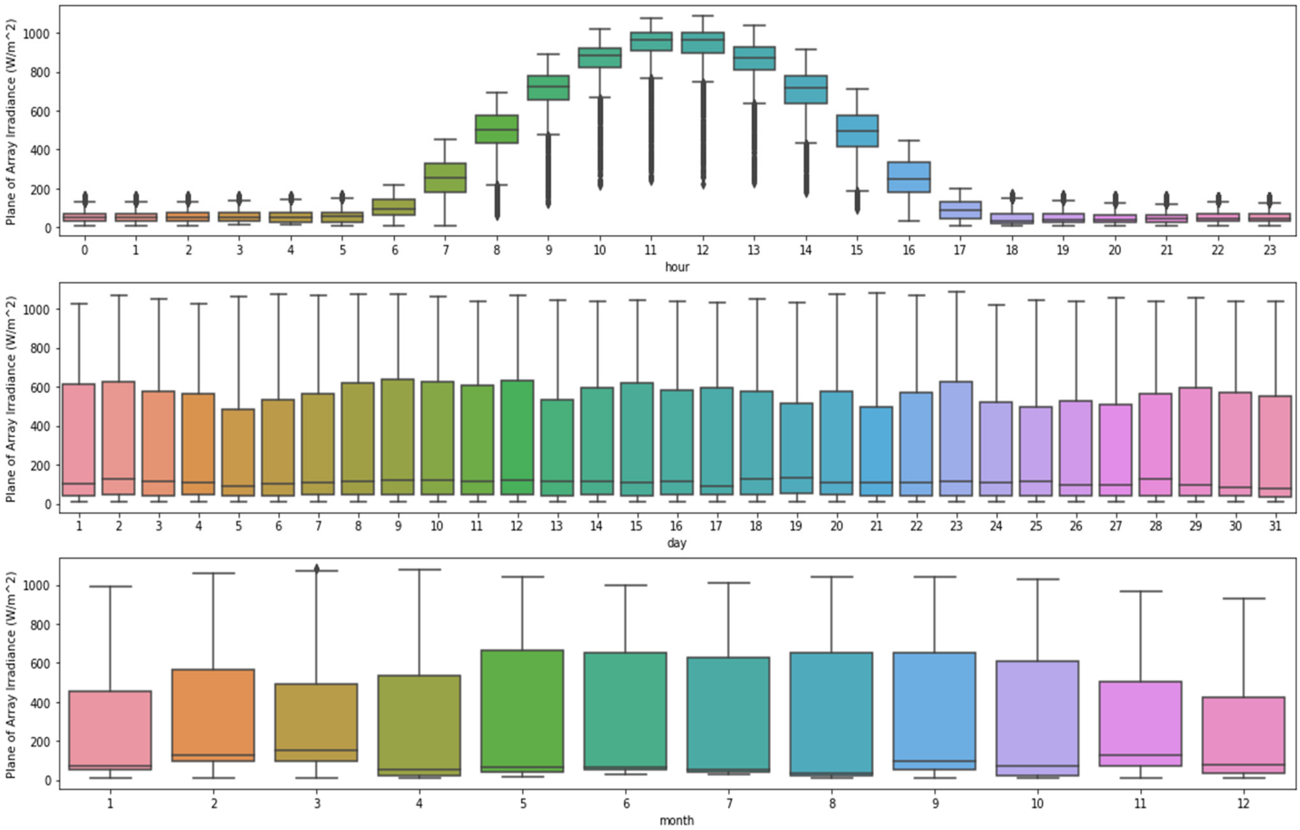

Figure A1. Hourly, daily, and monthly plane of array irradiation for UAE location.

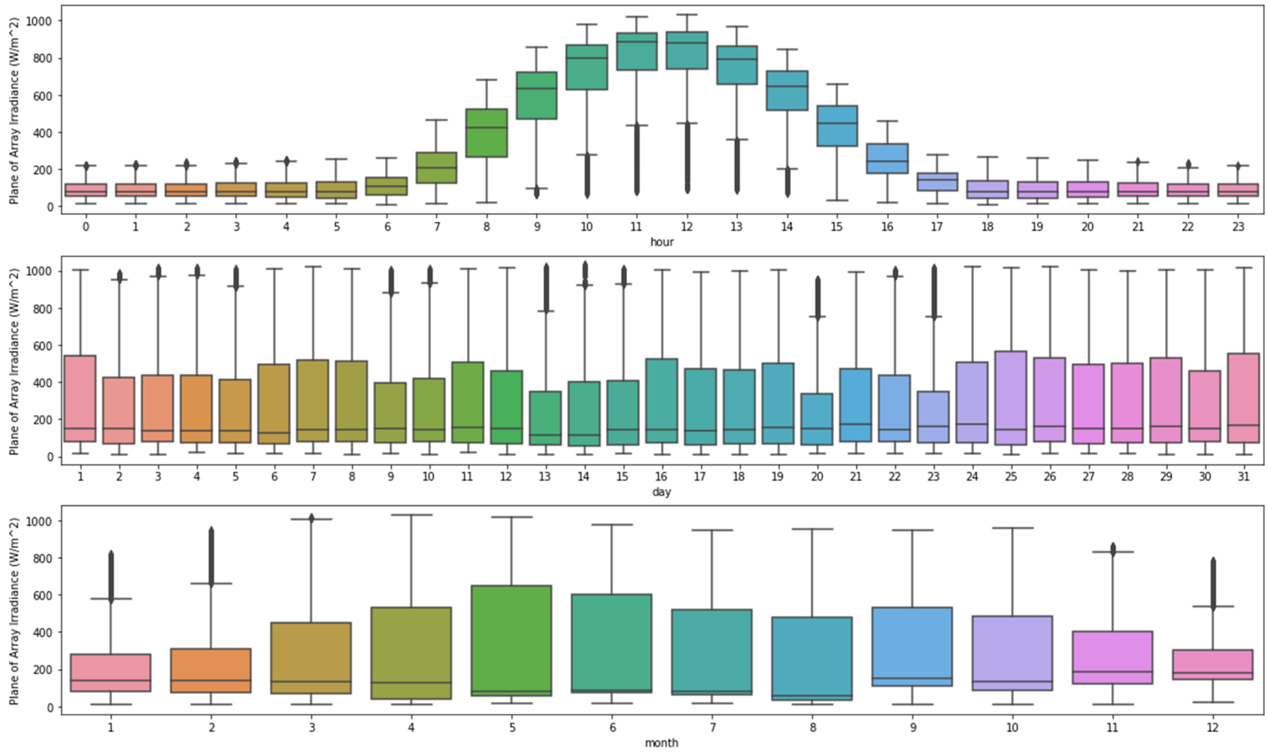

Figure A2. Hourly, daily, and monthly plane of array irradiation for Islamabad location.

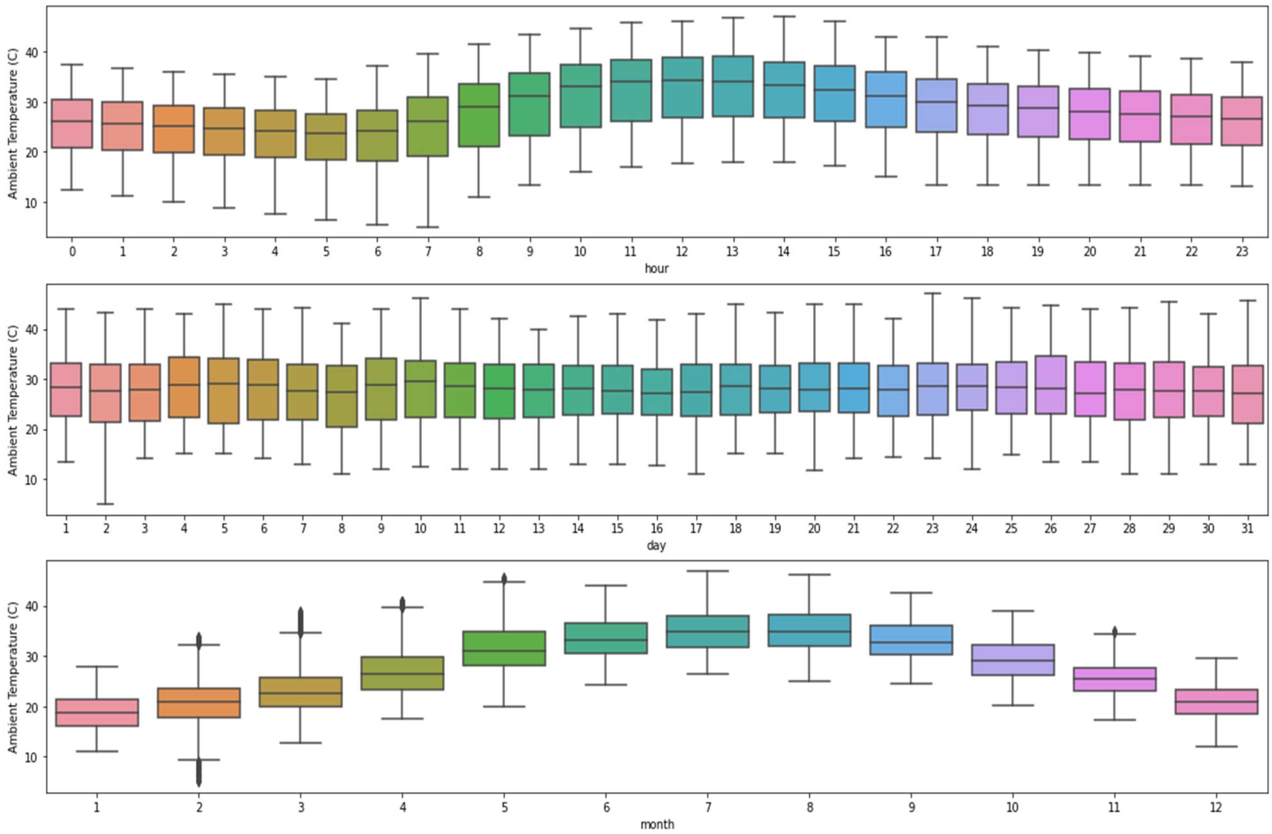

Figure A3. Hourly, daily, and monthly ambient temperature for UAE location.

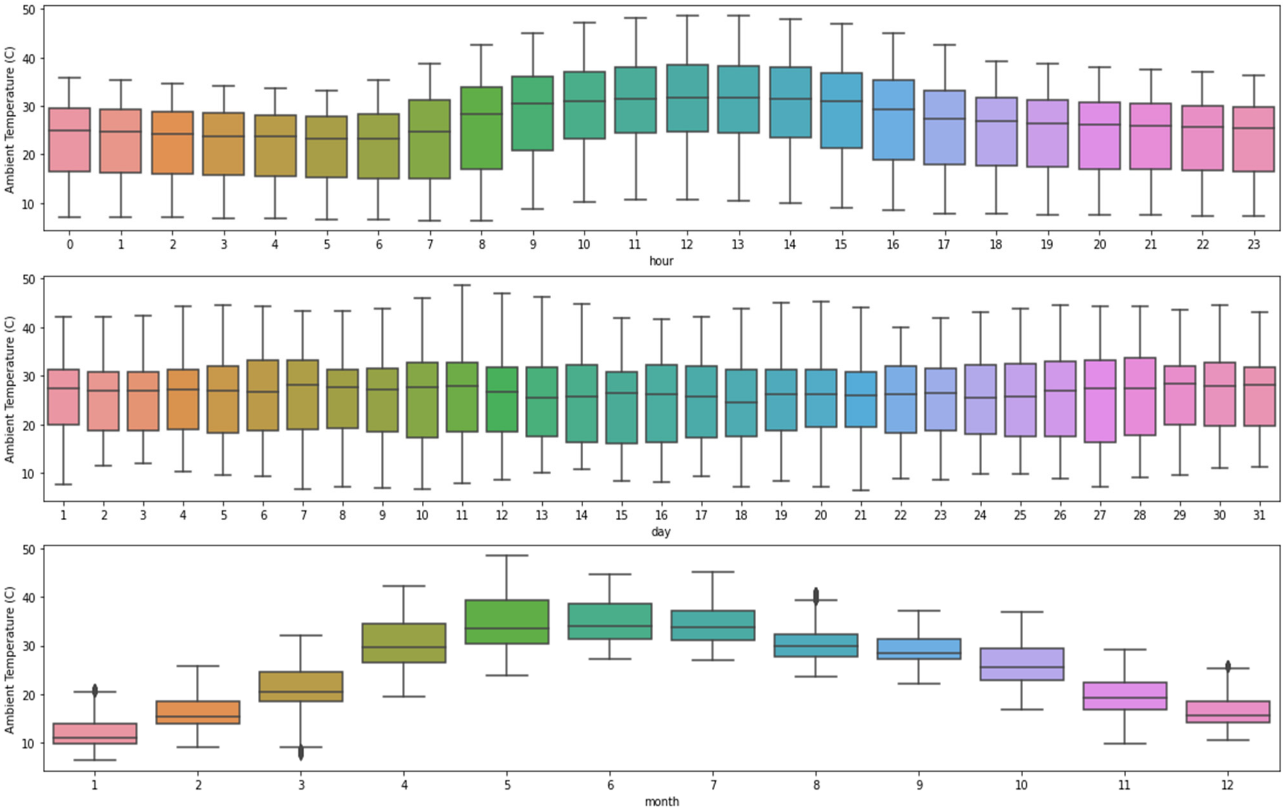

Figure A4. Hourly, daily, and monthly ambient temperature for Islamabad location.

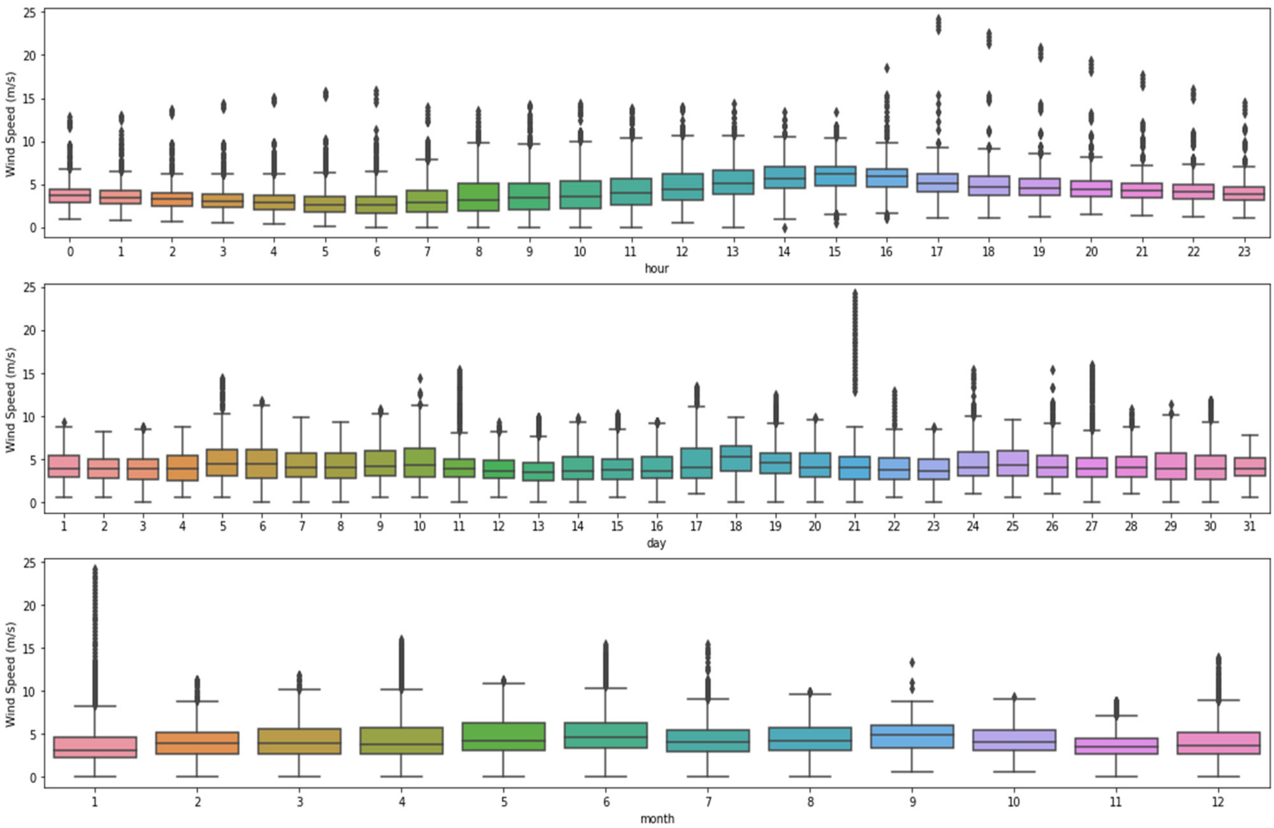

Figure A5. Hourly, daily, and monthly wind for UAE location.

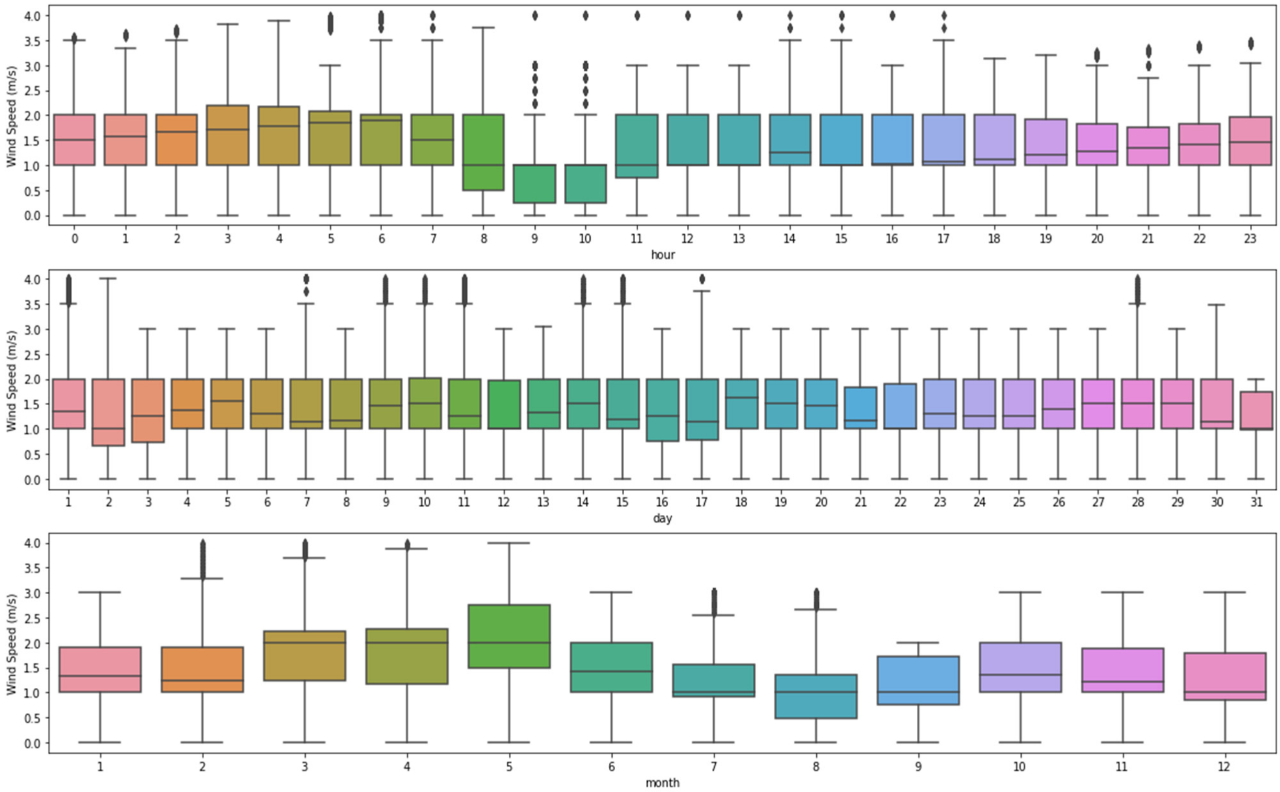

Figure A6. Hourly, daily, and monthly wind for Islamabad location.

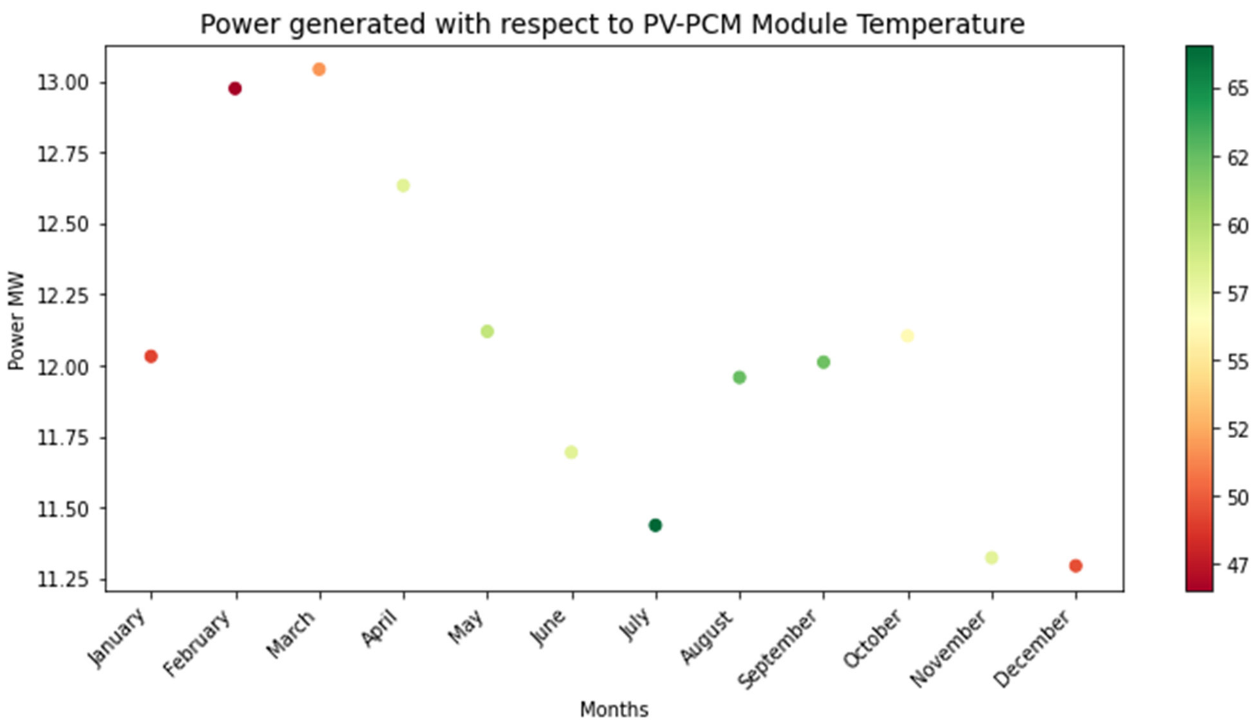

Figure A7. Monthly power and PV-PCM temperature correlation for UAE location.

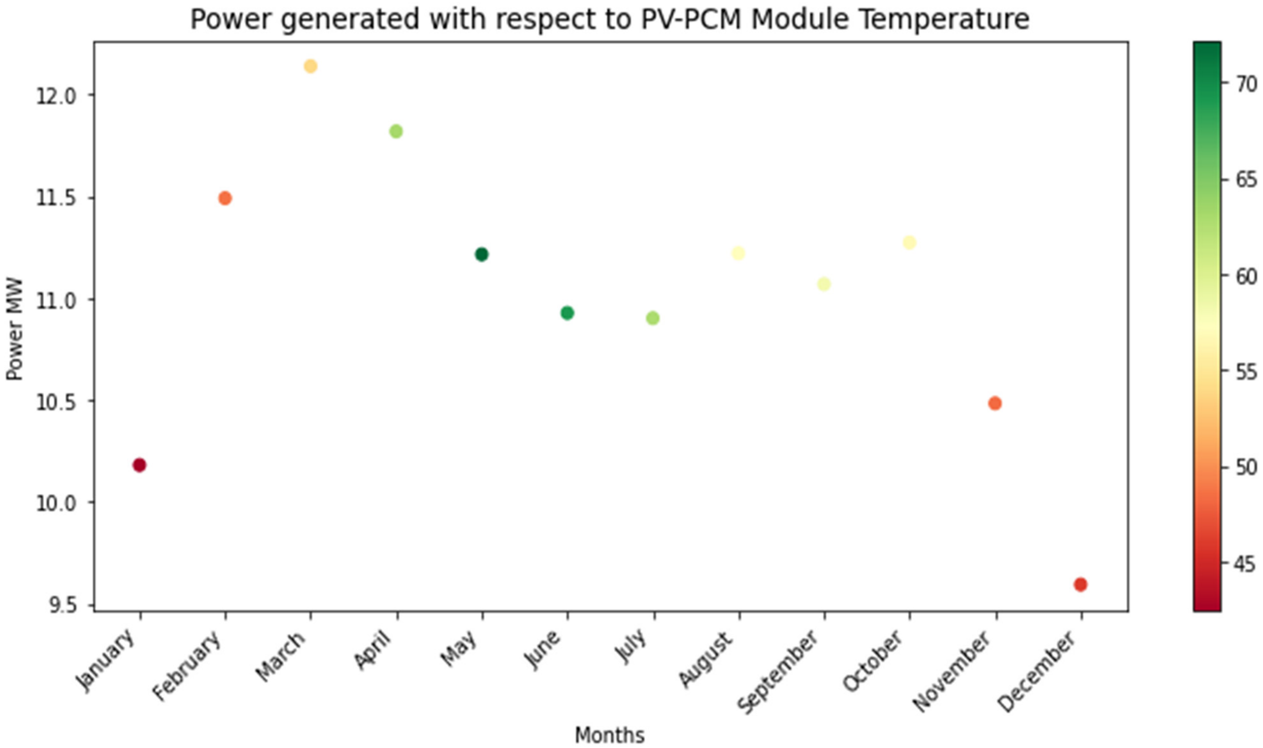

Figure A8. Monthly power and PV-PCM temperature correlation for Islamabad location.

References

1. Jin, X.; Chen, Y.; Wang, L.; Han, H.; Chen, P. Failure prediction, monitoring and diagnosis methods for slewing bearings of large-scale wind turbine: A review. *Measurement* **2021**, *172*, 108855. [CrossRef]
2. Xiao, G.; Chen, B.; Li, S.; Zhuo, X. Fatigue life analysis of aero-engine blades for abrasive belt grinding considering residual stress. *Eng. Fail. Anal.* **2022**, *131*, 105846. [CrossRef]
3. Zhong, C.; Li, H.; Zhou, Y.; Lv, Y.; Chen, J.; Li, Y. Virtual synchronous generator of PV generation without energy storage for frequency support in autonomous microgrid. *Int. J. Electr. Power Energy Syst.* **2022**, *134*, 107343. [CrossRef]
4. Enshasy, H.; Abu Al-Haija, Q.; Al-Muhaisen, S.; Al-Nashri, M.; Al-Amri, H. A Schematic Design of HHO Cell As Green Energy Storage. *Tien Tzu Hsueh Pao/Acta Electron. Sin.* **2019**, *3*, 9–15. [CrossRef]
5. Cazzaniga, R.; Rosa-Clot, M. The booming of floating PV. *Sol. Energy* **2020**, *219*, 3–10. [CrossRef]
6. Dabaieh, M.; Johansson, E. Building Performance and Post Occupancy Evaluation for an off-grid low carbon and solar PV plus-energy powered building. *A Case West. Desert Egypt. J. Build. Eng.* **2018**, *18*, 418–428.
7. Dini, H.S.; Putra, R.P. Automation and Mobile Phone Based-Monitoring Of Hydroponic Farming Style Using Solar Energy. *Acta Electron. Malays. (AEM)* **2021**, *5*, 5.
8. Velmurugan, K.; Karthikeyan, V.; Korukonda, T.B.; Poongavanam, P.; Nadarajan, S.; Kumarasamy, S.; Wongwuttanasatian, T.; Sandeep, D. Experimental studies on photovoltaic module temperature reduction using eutectic cold phase change material. *Sol. Energy* **2020**, *209*, 302–315. [CrossRef]
9. Zhang, X.; Tang, Y.; Zhang, F.; Lee, C.-S. A Novel Aluminum–Graphite Dual-Ion Battery. *Adv. Energy Mater.* **2016**, *6*, 1502588. [CrossRef]
10. Wang, M.; Jiang, C.; Zhang, S.; Song, X.; Tang, Y.; Cheng, H.-M. Reversible calcium alloying enables a practical room-temperature rechargeable calcium-ion battery with a high discharge voltage. *Nat. Chem.* **2018**, *10*, 667–672. [CrossRef]
11. Mu, S.; Liu, Q.; Kidkhunthod, P.; Zhou, X.; Wang, W.; Tang, Y. Molecular grafting towards high-fraction active nanodots implanted in N-doped carbon for sodium dual-ion batteries. *Natl. Sci. Rev.* **2020**, *8*, nwaa178. [CrossRef]
12. Cai, T.; Dong, M.; Liu, H.; Nojavan, S. Integration of hydrogen storage system and wind generation in power systems under demand response program: A novel p-robust stochastic programming. *Int. J. Hydrogen Energy* **2022**, *47*, 443–458. [CrossRef]
13. Li, X.; Gui, D.; Zhao, Z.; Li, X.; Wu, X.; Hua, Y.; Guo, P.; Zhong, H. Operation Optimization of Electrical-Heating Integrated Energy System Based on concentrating solar power plant hybridized with combined heat and power plant. *J. Clean. Prod.* **2020**, *289*, 125712. [CrossRef]
14. Wang, F.; Liu, X.-K.; Gao, F. Chapter 1—Fundamentals of Solar Cells and Light-Emitting Diodes. In *Advanced Nanomaterials for Solar Cells and Light Emitting Diodes*; Gao, F., Ed.; Elsevier: Amsterdam, The Netherlands, 2019; pp. 1–35.
15. Du, X.; Tian, W.; Pan, J.; Hui, B.; Sun, J.; Zhang, K.; Xia, Y. Piezo-phototronic effect promoted carrier separation in coaxial p-n junctions for self-powered photodetector. *Nano Energy* **2022**, *92*, 106694. [CrossRef]

16. Velmurugan, K.; Karthikeyan, V.; Korukonda, T.B.; Madhan, K.; Emsaeng, K.; Sukchai, S.; Sirisamphanwong, C.; Wongwuttanasatian, T.; Elavarasan, R.M.; Alhelou, H.H.; et al. Experimental Studies on PV Module Cooling with Radiation Source PCM Matrix. *IEEE Access* **2020**, *8*, 145936–145949. [CrossRef]
17. Chandel, S.S.; Agarwal, T. Review of cooling techniques using phase change materials for enhancing efficiency of photovoltaic power systems. *Renew. Sustain. Energy Rev.* **2017**, *73*, 1342–1351. [CrossRef]
18. Sharma, V.; Chandel, S.S. Performance analysis of a 190 kWp grid interactive solar photovoltaic power plant in India. *Energy* **2013**, *55*, 476–485. [CrossRef]
19. Ayompe, L.M.; Duffy, A.; McCormack, S.J.; Conlon, M. Measured performance of a 1.72 kW rooftop grid connected photovoltaic system in Ireland. *Energy Convers. Manag.* **2011**, *52*, 816–825. [CrossRef]
20. Shiva Kumar, B.; Sudhakar, K. Performance evaluation of 10 MW grid connected solar photovoltaic power plant in India. *Energy Rep.* **2015**, *1*, 184–192. [CrossRef]
21. Shravanth Vasisht, M.; Srinivasan, J.; Ramasesha, S.K. Performance of solar photovoltaic installations: Effect of seasonal variations. *Sol. Energy* **2016**, *131*, 39–46. [CrossRef]
22. Zhang, Y.; Shi, X.; Zhang, H.; Cao, Y.; Terzija, V. Review on deep learning applications in frequency analysis and control of modern power system. *Int. J. Electr. Power Energy Syst.* **2022**, *136*, 107744. [CrossRef]
23. Alami, A.H. Effects of evaporative cooling on efficiency of photovoltaic modules. *Energy Convers. Manag.* **2014**, *77*, 668–679. [CrossRef]
24. Fan, S.; Wang, Y.; Cao, S.; Sun, T.; Liu, P. A novel method for analyzing the effect of dust accumulation on energy efficiency loss in photovoltaic (PV) system. *Energy* **2021**, *234*, 121112. [CrossRef]
25. Verma, A.; Singhal, S. Solar PV Performance Parameter and Recommendation for Optimization of Performance in Large Scale Grid Connected Solar PV Plant—Case Study. *J. Energy Power Sources* **2015**, *2*, 40–53.
26. Abdolzadeh, M.; Ameri, M. Improving the effectiveness of a photovoltaic water pumping system by spraying water over the front of photovoltaic cells. *Renew. Energy* **2009**, *34*, 91–96. [CrossRef]
27. Moharram, K.A.; Abd-Elhady, M.S.; Kandil, H.A.; El-Sherif, H. Enhancing the performance of photovoltaic panels by water cooling. *Ain Shams Eng. J.* **2013**, *4*, 869–877. [CrossRef]
28. Wu, S.; Xiong, C. Passive cooling technology for photovoltaic panels for domestic houses. *Int. J. Low-Carbon Technol.* **2014**, *9*, 118–126. [CrossRef]
29. Phayom, W. Improvement of Photovoltaic Module for Increasing Energy Conversion Efficiency. *Appl. Mech. Mater.* **2014**, *448–453*, 1428–1432. [CrossRef]
30. Krauter, S. Increased electrical yield via water flow over the front of photovoltaic panels. *Sol. Energy Mater. Sol. Cells* **2004**, *82*, 131–137. [CrossRef]
31. Mehrotra, S.; Rawat, P.; Debbarma, M.; Sudhakar, K. Performance of a solar panel with water immersion cooling technique. *Int. J. Sci. Environ. Technol.* **2014**, *3*, 1035–1042.
32. Tina, G.M.; Rosa-Clot, M.; Rosa-Clot, P.; Scandura, P.F. Optical and thermal behavior of submerged photovoltaic solar panel: SP2. *Energy* **2012**, *39*, 17–26. [CrossRef]
33. Wang, Y.; Fang, Z.; Zhu, L.; Huang, Q.; Zhang, Y.; Zhang, Z. The performance of silicon solar cells operated in liquids. *Appl. Energy* **2009**, *86*, 1037–1042. [CrossRef]
34. Akbarzadeh, A.; Wadowski, T. Heat pipe-based cooling systems for photovoltaic cells under concentrated solar radiation. *Appl. Therm. Eng.* **1996**, *16*, 81–87. [CrossRef]
35. Chandrasekar, M.; Suresh, S.; Senthilkumar, T.; Ganesh Karthikeyan, M. Passive cooling of standalone flat PV module with cotton wick structures. *Energy Convers. Manag.* **2013**, *71*, 43–50. [CrossRef]
36. Tonui, J.K.; Tripanagnostopoulos, Y. Improved PV/T solar collectors with heat extraction by forced or natural air circulation. *Renew. Energy* **2007**, *32*, 623–637. [CrossRef]
37. Yun, G.Y.; McEvoy, M.; Steemers, K. Design and overall energy performance of a ventilated photovoltaic façade. *Sol. Energy* **2007**, *81*, 383–394. [CrossRef]
38. Mezoued, M.A.; Kaabi, A. Effect of Using Packing Material on the Performances of the Double Pass Photovoltaic-Thermal (PVT) Air Heater. *Int. J. Therm. Environ. Eng.* **2013**, *5*, 61–70.
39. Kumar, R.; Rosen, M.A. Performance evaluation of a double pass PV/T solar air heater with and without fins. *Appl. Therm. Eng.* **2011**, *31*, 1402–1410. [CrossRef]
40. Murugesan, S.; Nirmala, A.; Sakthivadivel, J.; Mukhilan, R.; Tennyson, S. Physicochemical and biological parameters of water at industrial sites of metropolitan city of Chennai, Tamil Nadu, India. *Water Conserv. Manag.* **2020**, *4*, 90–98.
41. Solanki, S.C.; Dubey, S.; Tiwari, A. Indoor simulation and testing of photovoltaic thermal (PV/T) air collectors. *Appl. Energy* **2009**, *86*, 2421–2428. [CrossRef]
42. Hernandez-Perez, J.G.; Carrillo, J.G.; Bassam, A.; Flota-Banuelos, M.; Patino-Lopez, L.D. Thermal performance of a discontinuous finned heatsink profile for PV passive cooling. *Appl. Therm. Eng.* **2020**, *184*, 116238. [CrossRef]
43. Babu, C.; Ponnambalam, P. The theoretical performance evaluation of hybrid PV-TEG system. *Energy Convers. Manag.* **2018**, *173*, 450–460. [CrossRef]
44. Kumar, N.M.; Subramaniam, U.; Mathew, M.; Ajitha, A.; Almakhles, D.J. Exergy analysis of thin-film solar PV module in ground-mount, floating and submerged installation methods. *Case Stud. Therm. Eng.* **2020**, *21*, 100686. [CrossRef]

45. Savvakis, N.; Tsoutsos, T. Theoretical design and experimental evaluation of a PV+PCM system in the mediterranean climate. *Energy* **2021**, *220*, 119690. [CrossRef]
46. Abdulmunem, A.R.; Mohd Samin, P.; Abdul Rahman, H.; Hussien, H.A.; Izmi Mazali, I.; Ghazali, H. Numerical and experimental analysis of the tilt angle's effects on the characteristics of the melting process of PCM-based as PV cell's backside heat sink. *Renew. Energy* **2021**, *173*, 520–530. [CrossRef]
47. Senthil Kumar, K.; Ashwin Kumar, H.; Gowtham, P.; Hari Selva Kumar, S.; Hari Sudhan, R. Experimental analysis and increasing the energy efficiency of PV cell with nano-PCM (calcium carbonate, silicon carbide, copper). *Mater. Today Proc.* **2021**, *37*, 1221–1225. [CrossRef]
48. Nomura, T.; Okinaka, N.; Akiyama, T. Technology of Latent Heat Storage for High Temperature Application: A Review. *ISIJ Int.* **2010**, *50*, 1229–1239. [CrossRef]
49. Karthikeyan, V.; Sirisamphanwong, C.; Sukchai, S.; Sahoo, S.K.; Wongwuttanasatian, T. Reducing PV module temperature with radiation based PV module incorporating composite phase change material. *J. Energy Storage* **2020**, *29*, 101346. [CrossRef]
50. Elavarasan, R.M.; Velmurugan, K.; Subramaniam, U.; Kumar, A.R.; Almakhles, D. Experimental Investigations Conducted for the Characteristic Study of OM29 Phase Change Material and Its Incorporation in Photovoltaic Panel. *Energies* **2020**, *13*, 897. [CrossRef]
51. Prasannaa, P.; Ramkumar, R.; Sunilkumar, K.; Rajasekar, R. Experimental study on a binary mixture ratio of fatty acid-based PCM integrated to PV panel for thermal regulation on a hot and cold month. *Int. J. Sustain. Energy* **2021**, *40*, 218–234. [CrossRef]
52. Savvakis, N.; Dialyna, E.; Tsoutsos, T. Investigation of the operational performance and efficiency of an alternative PV+PCM concept. *Solar Energy* **2020**, *211*, 1283–1300. [CrossRef]
53. He, Y.; Zhang, Y.; Xiao, L.; Wang, J. Effect of SA-LA Composite PCM Volume on PV/PCM Thermal Control Properties. *IOP Conf. Ser. Earth Environ. Sci.* **2021**, *701*, 012020. [CrossRef]
54. Velmurugan, K.; Kumarasamy, S.; Wongwuttanasatian, T.; Seithtanabutara, V. Review of PCM types and suggestions for an applicable cascaded PCM for passive PV module cooling under tropical climate conditions. *J. Clean. Prod.* **2021**, *293*, 126065. [CrossRef]
55. Divyateja, B.; Unnikrishnan, K.; Rohinikumar, B. Modelling and Numerical simulation of Nano-enhanced PV-PCM System for Heat Transfer Augmentation from the Panel. *J. Phys. Conf. Ser.* **2021**, *2054*, 012051. [CrossRef]
56. Hasan, A.; Sarwar, J.; Alnoman, H.; Abdelbaqi, S. Yearly energy performance of a photovoltaic-phase change material (PV-PCM) system in hot climate. *Sol. Energy* **2017**, *146*, 417–429. [CrossRef]
57. Waqas, A.; Ji, J. Thermal management of conventional PV panel using PCM with movable shutters—A numerical study. *Sol. Energy* **2017**, *158*, 797–807. [CrossRef]
58. Senthil, R.; Madurai Elavarasan, R.; Pugazhendhi, R.; Premkumar, M.; Vengadesan, E.; Navakrishnan, S.; Islam, M.R.; Natarajan, S.K. A holistic review on the integration of heat pipes in solar thermal and photovoltaic systems. *Sol. Energy* **2021**, *227*, 577–605. [CrossRef]
59. Anand, A.; Shukla, A.; Panchal, H.; Sharma, A. Thermal regulation of photovoltaic system for enhanced power production: A review. *J. Energy Storage* **2021**, *35*, 102236. [CrossRef]
60. Reji Kumar, R.; Samykano, M.; Pandey, A.K.; Kadirgama, K.; Tyagi, V.V. Phase change materials and nano-enhanced phase change materials for thermal energy storage in photovoltaic thermal systems: A futuristic approach and its technical challenges. *Renew. Sustain. Energy Rev.* **2020**, *133*, 110341. [CrossRef]
61. Browne, M.C.; Norton, B.; McCormack, S.J. Phase change materials for photovoltaic thermal management. *Renew. Sustain. Energy Rev.* **2015**, *47*, 762–782. [CrossRef]
62. Kandeal, A.W.; Thakur, A.K.; Elkadeem, M.R.; Elmorshedy, M.F.; Ullah, Z.; Sathyamurthy, R.; Sharshir, S.W. Photovoltaics performance improvement using different cooling methodologies: A state-of-art review. *J. Clean. Prod.* **2020**, *273*, 122772. [CrossRef]
63. Chehreh, S.S. Solar photovoltaic cells performance improvement by cooling technology: An overall review. *Int. J. Hydrogen Energy* **2021**, *46*, 10939–10972.
64. Maleki, A.; Haghighi, A.; El Haj Assad, M.; Mahariq, I.; Alhuyi Nazari, M. A review on the approaches employed for cooling PV cells. *Sol. Energy* **2020**, *209*, 170–185. [CrossRef]
65. Mahian, O.; Ghafarian, S.; Sarrafha, H.; Kasaeian, A.; Yousefi, H.; Yan, W.-M. Phase change materials in solar photovoltaics applied in buildings: An overview. *Sol. Energy* **2021**, *224*, 569–592. [CrossRef]
66. Potuganti, P.; Ponnapalli, C.S. Efficiency improvement of solar PV panels using active cooling. In Proceedings of the 2012 11th International Conference on Environment and Electrical Engineering, Venice, Italy, 18–25 May 2012.
67. Li, H.; Sun, Y. Performance optimization and benefit analyses of a photovoltaic loop heat pipe/solar assisted heat pump water heating system. *Renew. Energy* **2019**, *134*, 1240–1247. [CrossRef]
68. Karthikeyan, V.; Sirisamphanwong, C.; Sukchai, S. Investigation on Thermal Absorptivity of PCM Matrix Material for Photovoltaic Module Temperature Reduction. In *Key Engineering Materials*; Trans Tech Publications Ltd.: Bäch, Switzerland, 2018; Volume 777, pp. 97–101.
69. Babu, K.M.K.; Pant, R.S. A review of Lighter-than-Air systems for exploring the atmosphere of Venus. *Prog. Aerosp. Sci.* **2020**, *112*, 100587. [CrossRef]

70. Häusler, T.; Rogaß, H. *Photovoltaic Module with Latent Heat-Storage-Collector*; Office for Official Publications of the European Communities: Luxembourg, 1998.
71. Lim, J.-H.; Lee, Y.-S.; Seong, Y.-B. Diurnal Thermal Behavior of Photovoltaic Panel with Phase Change Materials under Different Weather Conditions. *Energies* **2017**, *10*, 1983. [CrossRef]
72. Indartono, Y.S.; Suwono, A.; Pratama, F.Y. Improving photovoltaics performance by using yellow petroleum jelly as phase change material. *Int. J. Low-Carbon Technol.* **2016**, *11*, 333–337. [CrossRef]
73. Sharma, S.; Sellami, N.; Tahir, A.; Reddy, K.S.; Mallick, T.K. Enhancing the performance of BICPV systems using phase change materials. In *AIP Conference Proceedings*; AIP Publishing LLC: Melville, NY, USA, 2015; Volume 1679, p. 110003.
74. Tsoutsos, N.S.A.T. Phase Change Materials in Photovoltaics:The Assessment of System Performance in the Present Mediterranean Climate Conditions. In *Power Systems*; Trivent Publishing: Budapest, Hungary, 2016.
75. Rajvikram, M.; Sivasankar, G. Experimental study conducted for the identification of best heat absorption and dissipation methodology in solar photovoltaic panel. *Sol. Energy* **2019**, *193*, 283–292. [CrossRef]
76. Rajvikram, M.; Leoponraj, S.; Ramkumar, S.; Akshaya, H.; Dheeraj, A. Experimental investigation on the abasement of operating temperature in solar photovoltaic panel using PCM and aluminium. *Sol. Energy* **2019**, *188*, 327–338.
77. Mahamudul, H.; Rahman, M.M.; Metselaar, H.S.C.; Mekhilef, S.; Shezan, S.A.; Sohel, R.; Abu Karim, S.B.; Badiuzaman, W.N.I. Temperature Regulation of Photovoltaic Module Using Phase Change Material: A Numerical Analysis and Experimental Investigation. *Int. J. Photoenergy* **2016**, *2016*, 8. [CrossRef]
78. Mahamudul, H.; Silakhori, M.; Metselaar, I.H.; Ahmad, S.; Mekhilef, S. Development of a temperature regulated photovoltaic module using phase change material for Malaysian weather condition. *Optoelectron. Adv. Mater.-Rapid Commun.* **2014**, *8*, 1243–1245.
79. Thongtha, A.; Chan, H.Y.; Luangjok, P. Influence of Phase Change Material Application on Photovoltaic Panel Performance. In *Key Engineering Materials*; Trans Tech Publications Ltd.: Bäch, Switzerland, 2017; Volume 730, pp. 563–568.
80. Indartono, Y.S.; Prakoso, S.D.; Suwono, A.; Zaini, I.N.; Fernaldi, B. Simulation and Experimental Study on Effect of Phase Change Material Thickness to Reduce Temperature of Photovoltaic Panel. *IOP Conf. Ser. Mater. Sci. Eng.* **2015**, *88*, 012049. [CrossRef]
81. Eqwan, M.R.; Aiman, Z.R. Experimental Investigation of the Effect of Solar Photovoltaic Back Plate Cooling Using Passive Heatsink and Candle Wax as Phase Change Material. *Int. J. Sci. Res. Sci. Eng. Technol.* **2017**, *3*, 410–417.
82. Klugmann-Radziemska, E.; Wcisło-Kucharek, P. Photovoltaic module temperature stabilization with the use of phase change materials. *Sol. Energy* **2017**, *150*, 538–545. [CrossRef]
83. Waqas, A.; Jie, J. Effectiveness of Phase Change Material for Cooling of Photovoltaic Panel for Hot Climate. *J. Sol. Energy Eng.* **2018**, *140*, 041006. [CrossRef]
84. Hendricks, J.H.C.; van Sark, W.G.J.H.M. Annual performance enhancement of building integrated photovoltaic modules by applying phase change materials. *Prog. Photovolt. Res. Appl.* **2013**, *21*, 620–630. [CrossRef]
85. Khanna, S.; Reddy, K.S.; Mallick, T.K. Optimization of solar photovoltaic system integrated with phase change material. *Sol. Energy* **2018**, *163*, 591–599. [CrossRef]
86. Huang, M.J.; Eames, P.C.; Norton, B. Thermal regulation of building-integrated photovoltaics using phase change materials. *Int. J. Heat Mass Transf.* **2004**, *47*, 2715–2733. [CrossRef]
87. Biwole, P.H.; Eclache, P.; Kuznik, F. Phase-change materials to improve solar panel's performance. *Energy Build.* **2013**, *62*, 59–67. [CrossRef]
88. Khanna, S.; Reddy, K.S.; Mallick, T.K. Performance analysis of tilted photovoltaic system integrated with phase change material under varying operating conditions. *Energy* **2017**, *133*, 887–899. [CrossRef]
89. Ahmad, A.; Navarro, H.; Ghosh, S.; Ding, Y.; Roy, J.N. Evaluation of New PCM/PV Configurations for Electrical Energy Efficiency Improvement through Thermal Management of PV Systems. *Energies* **2021**, *14*, 4130. [CrossRef]
90. Gan, G.; Xiang, Y. Experimental investigation of a photovoltaic thermal collector with energy storage for power generation, building heating and natural ventilation. *Renew. Energy* **2020**, *150*, 12–22. [CrossRef]
91. Darkwa, J.; Calautit, J.; Du, D.; Kokogianakis, G. A numerical and experimental analysis of an integrated TEG-PCM power enhancement system for photovoltaic cells. *Appl. Energy* **2019**, *248*, 688–701. [CrossRef]
92. Liu, X.; Zhou, Y.; Li, C.-Q.; Lin, Y.; Yang, W.; Zhang, G. Optimization of a New Phase Change Material Integrated Photovoltaic/Thermal Panel with The Active Cooling Technique Using Taguchi Method. *Energies* **2019**, *12*, 1022. [CrossRef]
93. Al Siyabi, I.; Khanna, S.; Mallick, T.; Sundaram, S. Multiple Phase Change Material (PCM) Configuration for PCM-Based Heat Sinks—An Experimental Study. *Energies* **2018**, *11*, 1629. [CrossRef]
94. Nehari, T.; Benlakam, M.; Nehari, D. Effect of the Fins Length for the Passive Cooling of the Photovoltaic Panels. *Period. Polytech. Mech. Eng.* **2016**, *60*, 89–95. [CrossRef]
95. Nehari, T.; Benlekkam, M.; Nehari, D.; Youcefi, A. The Effect of Inclination on the Passive cooling of the solar PV panel by using Phase change Material. *Int. J. Renew. Energy Res.* **2016**, *6*, 132–139.
96. Biwole, P.; Eclache, P.; Kuznik, F. Improving the performance of solar panels by the use of phase-change materials. In Proceedings of the World Renewable Energy Congress-Sweden, Linköping, Sweden, 8–13 May 2011; pp. 2953–2960.
97. Khanna, S.; Reddy, K.S.; Mallick, T.K. Optimization of finned solar photovoltaic phase change material (finned pv pcm) system. *Int. J. Therm. Sci.* **2018**, *130*, 313–322. [CrossRef]

98. Maiti, S.; Banerjee, S.; Vyas, K.; Patel, P.; Ghosh, P.K. Self regulation of photovoltaic module temperature in V-trough using a metal–wax composite phase change matrix. *Sol. Energy* **2011**, *85*, 1805–1816. [CrossRef]
99. Hachem, F.; Abdulhay, B.; Ramadan, M.; El Hage, H.; El Rab, M.G.; Khaled, M. Improving the performance of photovoltaic cells using pure and combined phase change materials—Experiments and transient energy balance. *Renew. Energy* **2017**, *107*, 567–575. [CrossRef]
100. August, A.; Reiter, A.; Kneer, A.; Selzer, M.; Nestler, B. Effective Thermal Conductivity of Composite Materials Based on Open Cell Foams. *Heat Mass Transf. Res. J.* **2018**, *2*, 33–45.
101. Abdulmunem, A.R. assive cooling by utilizing the combined PCM/aluminum foam matrix to improve solar panels performance: Indoor investigation. *Iraqi J. Mech. Mater. Eng.* **2017**, *17*, 712–723.
102. Fiorentini, M.; Cooper, P.; Ma, Z. Development and optimization of an innovative HVAC system with integrated PVT and PCM thermal storage for a net-zero energy retrofitted house. *Energy Build.* **2015**, *94*, 21–32. [CrossRef]
103. Elarga, H.; Goia, F.; Zarrella, A.; Dal Monte, A.; Benini, E. Thermal and electrical performance of an integrated PV-PCM system in double skin façades: A numerical study. *Sol. Energy* **2016**, *136*, 112–124. [CrossRef]
104. Gaur, A.; Ménézo, C.; Giroux-Julien, S. Numerical studies on thermal and electrical performance of a fully wetted absorber PVT collector with PCM as a storage medium. *Renew. Energy* **2017**, *109*, 168–187. [CrossRef]
105. Al-Waeli, A.H.; Chaichan, M.T.; Sopian, K.; Kazem, H.A. Energy Storage: CFD Modeling of Thermal Energy Storage for a Phase Change Materials (PCM) added to a PV/T using nanofluid as a coolant. *J. Sci. Eng. Res.* **2017**, *4*, 193–202.
106. Hasan, A.; Alnoman, H.; Shah, A. Energy Efficiency Enhancement of Photovoltaics by Phase Change Materials through Thermal Energy Recovery. *Energies* **2016**, *9*, 782. [CrossRef]
107. Sardarabadi, M.; Passandideh-Fard, M.; Maghrebi, M.-J.; Ghazikhani, M. Experimental study of using both ZnO/ water nanofluid and phase change material (PCM) in photovoltaic thermal systems. *Sol. Energy Mater. Sol. Cells* **2017**, *161*, 62–69. [CrossRef]
108. Carmona, M.; Palacio Bastos, A.; García, J.D. Experimental evaluation of a hybrid photovoltaic and thermal solar energy collector with integrated phase change material (PVT-PCM) in comparison with a traditional photovoltaic (PV) module. *Renew. Energy* **2021**, *172*, 680–696. [CrossRef]
109. Fu, Z.; Liang, X.; Li, Y.; Li, L.; Zhu, Q. Performance improvement of a PVT system using a multilayer structural heat exchanger with PCMs. *Renew. Energy* **2021**, *169*, 308–317. [CrossRef]
110. Naghdbishi, A.; Yazdi, M.E.; Akbari, G. Experimental investigation of the effect of multi-wall carbon nanotube—Water/glycol based nanofluids on a PVT system integrated with PCM-covered collector. *Appl. Therm. Eng.* **2020**, *178*, 115556. [CrossRef]
111. Fu, Z.; Li, Y.; Liang, X.; Lou, S.; Qiu, Z.; Cheng, Z.; Zhu, Q. Experimental investigation on the enhanced performance of a solar PVT system using micro-encapsulated PCMs. *Energy* **2021**, *228*, 120509. [CrossRef]
112. Ahmadi, R.; Monadinia, F.; Maleki, M. Passive/active photovoltaic-thermal (PVT) system implementing infiltrated phase change material (PCM) in PS-CNT foam. *Sol. Energy Mater. Sol. Cells* **2021**, *222*, 110942. [CrossRef]
113. Kazemian, A.; Taheri, A.; Sardarabadi, A.; Ma, T.; Passandideh-Fard, M.; Peng, J. Energy, exergy and environmental analysis of glazed and unglazed PVT system integrated with phase change material: An experimental approach. *Sol. Energy* **2020**, *201*, 178–189. [CrossRef]
114. Nižetić, S.; Jurčević, M.; Čoko, D.; Arıcı, M.; Hoang, A.T. Implementation of phase change materials for thermal regulation of photovoltaic thermal systems: Comprehensive analysis of design approaches. *Energy* **2021**, *228*, 120546. [CrossRef]
115. Hassan, A.; Wahab, A.; Qasim, M.A.; Janjua, M.M.; Ali, M.A.; Ali, H.M.; Jadoon, T.R.; Ali, E.; Raza, A.; Javaid, N. Thermal management and uniform temperature regulation of photovoltaic modules using hybrid phase change materials-nanofluids system. *Renew. Energy* **2020**, *145*, 282–293. [CrossRef]
116. Çiftçi, E.; Khanlari, A.; Sözen, A.; Aytaç, İ.; Tuncer, A.D. Energy and exergy analysis of a photovoltaic thermal (PVT) system used in solar dryer: A numerical and experimental investigation. *Renew. Energy* **2021**, *180*, 410–423. [CrossRef]
117. Yang, X.; Zhou, J.; Yuan, Y. Energy Performance of an Encapsulated Phase Change Material PV/T System. *Energies* **2019**, *12*, 3929. [CrossRef]
118. Arıcı, M.; Bilgin, F.; Nižetić, S.; Papadopoulos, A.M. Phase change material based cooling of photovoltaic panel: A simplified numerical model for the optimization of the phase change material layer and general economic evaluation. *J. Clean. Prod.* **2018**, *189*, 738–745. [CrossRef]
119. Yuan, W.; Ji, J.; Modjinou, M.; Zhou, F.; Li, Z.; Song, Z.; Huang, S.; Zhao, X. Numerical simulation and experimental validation of the solar photovoltaic/thermal system with phase change material. *Appl. Energy* **2018**, *232*, 715–727. [CrossRef]
120. Machniewicz, A.; Knera, D.; Heim, D. Effect of Transition Temperature on Efficiency of PV/PCM Panels. *Energy Procedia* **2015**, *78*, 1684–1689. [CrossRef]
121. Ali, H.M. Recent advancements in PV cooling and efficiency enhancement integrating phase change materials based systems—A comprehensive review. *Sol. Energy* **2020**, *197*, 163–198. [CrossRef]
122. Rathore, P.K.S.; Shukla, S.K. Enhanced thermophysical properties of organic PCM through shape stabilization for thermal energy storage in buildings: A state of the art review. *Energy Build.* **2021**, *236*, 110799. [CrossRef]
123. Khan, Z.; Khan, Z.; Ghafoor, A. A review of performance enhancement of PCM based latent heat storage system within the context of materials, thermal stability and compatibility. *Energy Convers. Manag.* **2016**, *115*, 132–158. [CrossRef]
124. Huang, M.J.; Eames, P.C.; Norton, B. Phase change materials for limiting temperature rise in building integrated photovoltaics. *Sol. Energy* **2006**, *80*, 1121–1130. [CrossRef]

125. Ma, T.; Li, Z.; Zhao, J. Photovoltaic panel integrated with phase change materials (PV-PCM): Technology overview and materials selection. *Renew. Sustain. Energy Rev.* **2019**, *116*, 109406. [CrossRef]
126. Murali, G.; Sravya, G.S.N.; Jaya, J.; Naga Vamsi, V. A review on hybrid thermal management of battery packs and it's cooling performance by enhanced PCM. *Renew. Sustain. Energy Rev.* **2021**, *150*, 111513. [CrossRef]
127. Wu, S.; Yan, T.; Kuai, Z.; Pan, W. Thermal conductivity enhancement on phase change materials for thermal energy storage: A review. *Energy Storage Mater.* **2020**, *25*, 251–295. [CrossRef]
128. Li, X.; Cui, W.; Simon, T.; Ma, T.; Cui, T.; Wang, Q. Pore-scale analysis on selection of composite phase change materials for photovoltaic thermal management. *Appl. Energy* **2021**, *302*, 117558. [CrossRef]
129. Li, C.; Li, Q.; Ding, Y. Carbonate salt based composite phase change materials for medium and high temperature thermal energy storage: From component to device level performance through modelling. *Renew. Energy* **2019**, *140*, 140–151. [CrossRef]
130. Abdulmunem, A.R.; Samin, P.M.; Rahman, H.A.; Hussien, H.A.; Ghazali, H. A novel thermal regulation method for photovoltaic panels using porous metals filled with phase change material and nanoparticle additives. *J. Energy Storage* **2021**, *39*, 102621. [CrossRef]
131. Mills, A.; Farid, M.; Selman, J.R.; Al-Hallaj, S. Thermal conductivity enhancement of phase change materials using a graphite matrix. *Appl. Therm. Eng.* **2006**, *26*, 1652–1661. [CrossRef]
132. Huang, Y.; She, X.; Li, C.; Li, Y.; Ding, Y. Evaluation of thermal performance in cold storage applications using EG-water based nano-composite PCMs. *Energy Procedia* **2019**, *158*, 4840–4845. [CrossRef]
133. Waqas, A.; Ji, J.; Xu, L.; Ali, M.; Alvi, J. Thermal and electrical management of photovoltaic panels using phase change materials—A review. *Renew. Sustain. Energy Rev.* **2018**, *92*, 254–271. [CrossRef]
134. Sarı, A.; Sarı, H.; Önal, A. Thermal properties and thermal reliability of eutectic mixtures of some fatty acids as latent heat storage materials. *Energy Convers. Manag.* **2004**, *45*, 365–376. [CrossRef]
135. Sharma, A.; Shukla, A. Thermal Cycle Test of Binary Mixtures of Some Fatty Acids as Phase Change Materials For Building Applications. *Energy Build.* **2015**, *99*, 196–203. [CrossRef]
136. Shukla, A.; Buddhi, D.; Sawhney, R.L. Thermal cycling test of few selected inorganic and organic phase change materials. *Renew. Energy* **2008**, *33*, 2606–2614. [CrossRef]
137. Anand, A.; Shukla, A.; Kumar, A.; Buddhi, D.; Sharma, A. Cycle test stability and corrosion evaluation of phase change materials used in thermal energy storage systems. *J. Energy Storage* **2021**, *39*, 102664. [CrossRef]
138. Mohseni, E.; Tang, W.; Khayat, K.H.; Cui, H. Thermal performance and corrosion resistance of structural-functional concrete made with inorganic PCM. *Constr. Build. Mater.* **2020**, *249*, 118768. [CrossRef]
139. Calabrese, L.; Brancato, V.; Palomba, V.; Proverbio, E. An experimental study on the corrosion sensitivity of metal alloys for usage in PCM thermal energy storages. *Renew. Energy* **2019**, *138*, 1018–1027. [CrossRef]
140. Moreno, P.; Miró, L.; Solé, A.; Barreneche, C.; Solé, C.; Martorell, I.; Cabeza, L.F. Corrosion of metal and metal alloy containers in contact with phase change materials (PCM) for potential heating and cooling applications. *Appl. Energy* **2014**, *125*, 238–245. [CrossRef]
141. Ferrer, G.; Solé, A.; Barreneche, C.; Martorell, I.; Cabeza, L.F. Corrosion of metal containers for use in PCM energy storage. *Renew. Energy* **2015**, *76*, 465–469. [CrossRef]
142. Socaciu, L. Thermal energy storage: An overview. *Appl. Math. Mech.* **2012**, *55*, 785–793.
143. Dincer, I.; Rosen, M.A. Thermal Energy Storage (TES) Methods. In *Thermal Energy Storage: Systems and Applications*, 2nd ed.; Wiley: Hoboken, NJ, USA, 2010; pp. 83–190.
144. Hassan, A.; McCormack, S.J.; Huang, M.J.; Norton, B. Energy and Cost Saving of a Photovoltaic-Phase Change Materials (PV-PCM) System through Temperature Regulation and Performance Enhancement of Photovoltaics. *Energies* **2014**, *7*, 1318–1331. [CrossRef]
145. Smith, C.J.; Forster, P.M.; Crook, R. Global analysis of photovoltaic energy output enhanced by phase change material cooling. *Appl. Energy* **2014**, *126*, 21–28. [CrossRef]
146. Sun, X.; Lin, Y.; Zhu, Z.; Li, J. Optimized design of a distributed photovoltaic system in a building with phase change materials. *Appl. Energy* **2022**, *306*, 118010. [CrossRef]
147. Kladisios, P.; Steggou-Sagia, A. Using phase change materials in photovoltaic systems for thermal regulation and electrical efficiency improvement: A review and outlook. *J. Therm. Eng.* **2016**, *2*, 897–906.
148. Yang, X.; Sun, L.; Yuan, Y.; Zhao, X.; Cao, X. Experimental investigation on performance comparison of PV/T-PCM system and PV/T system. *Renew. Energy* **2018**, *119*, 152–159. [CrossRef]
149. Elarga, H.; Dal Monte, A.; Andersen, R.K.; Benini, E. PV-PCM integration in glazed building. Co-simulation and genetic optimization study. *Build. Environ.* **2017**, *126*, 161–175. [CrossRef]
150. Nada, S.A.; El-Nagar, D.H.; Hussein, H.M.S. Improving the thermal regulation and efficiency enhancement of PCM-Integrated PV modules using nano particles. *Energy Convers. Manag.* **2018**, *166*, 735–743. [CrossRef]
151. Stropnik, R.; Stritih, U. Increasing the efficiency of PV panel with the use of PCM. *Renew. Energy* **2016**, *97*, 671–679. [CrossRef]
152. Nada, S.A.; El-Nagar, D.H. Possibility of using PCMs in temperature control and performance enhancements of free stand and building integrated PV modules. *Renew. Energy* **2018**, *127*, 630–641. [CrossRef]
153. Modjinou, M.; Ji, J.; Yuan, W.; Zhou, F.; Holliday, S.; Waqas, A.; Zhao, X. Performance comparison of encapsulated PCM PV/T, microchannel heat pipe PV/T and conventional PV/T systems. *Energy* **2019**, *166*, 1249–1266. [CrossRef]

154. Hosseinzadeh, M.; Sardarabadi, M.; Passandideh-Fard, M. Energy and exergy analysis of nanofluid based photovoltaic thermal system integrated with phase change material. *Energy* **2018**, *147*, 636–647. [CrossRef]
155. Zhou, Y.; Liu, X.; Zhang, G. Performance of buildings integrated with a photovoltaic–thermal collector and phase change materials. *Procedia Eng.* **2017**, *205*, 1337–1343. [CrossRef]
156. Nižetić, S.; Arıcı, M.; Bilgin, F.; Grubišić-Čabo, F. Investigation of pork fat as potential novel phase change material for passive cooling applications in photovoltaics. *J. Clean. Prod.* **2018**, *170*, 1006–1016. [CrossRef]
157. Lu, W.; Wu, Y.; Eames, P. Design and development of a Building Façade Integrated Asymmetric Compound Parabolic Photovoltaic concentrator (BFI-ACP-PV). *Appl. Energy* **2018**, *220*, 325–336. [CrossRef]
158. Park, J.; Kim, T.; Leigh, S.-B. Application of a phase-change material to improve the electrical performance of vertical-building-added photovoltaics considering the annual weather conditions. *Sol. Energy* **2014**, *105*, 561–574. [CrossRef]
159. Abdelrahman, H.E.; Wahba, M.H.; Refaey, H.A.; Moawad, M.; Berbish, N.S. Performance enhancement of photovoltaic cells by changing configuration and using PCM (RT35HC) with nanoparticles Al_2O_3. *Sol. Energy* **2019**, *177*, 665–671. [CrossRef]
160. Thaib, R.; Rizal, S.; Mahlia, T.M.I.; Pambudi, N.A. Experimental analysis of using beeswax as phase change materials for limiting temperature rise in building integrated photovoltaics. *Case Stud. Therm. Eng.* **2018**, *12*, 223–227. [CrossRef]
161. Cui, T.; Xuan, Y.; Li, Q. Design of a novel concentrating photovoltaic–thermoelectric system incorporated with phase change materials. *Energy Convers. Manag.* **2016**, *112*, 49–60. [CrossRef]
162. Atkin, P.; Farid, M.M. Improving the efficiency of photovoltaic cells using PCM infused graphite and aluminium fins. *Sol. Energy* **2015**, *114*, 217–228. [CrossRef]
163. Al-Waeli, A.H.A.; Sopian, K.; Chaichan, M.T.; Kazem, H.A.; Ibrahim, A.; Mat, S.; Ruslan, M.H. Evaluation of the nanofluid and nano-PCM based photovoltaic thermal (PVT) system: An experimental study. *Energy Convers. Manag.* **2017**, *151*, 693–708. [CrossRef]
164. Preet, S.; Bhushan, B.; Mahajan, T. Experimental investigation of water based photovoltaic/thermal (PV/T) system with and without phase change material (PCM). *Sol. Energy* **2017**, *155*, 1104–1120. [CrossRef]
165. Xu, D. Research on Supply Chain Management Strategy Of Longtang Electric Engineering Co. Ltd. *Acta Electron. Malays.* **2019**, *3*, 10–13. [CrossRef]
166. Zhang, W.; Zhang, Z. Deck Electrical System Support Technology of Port Tanker. *J. Coast. Res.* **2020**, *103*, 392–396. [CrossRef]
167. Material, P.C. *Rubitherm Data Sheet*; Rubitherm Technologies GmbH: Berlin, Germany, 2000.
168. Hale, D.V.; Hoover, M.J.; Oneill, M.J. *Phase Change Materials Handbook*; NASA Contractor Report; 1971; p. 65. Available online: https://ntrs.nasa.gov/citations/19720012306 (accessed on 15 July 2020).
169. Warren, M.; Roshsenow, J.P.H.; Cho, Y.I. *Handbook of Heat Transfer*, 3rd ed.; McGraw-Hill: New York, NY, USA, 1988.
170. Sharma, S.D.; Buddhi, D.; Sawhney, R.L. Accelerated thermal cycle test of latent heat-storage materials. *Sol. Energy* **1999**, *66*, 483–490. [CrossRef]
171. Lotos Group, S.A. Ceresin paraffin wax, Poland. Available online: https://www.lotos.pl/en/ (accessed on 15 July 2020).
172. Simone Raoux, M.W. Phase Change Materials. In *Science and Applications*; Springer Science: New York, NY, USA, 2009.
173. Chang, S.J.; Kang, Y.; Wi, S.; Jeong, S.-G.; Kim, S. Hygrothermal performance improvement of the Korean wood frame walls using macro-packed phase change materials (MPPCM). *Appl. Therm. Eng.* **2017**, *114*, 457–465. [CrossRef]
174. *PlusICE PCM Hydrated Salt*; Phase Change Material Products Limited: Yaxley, UK; Available online: https://www.pcmproducts.net/Phase-Change-Material-Solutions.htm (accessed on 15 July 2020).
175. Ma, T.; Zhao, J.; Li, Z. Mathematical modelling and sensitivity analysis of solar photovoltaic panel integrated with phase change material. *Appl. Energy* **2018**, *228*, 1147–1158. [CrossRef]
176. Tan, L.; Date, A.; Fernandes, G.; Singh, B.; Ganguly, S. Efficiency Gains of Photovoltaic System Using Latent Heat Thermal Energy Storage. *Energy Procedia* **2017**, *110*, 83–88. [CrossRef]
177. Wheelan, D. The Use of Phase Change Materials in Building Temeprature Regulation Applied Post-Construction. Post-Graduation Thesis, Trinity College, Dublin University, Dublin, Ireland, 2011.
178. Nouira, M.; Sammouda, H. Numerical study of an inclined photovoltaic system coupled with phase change material under various operating conditions. *Appl. Therm. Eng.* **2018**, *141*, 958–975. [CrossRef]
179. Japs, E.; Sonnenrein, G.; Krauter, S.; Vrabec, J. Experimental study of phase change materials for photovoltaic modules: Energy performance and economic yield for the EPEX spot market. *Sol. Energy* **2016**, *140*, 51–59. [CrossRef]
180. Al-Waeli, A.H.A.; Chaichan, M.T.; Sopian, K.; Kazem, H.A.; Mahood, H.B.; Khadom, A.A. Modeling and experimental validation of a PVT system using nanofluid coolant and nano-PCM. *Sol. Energy* **2019**, *177*, 178–191. [CrossRef]
181. Lu, W.; Liu, Z.; Flor, J.-F.; Wu, Y.; Yang, M. Investigation on designed fins-enhanced phase change materials system for thermal management of a novel building integrated concentrating PV. *Appl. Energy* **2018**, *225*, 696–709. [CrossRef]
182. Baetens, R.; Jelle, B.P.; Gustavsen, A. Phase change materials for building applications: A state-of-the-art review. *Energy Build.* **2010**, *42*, 1361–1368. [CrossRef]
183. Ma, T.; Zhao, J.; Han, J. A Parametric Study about the Potential to Integrate Phase Change Material into Photovoltaic Panel. *Energy Procedia* **2017**, *142*, 648–654. [CrossRef]
184. Hossain, M.S.; Pandey, A.K.; Selvaraj, J.; Rahim, N.A.; Islam, M.M.; Tyagi, V.V. Two side serpentine flow based photovoltaic-thermal-phase change materials (PVT-PCM) system: Energy, exergy and economic analysis. *Renew. Energy* **2018**, *136*, 1320–1336. [CrossRef]

185. Kazemian, A.; Hosseinzadeh, M.; Sardarabadi, M.; Passandideh-Fard, M. Experimental study of using both ethylene glycol and phase change material as coolant in photovoltaic thermal systems (PVT) from energy, exergy and entropy generation viewpoints. *Energy* **2018**, *162*, 210–223. [CrossRef]
186. Luo, Z.; Huang, Z.; Xie, N.; Gao, X.; Xu, T.; Fang, Y.; Zhang, Z. Numerical and experimental study on temperature control of solar panels with form-stable paraffin/expanded graphite composite PCM. *Energy Convers. Manag.* **2017**, *149*, 416–423. [CrossRef]
187. Ciulla, G.; Brano, V.L.; Cellura, M.; Franzitta, V.; Milone, D. A Finite Difference Model of a PV-PCM System. *Energy Procedia* **2012**, *30*, 198–206. [CrossRef]
188. Malik, M.; Dincer, I.; Rosen, M.A. Review on use of phase change materials in battery thermal management for electric and hybrid electric vehicles. *Int. J. Energy Res.* **2016**, *40*, 1011–1031. [CrossRef]
189. Lari, M.O.; Sahin, A.Z. Effect of retrofitting a silver/water nanofluid-based photovoltaic/thermal (PV/T) system with a PCM-thermal battery for residential applications. *Renew. Energy* **2018**, *122*, 98–107. [CrossRef]
190. Haji-Sheikh, A.; Eftekhar, J.; Lou, D. Some thermophysical properties of paraffin wax as a thermal storage medium. In Proceedings of the 3rd Joint Thermophysics, Fluids, Plasma and Heat Transfer Conference, St. Louis, MO, USA, 7 June–11 June 1982; American Institute of Aeronautics and Astronautics: Reston, VA, USA, 1982.
191. Mazraeh, A.E.; Babayan, M.; Yari, M.; Sefidan, A.M.; Saha, S.C. Theoretical study on the performance of a solar still system integrated with PCM-PV module for sustainable water and power generation. *Desalination* **2018**, *443*, 184–197. [CrossRef]
192. Klemm, T.; Hassabou, A.; Abdallah, A.; Andersen, O. Thermal energy storage with phase change materials to increase the efficiency of solar photovoltaic modules. *Energy Procedia* **2017**, *135*, 193–202. [CrossRef]
193. Browne, M.C.; Lawlor, K.; Kelly, A.; Norton, B.; Cormack, S.J.M. Indoor Characterisation of a Photovoltaic/ Thermal Phase Change Material System. *Energy Procedia* **2015**, *70*, 163–171. [CrossRef]
194. Mousavi Baygi, S.R.; Sadrameli, S.M. Thermal management of photovoltaic solar cells using polyethylene glycol 1000 (PEG1000) as a phase change material. *Therm. Sci. Eng. Prog.* **2018**, *5*, 405–411. [CrossRef]
195. Royo, P.; Ferreira, V.J.; López-Sabirón, A.M.; Ferreira, G. Hybrid diagnosis to characterise the energy and environmental enhancement of photovoltaic modules using smart materials. *Energy* **2016**, *101*, 174–189. [CrossRef]
196. Sarı, A.; Karaipekli, A. Preparation and thermal properties of capric acid/palmitic acid eutectic mixture as a phase change energy storage material. *Mater. Lett.* **2008**, *62*, 903–906. [CrossRef]
197. Hasan, A.; McCormack, S.J.; Huang, M.J.; Sarwar, J.; Norton, B. Increased photovoltaic performance through temperature regulation by phase change materials: Materials comparison in different climates. *Sol. Energy* **2015**, *115*, 264–276. [CrossRef]
198. Tyagi, V.V.; Buddhi, D. Thermal cycle testing of calcium chloride hexahydrate as a possible PCM for latent heat storage. *Sol. Energy Mater. Sol. Cells* **2008**, *92*, 891–899. [CrossRef]